

Texas General Land Office Offshore Sediment Resource Inventory: Geological and Geophysical Data Collection and Processing for Identification of Outer Continental Shelf Mineral Resources Offshore of Texas



THE WATER INSTITUTE
OF THE GULF®

U.S. Department of the Interior
Bureau of Ocean Energy Management
[BOEM Marine Minerals Program, New
Orleans, LA]

BOEM
Bureau of Ocean Energy
Management

Texas General Land Office Offshore Sediment Resource Inventory: Geological and Geophysical Data Collection and Processing for Identification of Outer Continental Shelf Mineral Resources Offshore of Texas

[June 2022]

Authors:

Beau Suthard (APTIM), Jeff Andrews (APTIM), Michael Lowiec (APTIM), Beth Forrest (APTIM), Patrick Bryce (APTIM), Alexandra Valente (APTIM), Chris Dvorscak (APTIM), Thomas Tuten (APTIM), Coty Granger (APTIM), Mike Miner (TWI), and John Swartz (TWI).

Prepared under Contract Number 18-127-014

By

Aptim Environmental & Infrastructure, LLC
725 US Highway 301 South
Tampa, FL 33619

And

The Water Institute of the Gulf
1110 River Road S.
Suite 200
Baton Rouge, LA 70802

**U.S. Department of the Interior
Bureau of Ocean Energy Management
[BOEM Marine Minerals Program, New
Orleans, LA]**



DISCLAIMER

Study collaboration and funding were provided by the U.S. Department of the Interior, Bureau of Ocean Energy Management (BOEM), Marine Minerals Program under Agreement Number [M21AC00005]. This report has been technically reviewed by BOEM, and it has been approved for publication. The views and conclusions contained in this document are those of the authors and should not be interpreted as representing the opinions or policies of BOEM, nor does mention of trade names or commercial products constitute endorsement or recommendation for use.

REPORT AVAILABILITY

To download a PDF file of this report, go to the U.S. Department of the Interior, Bureau of Ocean Energy Management Data and Information Systems webpage (<https://www.boem.gov/marine-minerals/marine-mineral-research-studies/marine-mineral-resource-evaluation-research>).

CITATION

Aptim Environmental & Infrastructure, LLC (APTIM) and The Water Institute of the Gulf 2022. Texas General Land Office Offshore Sediment Resource Inventory: Geological and Geophysical Data Collection and Processing for Identification of Outer Continental Shelf Mineral Resources Offshore of Texas. Final Report prepared for the Texas General Land Office. Contract No. 18-127-014: 94 p.

ACKNOWLEDGMENTS

Beau Suthard (Aptim Environmental & Infrastructure, LLC [APTIM]) was the Project Manager for this survey and the primary author of this report. He was responsible for project formulation and execution, including data analyses, interpretations, and report preparation. Mr. Suthard was supported by Jeffrey Andrews, Michael Lowiec, and APTIM's Geophysical and Hydrographic Survey teams with geophysical data collection, analysis, and interpretation. Beth Forrest (APTIM) and William "Quin" Robertson (Coastal Protection Engineering LLC) provided support throughout the study and contributed to written sections of the report. APTIM's field crew included Thomas Shahan, Richard Hart, Tim Moss, Alex Valente, Patrick Bryce, Thomas "Max" Tuten, Duke Thornburgh, Chris Dvorscak, Sabrina Porto, Sam Lohman (CPE-LLC), Sarah Finkle, Chase Beale, and Daniel Hope. John Swartz and Mike Miner from The Water Institute contributed to survey planning, synthesis of existing geologic and geophysical data and literature, data interpretation and development of conceptual geologic models, and report preparation.

Beau Suthard (APTIM) worked under the guidance of Texas General Land Office Coastal Erosion Planning and Response Act (CEPRA) Project Manager Kelly Brooks. Partners included The Water Institute (Mike Miner, Ph.D., P.G., and John Swartz, Ph.D.), Coastal Protection Engineering (William Robertson, Ph.D., PG, GISP), and the University of Texas Institute of Geophysics (John Goff, Ph.D., Sean Gulick, Ph.D., and Steffen Sastrup, Ph.D). Funding for this project was provided through BOEM Award Number M21AC00005 managed by the Texas General Land Office CEPRA program.

Contents

List of Figures	v
List of Tables	vii
List of Abbreviations and Acronyms	viii
1 Executive Summary	1
2 Introduction	4
3 Task 1 Historic Data Review/Survey Plan Development	6
3.1 Geologic Framework	6
3.1.1 Gulf Basin Evolution Early Gulf of Mexico Formation	6
3.1.2 Quaternary Geology	8
3.1.3 Late Quaternary Sea Level Changes (120,000 years ago to present)	10
3.1.4 Alluvial Plains	19
3.1.5 Paleo-Channel Fills	21
3.1.6 Transgressive Shelf Sand Bodies	25
3.1.7 Transgressive Ravinement	28
3.1.8 Highstand (~4,000 years ago to present)	28
3.1.9 Influence of Salt on Quaternary Geomorphology and Sediment Accumulation	28
3.2 Survey Planning	31
4 Task 2 Reconnaissance-Level Geophysical Survey	33
4.1 Geophysical Investigation	33
4.2 Equipment and Survey Methods	34
4.2.1 Navigation	36
4.2.2 HYPACK Inc.'s HYPACK 2020® Data Collection and Processing Program	37
4.2.3 Bathymetric Survey	37
4.2.4 Magnetometer Survey	38
4.2.5 Sidescan Sonar Survey	38
4.2.6 Seismic Reflection Profile Surveys	39
4.3 Mitigation Efforts to Minimize Potential High-Resolution Geophysical Impacts to Protected Species	41
4.3.1 Mitigation	41
4.3.2 Seismic Survey Mitigation and Protected Species Observer Protocols	41
4.3.3 Vessel Strike Avoidance and Injured/Dead Aquatic Protected Species Reporting Protocols	42
4.3.4 Gulf of Mexico Marine Trash and Debris Awareness and Elimination Survey Protocols	43
4.3.5 Navigation and Commercial Fisheries Operations Conflict Minimization Requirements	43
5 Task 3 Data Processing and Data Interpretation	44
5.1 Bathymetric Survey	44
5.2 Magnetometer Survey	49
5.3 Sidescan Sonar Survey	49
5.4 Sub-bottom Profile Survey	52
5.4.1 Seismic Unit Quaternary 1 (Q1)	55
5.4.2 Interpretation of Paleochannels, Potential Sand-Bearing Features, and Development of the Regional Geologic Model	60
5.4.3 Localized Features	68
5.4.4 Regional Geologic Summary	70
6 Vibrocore Planning	74
7 Conclusion	80
8 References	82

Appendix A: Desktop Study Report and Maps	88
Appendix B: Project Meeting Minutes	89
Appendix C: Mitigation Documents	90
Appendix D: PSO Observation Forms	91
Appendix E: Supplementary field operation notes and forms	92
Appendix F: Single Beam Bathymetry Map Series.....	93
Appendix G: Single Beam Bathymetric XYZ Data (Digital Only).....	94
Appendix H: Sidescan Sonar Mosaic Map Series	95
Appendix I: Sidescan Sonar Contacts and Magnetometer Targets Map Series.....	96
Appendix J: Sidescan Sonar Contact Sheets	97
Appendix K: Magnetic Anomaly Table.....	98
Appendix L: Seismic Features Map Series.....	99
Appendix M: Seismic Web Project (Digital Only).....	100
Appendix N: Seismic Interpretations Results Map Series	101
Appendix O: Geophysical Interpretations/Analysis Results geoMap	102
Appendix P: Geophysical Interpretations/MMIS File Geodatabase (Digital Only)	103
Appendix Q: Vibracore Site Selection Snapshots	104
Appendix R: Vibracore Planning Maps and Tables	105
Appendix S: Vibracore Selection Shapefile (Digital Only).....	106
Appendix T: Task 5 Pipeline Decommissioning Impacts on SSRA Blocks	107
Appendix U: Task 6 Environmental Mitigation Summary	108
Appendix V: Sidescan Sonar SonarWiz Project (Digital Only).....	109
Appendix W: Seismic SonarWiz Project (Digital Only)	110
Appendix X: Raw Geophysical Data (Digital Only).....	111

List of Figures

Figure 1. Texas GLO OCS Study Area..... 5

Figure 2. Gulf Basin physiology. 7

Figure 3. Satellite imagery of Texas coast and aerial image of High Island Salt Dome..... 8

Figure 4. Idealized dip cross section for the upper Texas coastal plain..... 9

Figure 5. Generalized dip cross-section for the eastern Texas-west Louisiana coastal plain Quaternary deposits..... 9

Figure 6. Sea level variability over the last 140,000 years..... 10

Figure 7. Falling stage fluvial deposits on the middle to upper Texas shelf..... 11

Figure 8. Plan view conceptual model of a valley fill..... 12

Figure 9. Map Showing the Trinity/Sabine Incised valley and Terrace Deposits..... 13

Figure 10. Interpreted Chirp Sonar Profile Over the Trinity incised valley and lithologic description from a platform geotechnical boring..... 13

Figure 11. Holocene (past ~10,000 years) sea level curve..... 14

Figure 12. Overfilled versus underfilled fluvial systems..... 15

Figure 13. Time-transgressive paleogeographic reconstruction of infilling of the upper (non-fluvial) section of the Trinity/Sabine Incised valley..... 16

Figure 14. Structure contour maps of Galveston Bay and Sabine Lake (left)..... 17

Figure 15. Thickness (in meters) of sandy fluvial deposits..... 18

Figure 16. Trinity/Sabine incised valley isopach map..... 18

Figure 17. Interpreted chirp sonar profile with geotechnical boring log used to validate interpretations... 19

Figure 18. Oblique view conceptual model (A) and generalized cross section of the Quaternary alluvial plains of the Colorado River, Texas (B)..... 20

Figure 19. Example sub-bottom profile sections across the offshore preserved Brazos Alluvial Plain..... 21

Figure 20. Paleochannel and paleovalley deposits..... 22

Figure 21. Sand deposit map of the Peveto Paleochannel offshore Holly Beach, Louisiana..... 23

Figure 22. Conceptual hierarchy of fluvial deposits..... 24

Figure 23. Sub-bottom profile sections across a Pleistocene channel belt in Texas state waters..... 25

Figure 24. Map showing occurrence of sand banks relative to the Trinity/Sabine incised valley and tidal deposits..... 26

Figure 25. Three-stage conceptual model..... 27

Figure 26. Dip-oriented cross-section across Sabine Bank..... 27

Figure 27. Geologic map showing Weeks Island and Cote Blanche Island salt domes in coastal Louisiana..... 30

Figure 28. Chirp profile collected during the McFaddin Beach restoration sand search..... 30

Figure 29. Conceptual model for development and preservation of salt dome colluvial aprons..... 31

Figure 30: Planned survey lines from Desktop Study..... 32

Figure 31. As run tracklines..... 34

Figure 32. Schematic diagram showing the typical deployment of sensors.	36
Figure 33. Geometrics G-882 Digital Cesium Marine Magnetometer.	38
Figure 34. EdgeTech 4200 Sidescan Sonar Towfish.	39
Figure 35. EdgeTech X-STAR SB-512i sub-bottom profiling system.	40
Figure 36. Sound Velocity cast profile example.	46
Figure 37. Texas OCS sounding standard deviation chart.	47
Figure 38. Tide Comparison Plot (11/4/20).	48
Figure 39. Example classification of sub-bottom profiler data based on seismic horizon reflection character and geometry.	54
Figure 40. Historic vibracores utilized for geophysical data interpretation.	56
Figure 41. Seismic line 048.001.	57
Figure 42. Seismic line 020.001.	58
Figure 43. Seismic Unit Q1 isopach generated by APTIM compared to the Modeled Shoals provided by BOEM MMIS.	59
Figure 44. Mapped sub-surface geologic features.	61
Figure 45. Example sub-bottom profiler data across Channel Belt 1.	62
Figure 46. Example sub-bottom profiler data across Channel Belt 2.	63
Figure 47. Example sub-bottom profiler data across Channel Belt 3.	64
Figure 48. Example sub-bottom profiler data across Channel Belt 4.	65
Figure 49. Example sub-bottom profiler data across Channel Belt 5.	65
Figure 50. South Sabine Fluvial Terrace.	66
Figure 51. Sabine Incised Valley stratigraphy.	67
Figure 52. Localized potential sand deposit (yellow) in paleochannel (black) on seismic Line 206.	69
Figure 53. Seismic Line 040.003.	69
Figure 54. Localized features identified in the survey area.	70
Figure 55. Generalized cross section of major features observed in the OCS.	72
Figure 56. Late Pleistocene Stratigraphy of Southwest Louisiana.	73
Figure 57. Proposed vibracore sites in the outer continental shelf study area.	75

List of Tables

Table 1. Geophysical investigations conducted in 2020.....	33
Table 2. Equipment used during the geophysical investigation.....	35
Table 3. Texas OCS Cross Check Statistical Report.	47
Table 4. Sidescan sonar bottom feature classification.	51
Table 5. Historic vibracore classification scheme.	56
Table 6. Calculated potential gross volume.	59
Table 7. Potential gross volume identified within study area.....	68
Table 8. Proposed Vibracore locations and general description of targeted stratigraphy.	76

List of Abbreviations and Acronyms

%	percent
~	approximately
AEZ	Acoustic Exclusion Zone
AGC	Automatic Gain Control
APTIM	Aptim Environmental & Infrastructure, LLC
APTIM-CPE	APTIM (formerly known as Coastal Planning & Engineering, Inc.)
BCY.	billion cubic yards
BOEM	Bureau of Ocean Energy Management
BSEE	Bureau of Safety and Environmental Enforcement
CEPRA	Coastal Erosion Planning and Response Act
CPE-LLC	Coastal Protection Engineering LLC
DGPS	Differential Global Positioning System
EGN	Empirical Gain Normalization
ft	feet (foot)
GLO	General Land Office
GNSS	Global Navigation Satellite System
GOM	Gulf of Mexico
GPS	Global Positioning System
HRG	High Resolution Geophysical
Hz	hertz
kHz	kilohertz
km	kilometer(s)
m	meter(s)
m/ms	meter(s) per millisecond
mbsl	meter(s) below sea level
MCY	million cubic yards
mi	mile(s)
mm/yr	millimeter(s) per year
MMIS	Marine Minerals Information System
MMP	Marine Minerals Program
MRU	Motion Reference Unit
NAD	North American Datum
NAVD	North American Vertical Datum
nm	nautical mile(s)
NMFS	National Marine Fisheries Service
NOAA	National Oceanic and Atmospheric Administration
nT	nanotesla
OCS	Outer Continental Shelf
P-P	Peak to Peak
PAM	Passive Acoustic Monitoring
PPK	Post-Processing Kinematic
PSO	Protected Species Observer
Q1	Quaternary 1
SSRA	Significant Sediment Resource Areas
SVP	Sound Velocity Profiler
TBC	Trimble Business Center
TSV	Trinity Sabine Valley
TVG	Time-Varying Gain

TWI
UGC
USCG

The Water Institute of the Gulf
User-Defined Gain Control
U. S. Coast Guard

1 Executive Summary

The Texas General Land Office (GLO) and the Bureau of Ocean Energy Management (BOEM) contracted Aptim Environmental & Infrastructure, LLC (APTIM), with team members The Water Institute of the Gulf (TWI) and Coastal Protection Engineering LLC (CPE-LLC), to conduct geophysical surveys to assist the GLO and BOEM with identifying and delineating sediment resources along the Texas Continental Shelf. The APTIM Team conducted an extensive review of existing geophysical and geotechnical data to ensure no duplication of data occurred. Marine hazard and resource data were also acquired and compiled, reviewed, and incorporated to further develop the geophysical survey plan. APTIM reviewed the existing data to assess seafloor depth, seafloor hazards, base of overburden, top of sand, base of sand, channels/paleochannels, and ravinement surfaces. Based on this evaluation, the APTIM Team developed a survey plan that made the most efficient use of existing data while avoiding collecting duplicate data.

Between October 23 and November 14, 2020, the APTIM crew conducted 24-hour survey efforts and collected 1,133 nautical miles (nm) of full-suite geophysical (sub-bottom, sidescan sonar, magnetometer, and single-beam bathymetry) data along Sabine and Heald Bank (and adjacent areas) within the investigation area in support of the GLO Sediment Management Plan Surveys of the Federal Outer Continental Shelf (OCS). Following the initial desktop study an initial survey plan was developed consisting of 1,067 nm full suite geophysical and single-beam bathymetry data. However, during survey operations, APTIM scientists marked areas of potential interest that were highly indicative of potential sand resources and, before completing the data collection efforts, APTIM and TWI worked with the GLO to select areas for additional data coverage and acquired an additional 66 nm of geophysical data for a total of 1,133 nm of data. From the findings presented herein, APTIM has completed a reconnaissance geophysical survey throughout the survey area consisting of 1 nm spaced shore perpendicular lines and 5 nm spaced shore parallel lines, covering a roughly 740,000-acre area that encompasses the Sabine, Heald, and neighboring sand banks.

Interpretation of the reconnaissance geophysical survey data identified major regional stratigraphic features located within the OCS and developed a regional geologic framework of major depositional systems that have the potential to contain accessible sand resources. The east Texas OCS contains a significant number of potential sand-bearing units located within the study area in the form of fluvial deposits and sand bank features, and surficial units. As part of this study, five (5) potential sand-bearing Pleistocene channel belt systems were identified and mapped, along with two (2) Pleistocene fluvial terraces and the previously identified Sabine Incised Valley.

The Pleistocene Channel Belts 1 and 2 are located on the eastern side of the study area and are characterized by a basal erosional unconformity overlaid by variable amplitude steeply dipping clinoforms and occasional areas of semi-transparent to chaotic acoustic facies, with the upper portion of these units being either a transition to a more-layered seismic facies or are truncated by transgressive ravinement. Channel Belts 1 and 2 are roughly 25-50 feet (ft) (7.6-15.2 meters [m]) thick with 0-10 feet (ft) (0-3 m) of overburden and 20-50 ft (6.1-15.24 m), with 0-5 ft (0-1.5 m) of overburden, respectively, and have a potential gross volume of 121 million cubic yards (MCY) and 49 MCY respectively. Potential

gross volumes of geologic features throughout this report are based on the seismic facies (attenuation and geometry) signature and are calculated for the entire outlined deposit and do not include overburden.

Pleistocene Channel Belts 3-5 are located on the central portion of the study area, seaward and under Heald Bank. This channel belt system shows variable geometry and occasional cross-cutting by incisional drainages feeding into Sabine Valley and are characterized by basal erosional unconformities overlain by steeply dipping clinoforms that grade into U-shaped channel forms at the edge of the belt deposit. The likely sandier portion of the system is roughly 20-50 ft (6.1-15.24 m) thick and between 0-20 ft (0-6.1 m) of overburden with a potential gross volume of 78 MCY, 67 MCY, and 107 MCY for Channel Belts 3, 4, and 5, respectively.

The two identified terraces are located to the north and south of the Holocene Sabine Incised Valley and are characterized by a thick unit with steeply dipping clinoforms and 0 and 15 ft (4.6 m) of overburden. The Sabine North Terrace has a gross estimated volume of 472 MCY and the Sabine South Terrace has an estimated potential gross volume of 1,240 MCY.

The Sabine Incised Valley system is a major stratigraphic unit across the entire study area. The edges of the system are well defined within this investigation; however, the actual base of the valley is not observed due to an amalgamated sand-rich fluvial unit formed during the lowstand and early stage of the transgression that has a very high-amplitude acoustic return and allows for little penetration past it. Therefore, this investigation was unable to estimate a gross volume of the Incised Valley system; however, it is expected to be quite large and is buried under a roughly 30-40 ft (6.1-15.24 m) thick estuarine unit, with some smaller areas being closer to the seafloor. The thick estuarine unit that sequesters the Sabine Incised Valley system sediments is considered overburden. Due to the thickness of the estuarine overburden section, basal valley fluvial sediments are not considered as a potential sand source at this time.

As part of the seismic data processing and interpretation, APTIM was able to delineate Sabine and Heald banks, several smaller shoals in their vicinity, and a broader surficial sedimentary unit that appears related to the previously identified banks and has a similar seismic facies. This uppermost surficial unit overlies the transgressive ravinement and is upwardly bound by the modern seafloor. In this report it is referred to as Seismic Unit Q1 (Quaternary 1), and further details of its identification, mapping, and potential composition are provided in Section 5.4.1. It is estimated, from this mapping effort, that this surficial seismic unit contains a total gross sediment volume of approximately (~) 5.9 billion cubic yards (BCY), but specific composition and sand content will require further geological investigation. Furthermore, smaller localized potential sand deposits in the area were also identified. However, due to the reconnaissance level line spacing, these potential deposits are not traceable across multiple lines and require additional data coverage to be fully delineated. These smaller localized features are normally isolated channels or sediment pockets which are indicative of sand or mixed sediments and are observed throughout the study area and many have a high-potential for sand-bearing deposits, but are not quantified as they are not correlatable across multiple lines. The lower fluvial section of the Sabine and Trinity Valley fill, despite potentially being composed of a large volume of sandy material (Anderson 2007) is overlain by a thick (40-60 ft) estuarine overburden section that impede characterization and economic accessibility, and so is not considered in this report as a viable economic sand resource at this time. This

report does provide the most detailed map of its extent within the OCS, however, and we include it for its importance in understanding recent shelf geologic evolution.

The features identified in this investigation are not exhaustive or inclusive of all potential sand-bearing stratigraphy within the region, but rather represent systems that are sufficiently regionally extensive and contiguous to be confidently interpreted across the 1-mile (mi) x 5-mile (1.6 x 8 kilometers [km]) spaced survey grid. The major sub-surface geologic systems observed represent a cumulative gross volume of ~2.1 BCY without overburden of varying sediment lithologies while the overlying surficial Seismic Unit Q1 represents a total gross volume of ~5.9 BCY. The precise composition of these deposits is likely highly variable and requires more detailed geological investigation.

2 Introduction

The Texas General Land Office (GLO) awarded Aptim Environmental & Infrastructure, LLC (APTIM), along with team members Coastal Protection Engineering LLC (CPE-LLC) and The Water Institute of the Gulf (TWI), to conduct geophysical surveys across Sabine and Heald Banks as well as what used to be Shepard Bank (**Figure 1**). The goal of the project was to primarily assist in a multi-agency response to categorize sediment resources offshore for development of policies and inventories for coastal restoration, with the purpose of better maintaining ports and navigation channels (dredging), determining appropriate sediment disposal sites, and determining the location of sediment deposits for their restoration efforts intended to mitigate beach erosion caused by storms and currents. A secondary goal of the project was to provide the General Land Office (GLO) with a dataset that correlated recent state-side geophysical data (August 19 through October 23, 2020) (**Figure 1**) with Outer Continental Shelf (OCS) data for a more comprehensive understanding and mapping of geologic features in the area.

In order to efficiently coordinate this investigation, the GLO, Bureau of Ocean Energy Management (BOEM), and APTIM developed a two-phase project approach. The first phase consisted of the desktop study, previously submitted, followed by the second phase reconnaissance-level geophysical data collection (chirp sub-bottom, sidescan sonar, magnetometer, and single-beam fathometer) and data processing and interpretation in order to delineate potential sand deposits along the OCS and identify proposed vibrocore sites. Additionally, the project included a Pipeline Decommissioning Impacts on Significant Sediment Resource Areas (SSRA) Block's assessment (**Appendix T**), as well as an Environmental Mitigation Summary report (**Appendix U**).

The Task 1 desktop study consisted of historical data compilation followed by a review of the data to provide a comprehensive understanding of existing data coverage and geological framework. APTIM compiled bathymetric and sub-bottom data as well as geotechnical information (vibrocores and grab samples) and analyzed previously delineated sediment deposits. These data were correlated with scientific reports to assist in the identification of potential sand resources. Task 1 resulted in the development of a survey plan. Information on the compiled data, resources used, and data types of Task 1 that support the survey plan are described within the Desktop Study, previously submitted and attached in **Appendix A**. After the desktop study was completed, APTIM transitioned into the Task 2 geophysical survey data collection and processing portion of the project. APTIM proposed to collect up to 1,050 nautical miles (nm) of geophysical data.

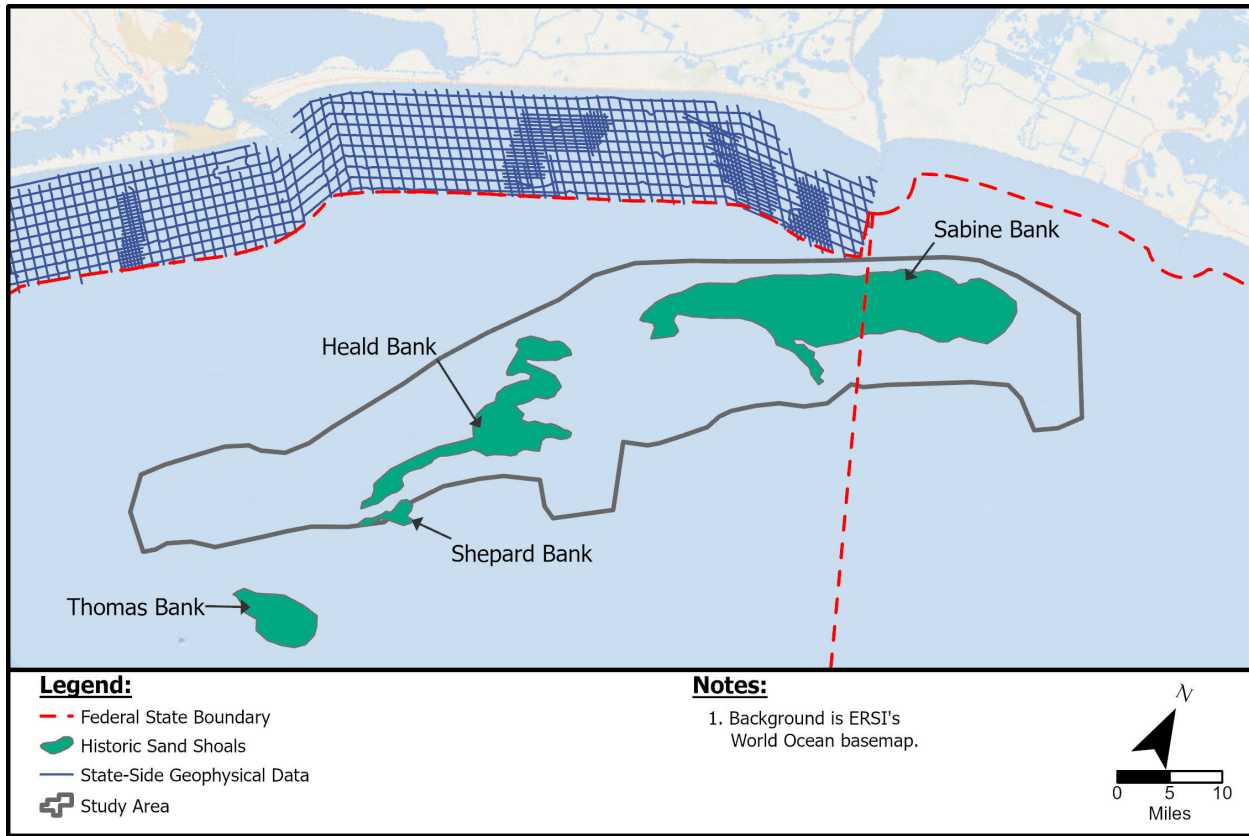


Figure 1. Texas GLO OCS Study Area.

Historic sand shoals digitized from Rodriguez et al. (1999).

Between October 23, 2020 and November 14, 2020, APTIM collected a total of 1,133 nm of geophysical data offshore western Louisiana and eastern Texas along Sabine, Heald, and adjacent sand banks. Upon completion of the geophysical data collection, APTIM began processing and interpreting the data. Sidescan sonar and magnetometer data were reviewed for any potential hazards and areas to avoid and to delineate any characterizations of the seafloor. The seismic sub-bottom data were used to delineate the shoal deposits within the study area and estimate a potential gross volume of sediments that could be available for different coastal restoration efforts. Moreover, the seismic data were reviewed for any features/structures that could provide additional information on the overall geologic framework of the area and be compared to the information gathered during the desktop study and potentially assist with revising some of the previous conclusions about the framework of the area. Lastly, APTIM and TWI were tasked with analyzing the data to identify areas that could benefit from geotechnical data collection/ground-truthing to further characterize the sediment deposit type.

3 Task 1 Historic Data Review/Survey Plan Development

3.1 Geologic Framework

Below is a description of the formation and framework geology of the Gulf of Mexico (GOM) Basin as well as the Texas continental shelf with relevance to coastal evolution and sediment resources.

3.1.1 Gulf Basin Evolution Early Gulf of Mexico Formation

The GOM Basin is the product of crustal extension, rifting, and seafloor spreading during the breakup of the supercontinent Pangea as the North American Plate separated from the South American and African Plates (Salvador 1991; Buffler et al. 1994; Galloway 2008). The basin is filled with up to 9.5-mile (mi) (15 kilometers [km])-thick sedimentary deposits that range from Jurassic to recent ages with some older Triassic sedimentary rocks preserved locally in graben structures associated with Triassic rifting (Salvador 1991). Extension continued through the early Jurassic when flooding of the basin from the Pacific Ocean and subsequent evaporation of sea water resulted in deposition of thick evaporate deposits, primarily the Jurassic Louann Salt (Burke 1975; Galloway 2008). Widespread salt deposition would turn out to be a defining event in Gulf basin geologic evolution that has influenced surface morphology, brittle deformation, development of shelf stratigraphic sequences, and hydrocarbon production (Galloway 2008). Subsequent to salt deposition, a later phase of seafloor spreading continued opening the basin to develop basaltic oceanic crust that underlies much of the deepwater GOM (Nguyen and Mann 2016). Early Cretaceous carbonate reefs and platforms rimmed the basin and defined its modern extent; however, by the late Cretaceous the area of the North American continent draining into the Gulf greatly increased as did attendant terrigenous deposition, inhibiting further carbonate development. This continental scale drainage reorganization led to burial of carbonates by thick clastic (sandstones and mudstones) deposits that persisted from late Cretaceous through Quaternary time producing the broad continental shelf and slope of the northern Gulf (**Figure 2**; Galloway 2008).

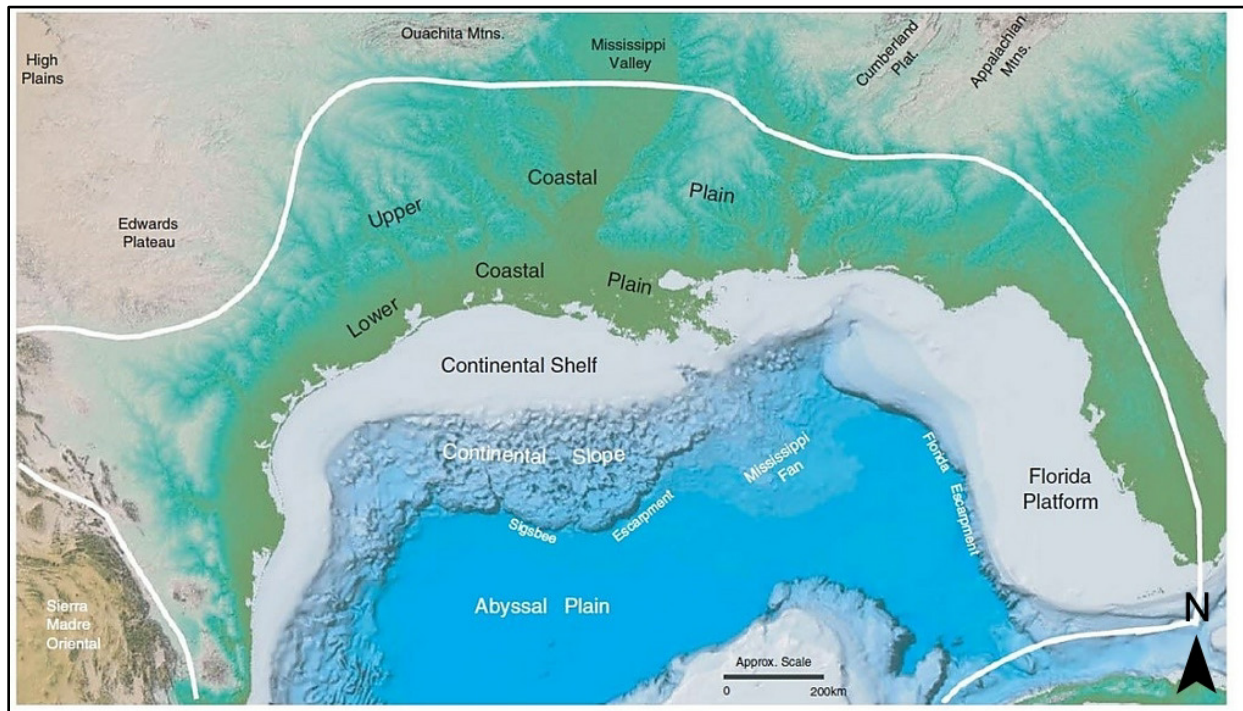


Figure 2. Gulf Basin physiology.

Note the broad continental shelf and Sigsbee Escarpment along the base of the continental slope that is the result of basinward salt extrusion. From Galloway (2008).

Loading of the Louann salt resulted in extrusion of salt vertically upward through overlying sections in the form of salt diapirs and tongues, as well as lateral sheet formation (Diegel et al. 1995). Salt-involved deformation influenced Cenozoic structural evolution of the Gulf as continued loading by younger deposits forced salt motion and attendant deformation of the overlying strata. This process results in areas of uplift where salt migrates vertically and laterally, and subsidence occurs over regions of salt withdrawal (Diegel et al. 1995). The accommodation for sediment deposition created by salt evacuation facilitates a feedback where sediment loading forces extrusion and continued subsidence facilitates further loading and extrusion. The influence of salt along the Gulf of Mexico coast and near-shore is readily apparent in the modern landscape. High Island (**Figure 3**) and at least three (3) offshore salt diapirs have influenced recent geomorphology and seafloor sedimentary character locally.



Figure 3. Satellite imagery of Texas coast and aerial image of High Island Salt Dome. Location of High Island Salt Dome outlined (left, NASA Earth Observatory). Aerial image of High Island Salt Dome during floodwaters of Hurricane Ike (right, Houston Chronicle).

3.1.2 Quaternary Geology

The Quaternary coastal plain of east Texas and offshore inner continental shelf consists of fluvial deposits and coastal deposits associated with sea level fluctuations and basin subsidence. Stratigraphically, this has resulted in a series of unconformity-bounded, seaward dipping clastic wedges that are Pliocene to Late Pleistocene age producing a coastal plain topography characterized by coast-parallel terraces due to variations in erosional resistance (Fisher et al. 1972 and 1973; Morton and Gibeaut 1993; Young et al. 2012; Heinrich et al. 2020). Each of these wedge units are characterized by terrestrial deposits that grade basinward into coastal and shallow marine deposits (**Figure 4**). Of interest to this discussion is the most recent Pleistocene unit, the Beaumont Formation that comprises a complex of Pleistocene depositional units (**Figure 5**). The surface of the Beaumont Formation is often characterized by oxidized sands and stiff clays (paleo-soil horizons) due to subaerial exposure during the most recent sea level lowstand. In most areas of the lower coastal plain, the Beaumont Formation forms the land surface where Holocene coastal and alluvial deposits are absent. Detailed discussion of the Quaternary geology of the upper Texas coastal plain can be found in Young et al. (2012) and the Environmental Geologic Atlas of the Texas Coastal Zone series produced by the Texas Bureau of Economic Geology (McGowen et al. 1976; Fisher et al. 1972 and 1973).

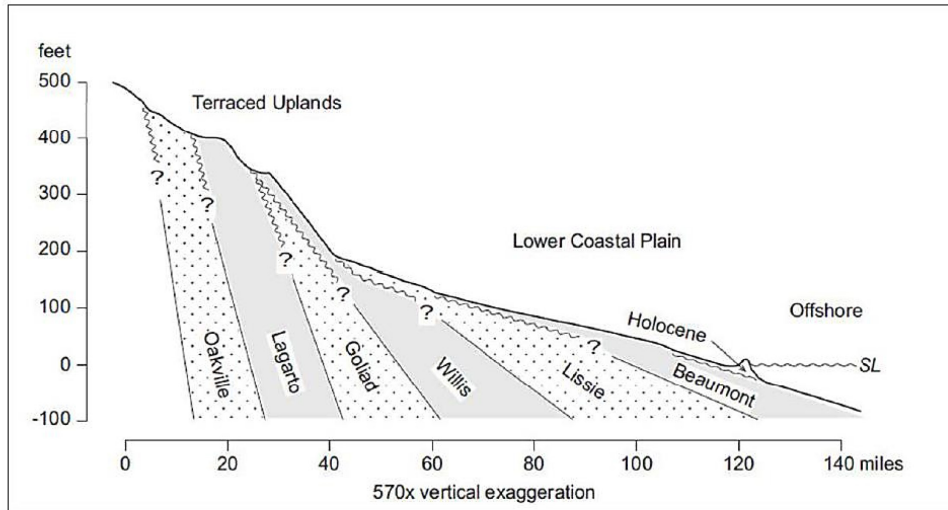


Figure 4. Idealized dip cross section for the upper Texas coastal plain.
 From Young et al. (2012).

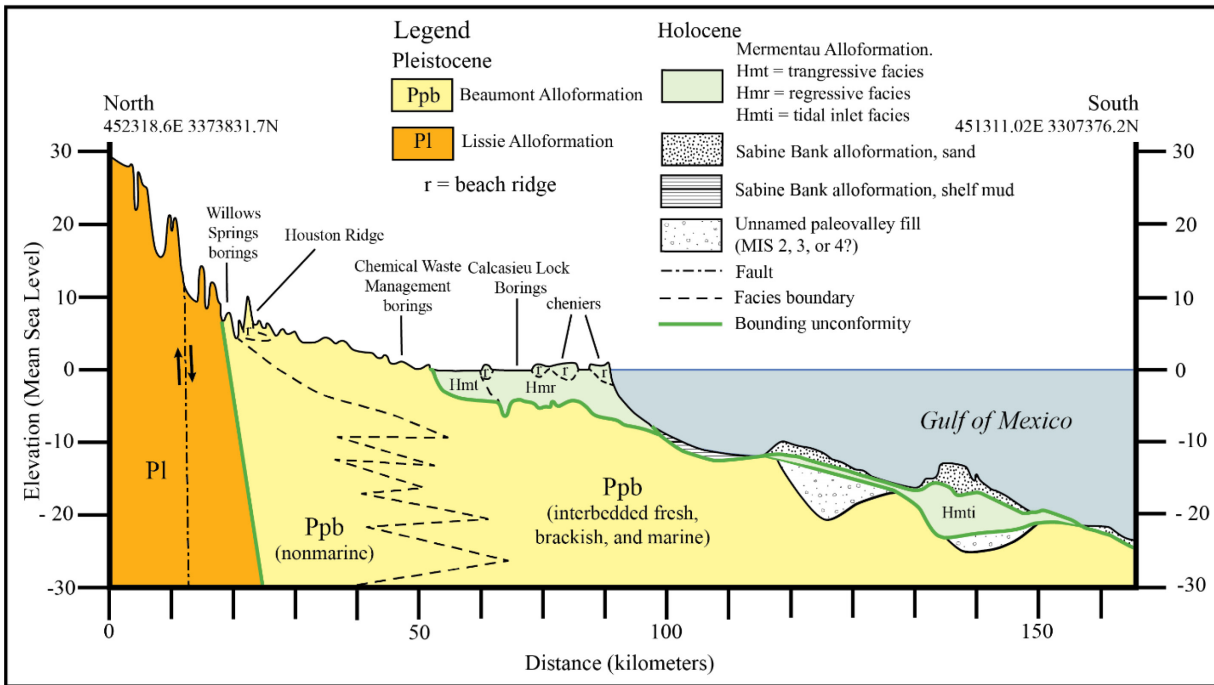


Figure 5. Generalized dip cross-section for the eastern Texas-west Louisiana coastal plain Quaternary deposits.
 From Heinrich et al. (2020).

3.1.3 Late Quaternary Sea Level Changes (120,000 years ago to present)

Coastal and fluvial response to sea level changes in the study area has dominated the geomorphic evolution (deposition and erosion of sediments) of the study area since the mid-Pleistocene ~900,000 years ago. These changes in sea level are the results of periodic growth of continental ice sheets that reduce the volume of seawater and lower sea levels on the order of hundreds of feet and result in Gulf of Mexico shorelines migrating basinward to coincide with the shelf edge during maximum lowstands of sea level (the stable, shoreline low points of a falling stage sea level). Conversely, melting glacial ice results in sea level rise, a term referred to as *transgression*, resulting in sea level highstands, or stable shoreline high points of a rising stage sea level. For the purpose of this discussion relative to sediment resources within the study area, an understanding of the most recent glacio-eustatic cycle (beginning ~120,000 years ago) is important (**Figure 6**). During this time sea level was ~ 30 feet (ft) (9.1 meters [m]) above present levels (Simms et al. 2013), and the shoreline correlated with the preserved Ingleside Shoreline that extends from eastern Louisiana to Corpus Christi, Texas. The Ingleside Shoreline represents the highstand barrier island shoreline dating to approximately 120,000 years ago (Price 1933; Otvos and Howat 1996; Simms et al. 2013). After this highstand, sea level began to fall until about 70,000 years ago when it was ~ 250 ft (76.2 m below present levels). This was followed by a warming period where sea level rose to approximately 50 ft (15.2 m) below present and then fell to about 400 ft (121.9 m) below present by 22,000 years ago with the shoreline located at the shelf edge (Anderson et al. 2004; Anderson et al. 2015). This most recent lowstand of sea level persisted from approximately 22,000 to 17,000 years ago (Anderson et al. 2004). Between 17,000 and 4,000 years ago sea level rose ~400 ft (121.9 m), to its present position along the modern coastline (Anderson et al. 2015).

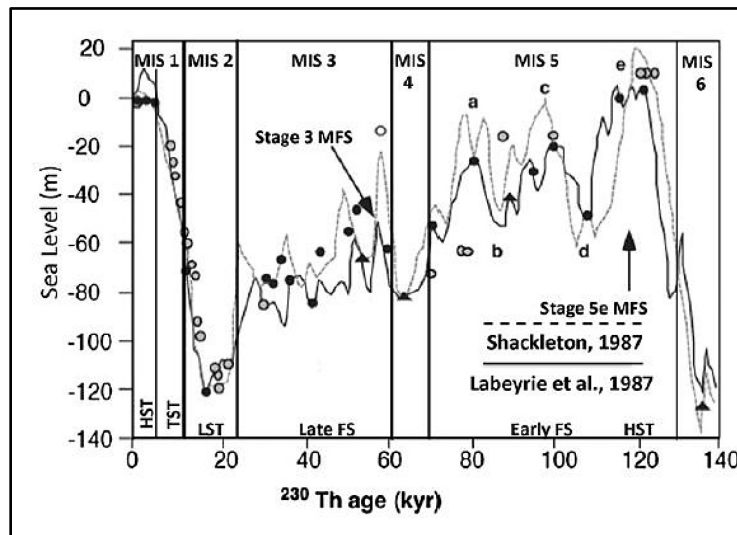


Figure 6. Sea level variability over the last 140,000 years.

Note the present and 120,000 yr highstands (HS), falling stage (FS) between 120,000 and 22,000 years ago, the lowstand (LST) from 22,000 to 17,000, and transgression (TST) from 17,000 to 4,000 years ago. From Anderson et al. (2015).

The following sections discuss depositional and erosional response within the study area to changes in sea level and the development of shelf sand deposits. The discussion is divided into falling stage and lowstand, transgression (sea level rise), and highstand deposits.

3.1.3.1 Falling Stage and Lowstand (~120,000-17,000 years ago)

During the falling stage of sea level ~120,000–22,000 years ago, river channels began vertically incising down into pre-existing shelf deposits (e.g., Beaumont Formation and older); however, development of deep incised valleys did not dominate until late falling stage and into the lowstand (Anderson et al. 2015). Falling stage deltas formed and migrated basinward producing a series of large deltaic deposits that are elongate in dip direction (in contrast to the more lobate transgressive deltas discussed below; **Figure 7**; Anderson et al. 2015). Limited accommodation space for sediment deposition on the shelf coupled with extended subaerial exposure in the weathering environment during lowstand and subsequent wave ravinement (erosion) during transgression led to the delta tops and sandy mouth bars being eroded (Morton and Suter 1996; Anderson et al. 2015).

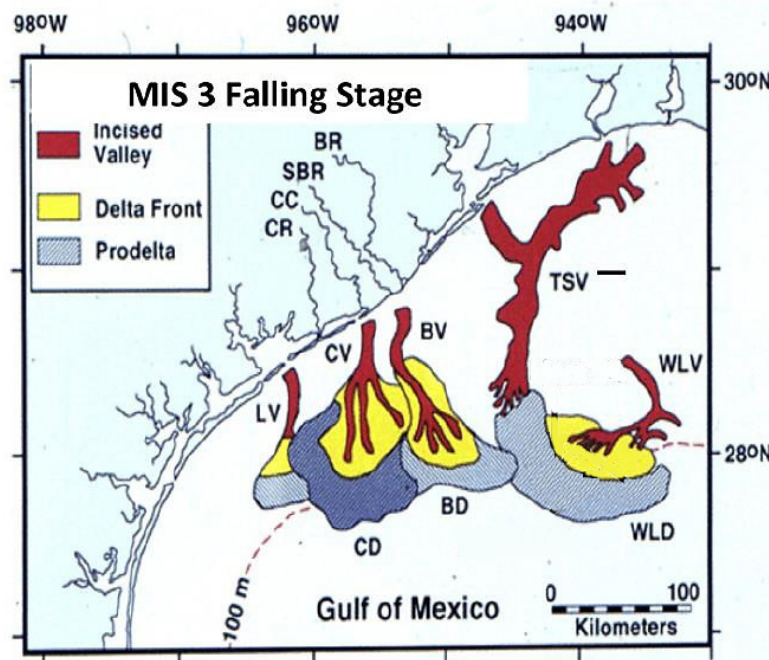


Figure 7. Falling stage fluvial deposits on the middle to upper Texas shelf.

Note that these deposits are not fully preserved due to subsequent erosion during transgression. TSV stands for the merged Trinity-Sabine Valley. Modified from Anderson et al. (2015).

During sea level lowstands, large rivers incise valleys deep into the exposed continental shelf in order to reach a lowered Gulf level. These lowstand shelf valleys result in sediment bypassing of the adjacent, topographically high interfluves, and develop shelf-edge deltas (Anderson et al. 2015). The prominent

incised valleys in the study area are associated with the Trinity and Sabine Rivers that, during the most recent lowstand, extended from their present locations of Trinity Bay and Sabine Lake across the shelf and to the shelf edge (Thomas and Anderson 1994; Swartz 2019). Midway on the shelf there is a confluence where the Trinity and Sabine incised valleys (referred to as the Trinity Sabine Valley [TSV]) merge and extend seaward as a single larger valley (**Figure 7**). During this time of maximum sea level lowstand (22,000 to 17,000 years ago), exposure of the entire continental shelf resulted in a regionally correlative erosional surface referred to as the Late Wisconsinan Unconformity (Anderson et al. 2015; Heinrich et al. 2020). Incised valley depths relative to the adjacent interfluvial surface ranged from 100-130 ft (30.5-39.6 m) deep; however, due to infilling during sea level rise the valley is completely full and there is no bathymetric expression on the modern seafloor (Thomas and Anderson 1994; Swartz 2019).

During sea level fall and valley incision, floodplains that flank the stream channels become abandoned at higher elevations and a new floodplain forms deeper in the valley. This results in the formation of *fluvial terraces* (**Figure 8** and **Figure 9**). If lateral channel migration does not erode terrace deposits, they can be preserved as part of the incised valley fill (see discussion below on transgression and incised valley fills). Floodplain development in meandering streams is often a combination of lateral accretion of sandy point bar and channel deposits followed by vertical accretion of fine-grained material during floods (**Figure 8**). However, some portions of the floodplain are dominated by vertical accretion. Therefore, the terraces preserved within incised valleys are potentially sand-rich deposits with interbedded clays (Swartz 2019). These terrace deposits comprise potential sand resources that may have significantly less overburden than the thick fluvial sands discussed below that fill the lower portion (**Figure 10**) of the valley during sea level rise (Anderson 2007; Thomas and Anderson 1994; Swartz 2019).

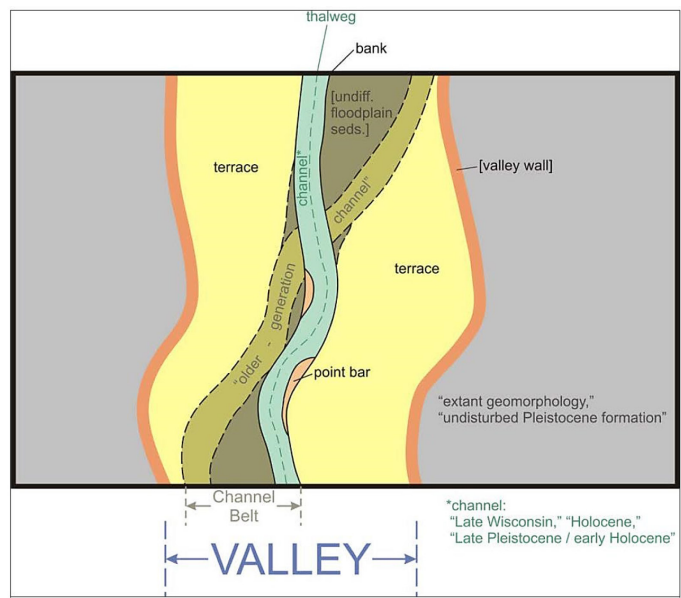


Figure 8. Plan view conceptual model of a valley fill.

View shows multiple generations of channel belts, active point bars, floodplains, and fluvial terraces (abandoned, perched floodplains). From Heinrich et al. (2020).

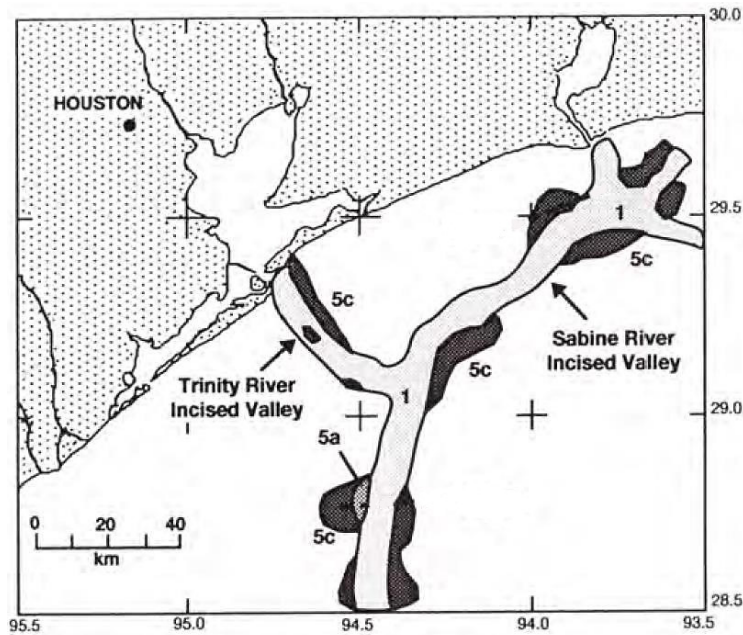


Figure 9. Map Showing the Trinity/Sabine Incised valley and Terrace Deposits.
 Interpreted from High Resolution Single Channel Seismic Data. Modified from Thomas and Anderson (1994).

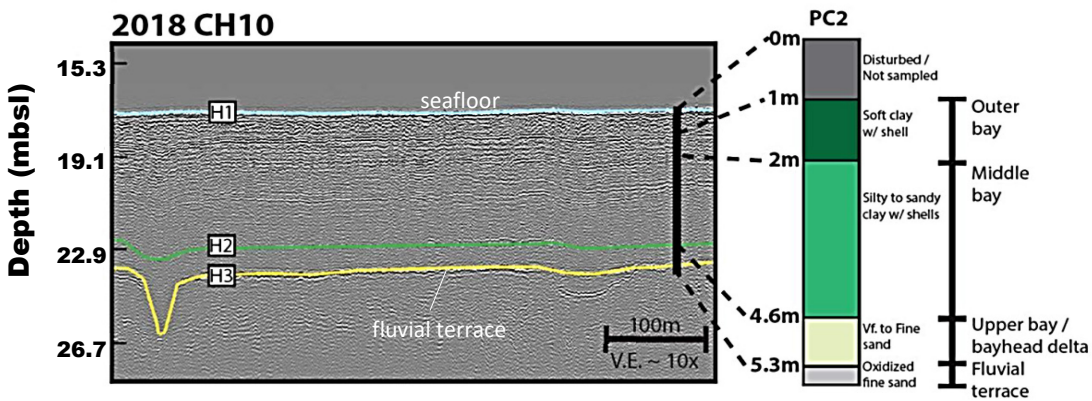


Figure 10. Interpreted Chirp Sonar Profile Over the Trinity incised valley and lithologic description from a platform geotechnical boring.

Note the interpreted fluvial terrace surface at 4.6 m depth below the seafloor that contains sands in the boring. From Swartz (2019).

As previously mentioned, development of incised valleys results in sediment delivered from continental drainage being transported to the shelf edge, starving the vast interfluvial areas of alluvium. However, recent works have demonstrated the presence of smaller, high gradient paleo gully and stream networks

draining interfluvies into adjacent valleys (Heinrich et al. 2020). The high gradient setting suggests and limited geophysical and platform boring data indicate that these paleo drainage features may potentially have a coarse basal lag deposit, but overall be infilled by fine-grained estuarine and bay material (J. Swartz personal communication).

3.1.3.2 Transgression (~17,000–4,000 years ago)

During the period from ~17,000–10,000 years ago rapid sea level rise (~4.2 millimeters per year [mm/yr]; **Figure 11**) did not facilitate extensive transgressive deposition on the shelf (Anderson et al. 2015). After that time, sea level slowed resulting in development and preservation of deposits—relevant to this sand resources discussion—comprising incised valley fills and sand banks on the inner shelf that potentially represent reworked barrier island deposits or modern marine sand shoals (Morton and Price 1987; Rodriguez et al. 2004).

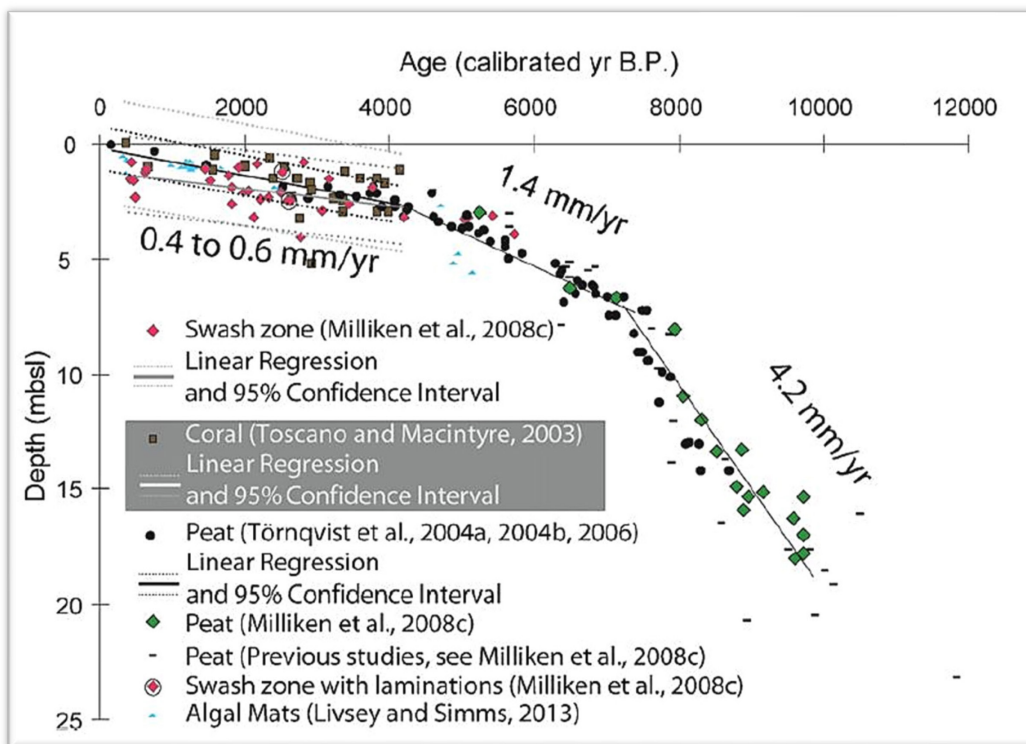


Figure 11. Holocene (past ~10,000 years) sea level curve.
From Anderson et al. (2015).

3.1.3.2.1 Incised Valley Fills

Within the East Texas study area, the Trinity/Sabine and Brazos fluvial systems had contrasting fluvial infilling that has been termed underfilled and overfilled, respectively (**Figure 12**; Simms et al. 2006,

Anderson et al. 2015). The underfilled Trinity/Sabine did not completely fill with fluvial deposits during transgression, and instead the broad valley became a site of estuarine development and deposition of muddy estuarine deposits and somewhat sandier bayhead delta deposits overlying the fluvial section (**Figure 13**; Morton and Price 1987; Thomas and Anderson 1994; Swartz 2019). Conversely, the Brazos (which flanks the western boundary of the study area) completely infilled with fluvial deposits (mostly muddy floodplain deposits with isolated channel sands; Abdulah 1995; Abdulah et al. 2004; Taha and Anderson 2008). The Trinity/Sabine incised valley fill is characterized with vertical sequences that fine upward from basal channel sands and amalgamated point bar deposits (in contrast to the discrete channel sands observed in the Brazos incised valley) into bayhead deltas, estuarine, and tidal-associated deposits that backstep landward tracking with the transgressive shoreline position (**Figure 13** and **Figure 14**; Thomas and Anderson 1994; Swartz 2019). As discussed below, the lower fluvial section of the Trinity Valley fill comprises the largest volume of beach quality sand identified on the Texas shelf to date (Anderson 2007); however, the thick, muddy overburden and depth to this sandy unit have impeded development as a viable sand resource.

J.B. Anderson et al. / Earth-Science Reviews xxx (2015) xxx-xxxx

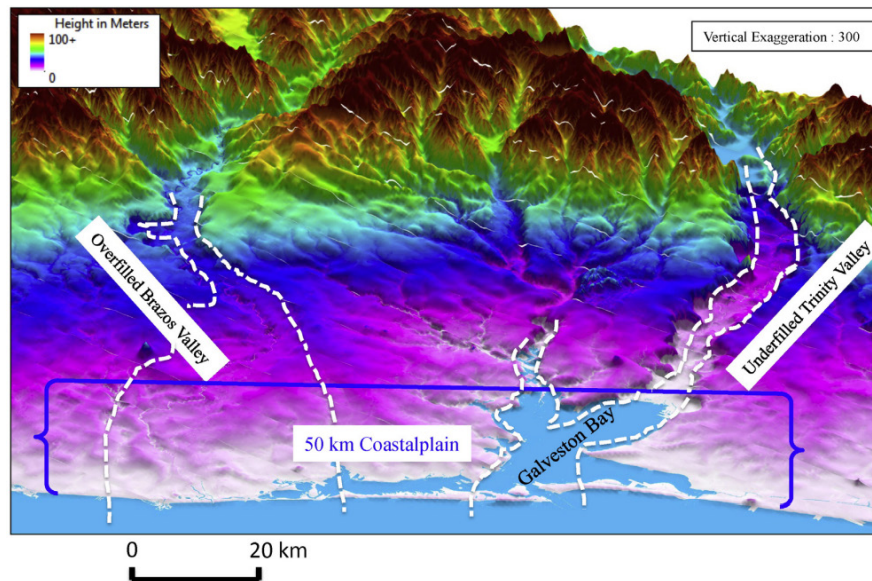


Figure 12. Overfilled versus underfilled fluvial systems.

The Holocene and Modern Brazos River has completely filled any previous erosional valley form and built a broad avulsive alluvial plain. The Modern Trinity River remains confined within the erosional valley created during the Pleistocene and Holocene. From Anderson et al. (2015).

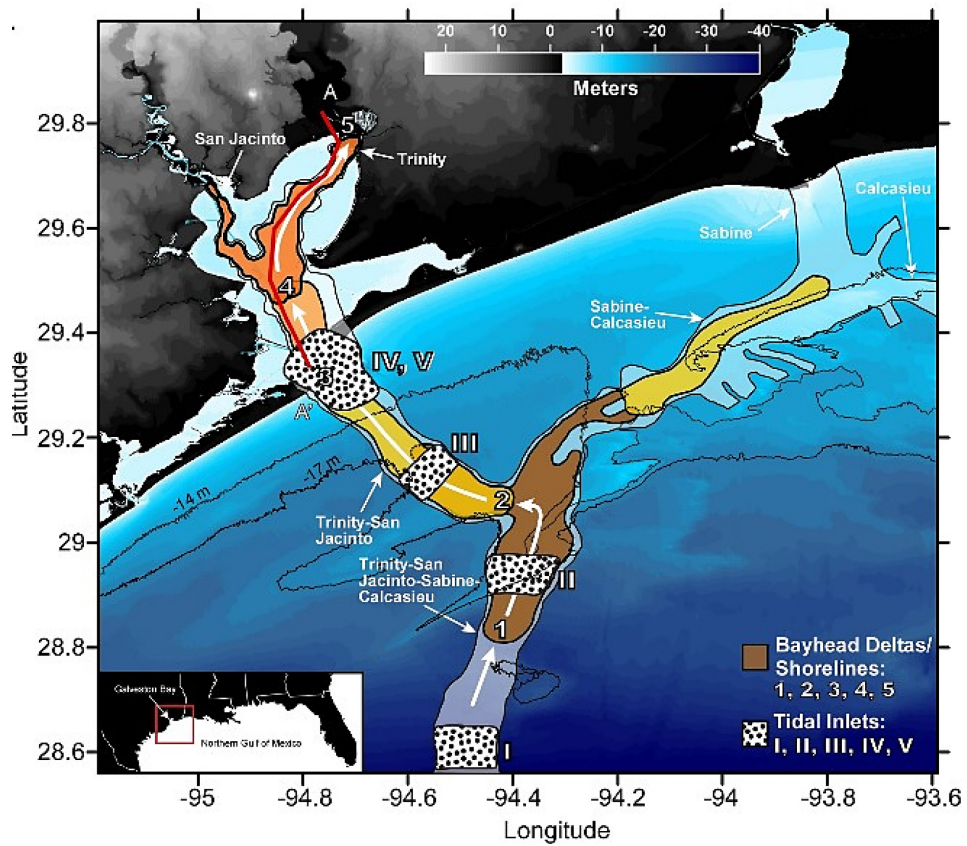


Figure 13. Time-transgressive paleogeographic reconstruction of infilling of the upper (non-fluvial) section of the Trinity/Sabine Incised valley.
 Bayhead deltas and tidal inlet/deltas are displayed as these “backstep” landward during sea level rise.
 From Anderson et al. (2015).

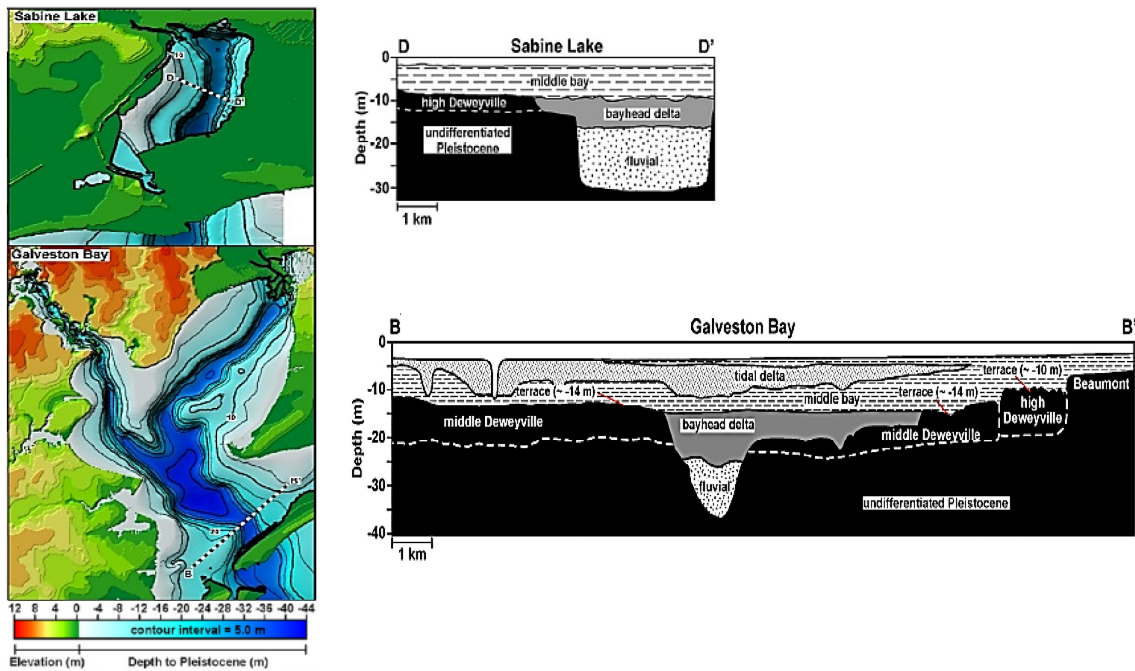


Figure 14. Structure contour maps of Galveston Bay and Sabine Lake (left).

Sabine Lake (left) showing depth to the top of the Pleistocene (Late Wisconsinan Unconformity surface) and representative cross sections (right) showing the valley infill deposits underlying the modern bays. Note that the offshore equivalents of these valley fill deposits do not contain significant tidal delta sands because of removal during transgressive ravinement. Also note the fluvial terraces labeled "Deweyville". From Anderson et al. (2015).

Incised valley fills of the Trinity/Sabine system have been demonstrated to contain large volumes of beach quality sand (Thomas et al. 1994; Morton et al. 1996; Anderson 2007; Anderson et al. 2015; Swartz 2019). The thick (average ~25 ft [7.6 m]) sand units comprising the fluvial infill of these valleys are the largest potential sand resource for the Upper Texas Coast with volumes in excess of 1 billion cubic yards (BCY); however, these deposits are overlain by ~50 ft (15.2 m) thick muddy estuarine deposits (**Figure 15**, **Figure 16**, and **Figure 17**; Thomas and Anderson 1994; Anderson 2007; Anderson et al. 2014; Swartz 2019) that would require significant operational and regulatory creativity to be considered economically recoverable.

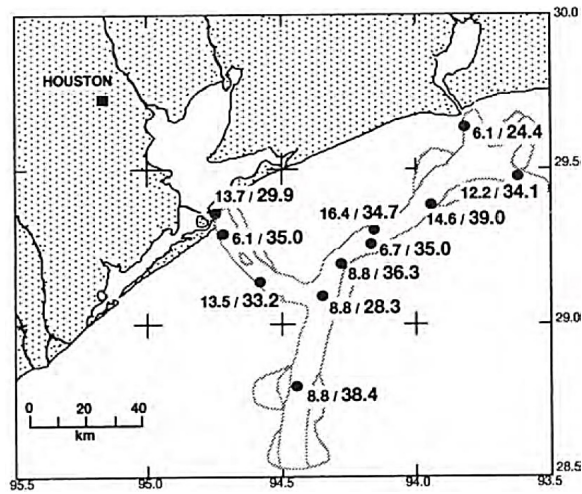


Figure 15. Thickness (in meters) of sandy fluvial deposits.

Thickness (labeled with small type preceding slash) and depth (in meters) to base of fluvial section (Late Wisconsinan Unconformity) below the seafloor for the Trinity/Sabine incised valley fill. From Thomas and Anderson (1994).

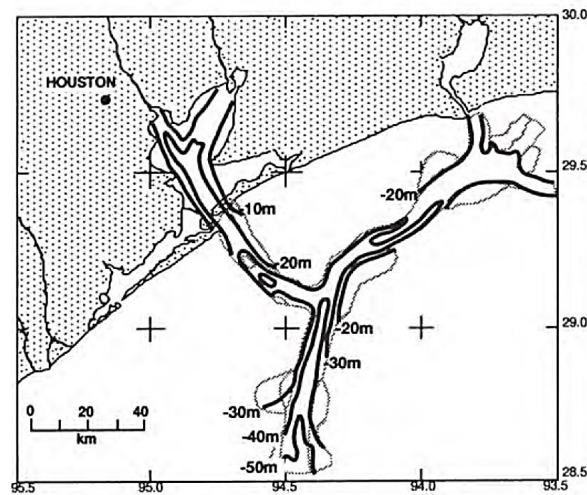


Figure 16. Trinity/Sabine incised valley isopach map.

Map shows thickness of muddy overburden above sandy transgressive fluvial deposits in the Trinity/Sabine incised valley. Note that values are expressed as depth below seafloor in meters to the top of the fluvial section. Note that fluvial terrace deposits with potential sand reserves (Figures 10 and 11) are not included in the isopach. From Thomas and Anderson (1994).

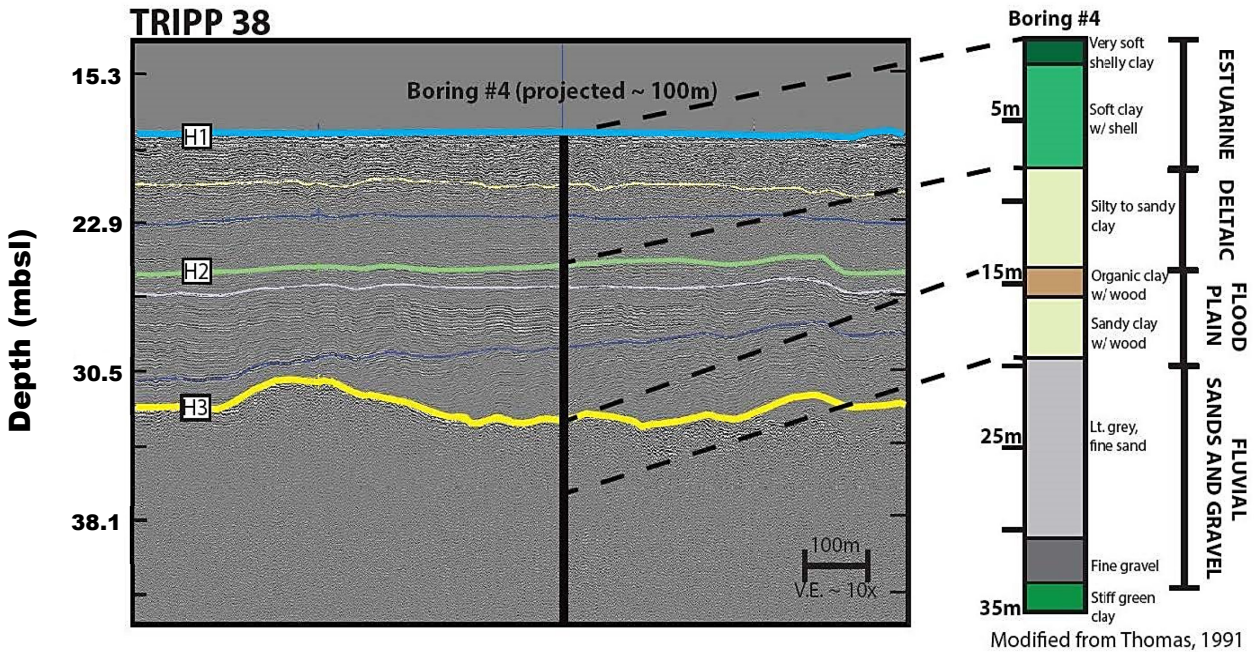


Figure 17. Interpreted chirp sonar profile with geotechnical boring log used to validate interpretations.

Note the thick (30 ft [9.1 m]) fluvial sands that are first encountered approximately 60 ft (18.3 m) below the seafloor. Water depth at this location is approximately 55 ft (16.8 m). From Swartz (2019).

3.1.4 Alluvial Plains

Unlike the incised valley systems that contain multiple fluvial channels bounded by a valley unconformity defining the lateral extents of the fluvial system during the lowstand and subsequent transgression, along the East Texas coast there also exist alluvial plain systems such as the modern Colorado and Brazos rivers (Blum and Price 1998). These fluvial systems built broad reaches of the lower Texas coast through the process of avulsion where on a timescale of 100s to 1000s of years the river reaches a critical super-elevation relative to the floodplain, leading to avulsion and relocation of the main river channel (Mohrig et al. 2000). Systems such as the Colorado and Brazos have avulsed dozens of times over the Quaternary and in particular during the Holocene Transgression (Blum and Price 1998), leading to multiple overlapping alluvial plains composed of discrete channel belts (**Figure 18**).

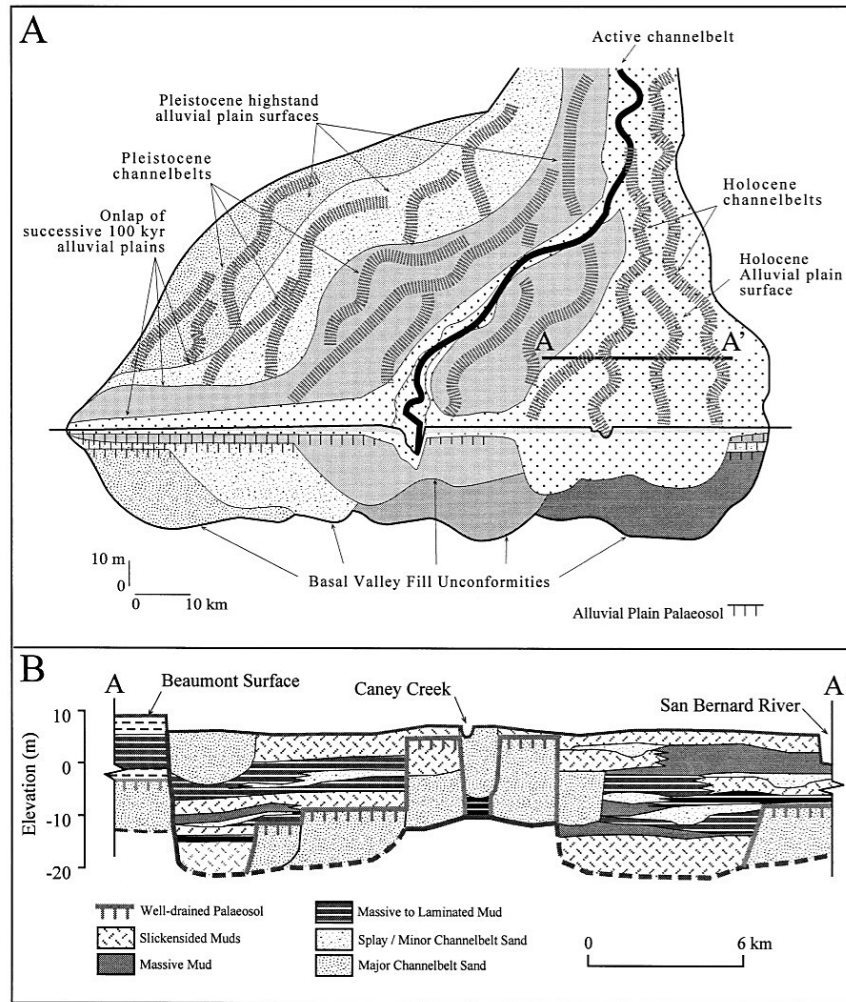


Figure 18. Oblique view conceptual model (A) and generalized cross section of the Quaternary alluvial plains of the Colorado River, Texas (B).

Note the presence of numerous adjacent overlapping channel belts exposed sub-aerially as well as thick successions of fluvial sediments within the subsurface. Figure modified from Blum and Price (1998).

The development of alluvial plains along the Texas coast has been interpreted to have occurred throughout the Quaternary during both low-stand and transgressive intervals depending on sediment supply and antecedent topography (Blum and Törnqvist 2000). While most well studied along the modern coastal plain where these fluvial channel belts comprise the Pleistocene Beaumont, Lissie formations, and modern Holocene alluvium, prior work also suggests that they might comprise portions of the inner continental shelf stratigraphy offshore of modern rivers such as the Brazos and Colorado (Anderson et al. 2015). Despite the prevalence of these features and their importance in constructing the modern Texas coastal plain there has been little work aimed specifically at understanding their equivalent stratigraphy

offshore, despite early studies noting the presence of subsurface fluvial channel forms located outside the main interpreted incised valley systems (Winker 1979).

An investigation of potential sand-bearing stratigraphy within Texas state waters adjacent to the study area of this report found a number of potential sediment resource units that have been interpreted to be an alluvial plain constructed from fluvial avulsions and deposits during the Holocene (**Figure 19**, APTIM 2021; Anderson et al. 2015). This interpreted alluvial plain feature covers a broad 7 x 7 mile) region with a variable 20-30 ft thickness, geometries analogous to the interpreted Holocene Brazos plain located along the modern terrestrial coastal plain (Anderson et al. 2016).

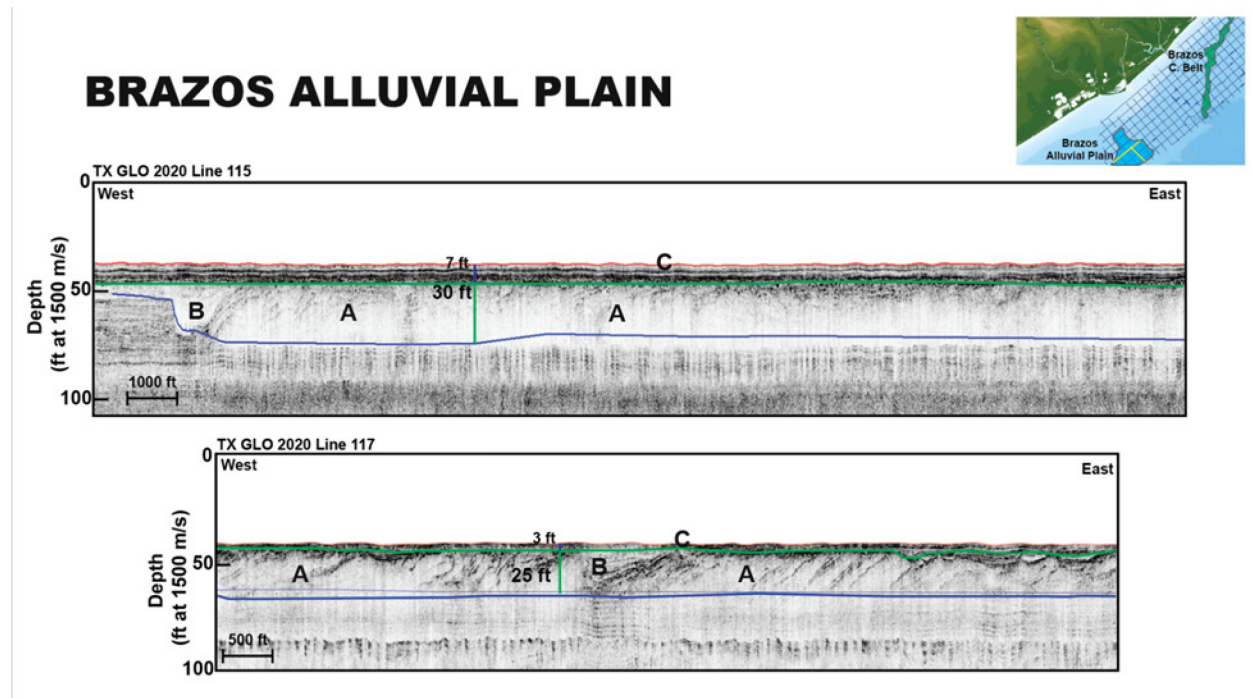


Figure 19. Example sub-bottom profile sections across the offshore preserved Brazos Alluvial Plain.

The blue horizon marks the basal unconformity separated layered Beaumont stratigraphy from the above dipping clinoforms and variable transparent/chaotic seismic reflectors. The green horizon is the top of the dipping reflector package. From APTIM (2021).

3.1.5 Paleo-Channel Fills

In contrast to incised valley fills that contain multiple channel belts, discrete near-surface channel fills have been observed throughout the study area representing stream systems that incised into interfluvial areas during lowstand or were preserved basal channel fills from previous highstand or falling stage streams. An analysis that mosaiced over 300 shallow hazards surveys conducted for oil and gas development offshore western Louisiana and east Texas (Heinrich et al. 2020) demonstrated the ubiquity of these

features in the study area (**Figure 20**). Dellapenna et al. (2010) collected sediment cores in some of these features that had been identified from geophysical data, and sand content was minimal or below the depth of core penetration. However, as demonstrated by Coastal Planning & Engineering, Inc. (APTIM-CPE) (2001) in support of Holly Beach, Louisiana Restoration (immediately adjacent to the study area), high density geophysical and geological data can identify the elusive channel sands that occur within sinuous ribbons of muddy sediment within the fluvial channel belt (**Figure 21** and **Figure 22**; Heinrich et al. 2020).

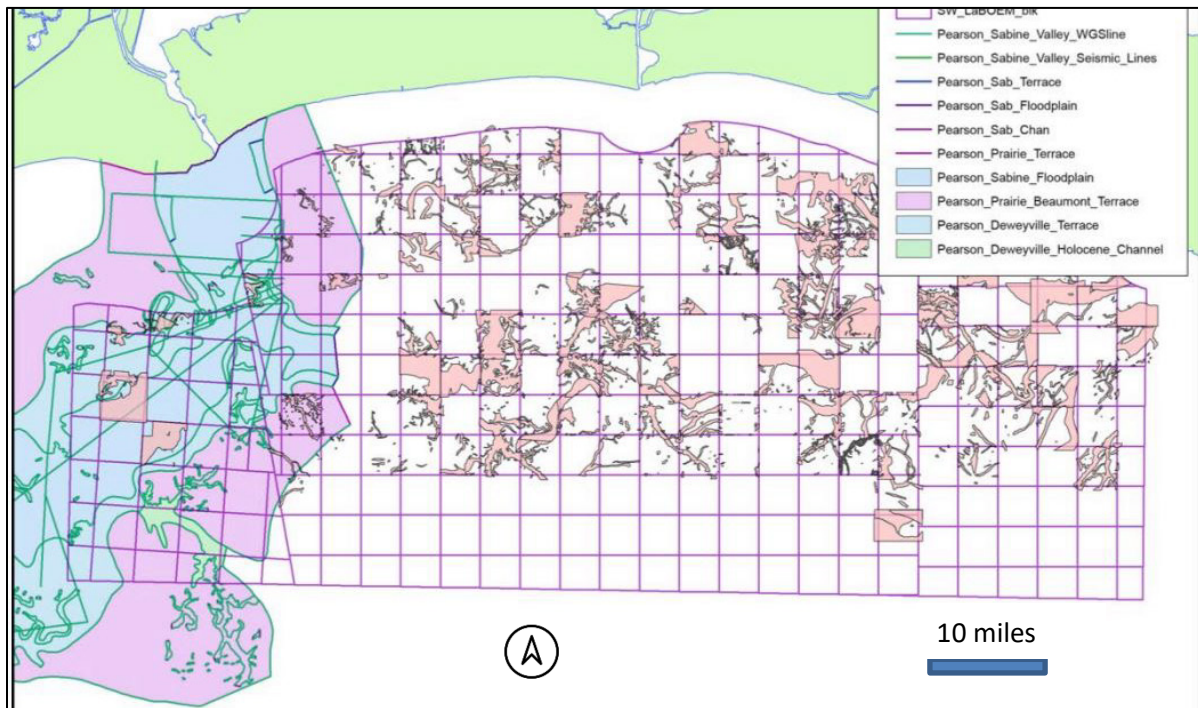


Figure 20. Paleochannel and paleovalley deposits.

Interpreted on over 300 individual oil and gas hazards survey reports conducted on Federal offshore lease blocks (defined by irregular purple grid) offshore Sabine and Calcasieu Passes. Deweyville Holocene Channels shown as pink shapes. Over 300 shallow hazard survey interpretations were mosaiced to develop this map. From Heinrich et al. (2020).

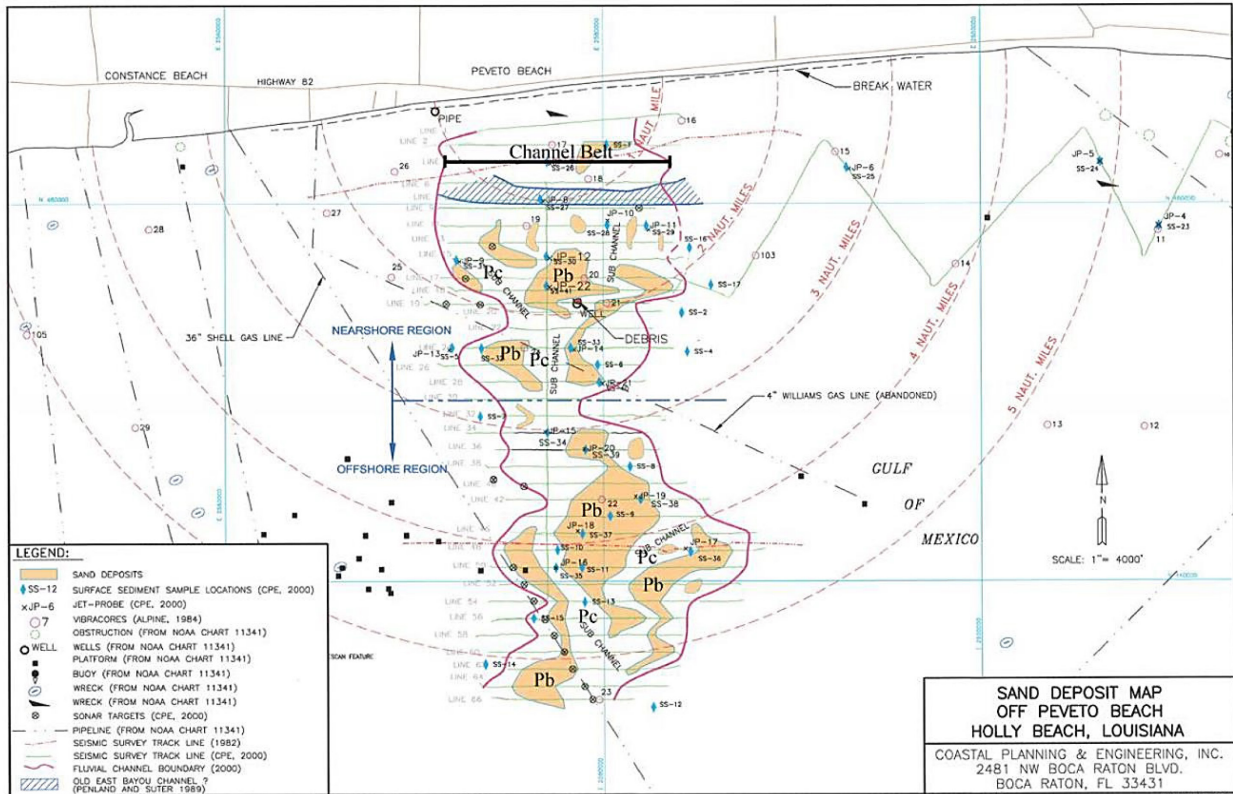


Figure 21. Sand deposit map of the Peveto Paleochannel offshore Holly Beach, Louisiana. Map demonstrates the complexity of locating channel sands within the channel fill and floodplain muddy deposits. The southernmost deposits on this map were ultimately extracted to construct the Holly Beach Restoration Project. See **Figure 20** for a conceptual model of paleochannel fills. From Heinrich et al. (2020), modified from APTIM-CPE (2001).

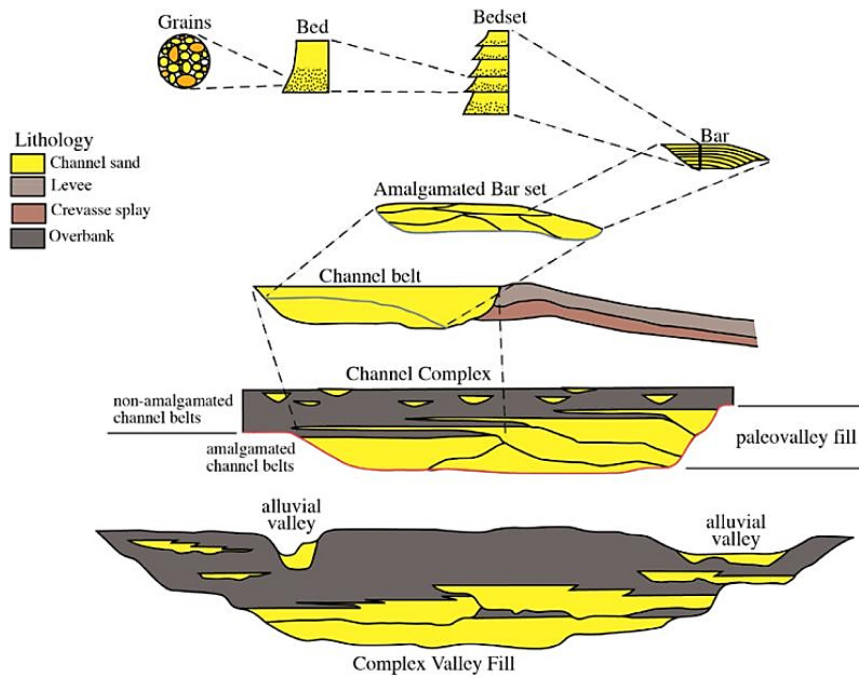


Figure 22. Conceptual hierarchy of fluvial deposits.

From Heinrich et al. (2020) modified from SEPM web.

The Texas state continental shelf adjacent to this study's region of interest contains numerous paleo-channel fills and amalgamated fluvial channel belts that were interpreted to represent deposits formed during the Pleistocene by ancestral versions of the current Brazos, Trinity, Sabine, and Neches rivers (APTIM 2021). These discrete fluvial channel belts maintained a relatively uniform width and thickness for 5-20 mi (8-32 km) and were primarily composed of steeply inclined dipping clinoforms that have the potential to be sand-bearing stratigraphic units (**Figure 23**). It is likely that these features either continue into the area of current investigation or have equivalent stratigraphic features present.

BRAZOS PLEISTOCENE CHANNEL BELT

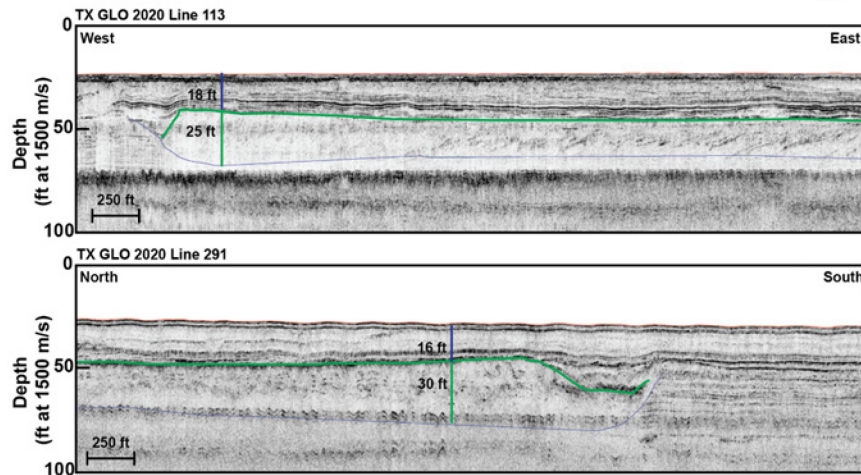
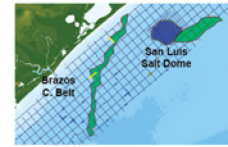


Figure 23. Sub-bottom profile sections across a Pleistocene channel belt in Texas state waters. The blue horizon marks the basal unconformity separated layered Beaumont stratigraphy from the above dipping clinoforms and variable transparent/chaotic seismic reflectors. The green horizon is the top of the dipping reflector package. Note the transition from dipping clinoforms to channel form at the edge of the feature. From APTIM (2021).

3.1.6 Transgressive Shelf Sand Bodies

The eastern Texas shelf contains multiple transgressive shelf sand bodies locally referred to as sand banks with attendant thinner sand sheets comprising sand reworked during transgression and the present highstand of sea level. Within the study area these sand banks include (from northeast to southwest, trending along the Trinity/Sabine incised valley) Sabine Bank, Heald Bank, Shepard Bank, and Thomas Bank (**Figure 24**). The purpose of this investigation is to map and delineate the deposits associated with Sabine and Heald Banks. Limited data suggest that thinner sand deposits (“sand sheets”) exist landward of Sabine and Heald Banks on the shelf. The discussion below primarily focuses on Sabine and Heald Banks because they comprise the most viable sand resource targets identified to date for implementation of large-scale restoration programs.

Sabine Bank is a shore-parallel elongate sand body located approximately 17 mi (27 km) offshore Sabine Pass at the Texas/Louisiana border generally delineated by the 30 ft (9.1 m) isobath, 30 mi (48 km)-wide (east-west) and 5 mi (8 km) long (north-south). The shallowest portions of Sabine Bank are less than 15 ft (4.6 m) deep. Heald Bank is 28 mi (45 km) offshore, is delineated by the 40 ft (12.2 m) isobath, and shoals to 25 ft (7.6 m). These banks are hypothesized to represent the sands of former barrier islands that underwent transgressive submergence (Penland et al. 1988; **Figure 25**). Transgressive submergence describes the process of barrier island submergence in response to sea level rise and involves a transition

from a transgressive (landward-migrating in response to sea level rise) barrier island that can no longer maintain exposure and becomes submerged. As sea level rise continues, the newly formed shoal continues to migrate landward across the shelf until all geologic evidence of the former barrier island has been reworked. It is important to distinguish barrier island transgressive submergence from in-place drowning. If in-place drowning occurs, the barrier island deposits would be preserved on the seafloor as a shoal and would have implications for how sand resources might be organized within the shoal as well as for preservation intact cultural resources. Based on existing geophysical and geological data, Heald Bank does not contain any preserved barrier island deposits (Rodriguez et al. 2004; Swartz et al. 2016). In other words, the sand body has been completely reworked on the shelf. The basal portions of Sabine Bank do contain basal barrier island deposits associated with subaqueous depositional environments (tidal inlets and flood tidal deltas), however, none of the subaerial barrier deposits are preserved (Rodriguez et al. 1999 and 2004)

Both Sabine and Heald Banks are composed of three distinct sedimentary units (**Figure 26**; Rodriguez et al. 1999). The sedimentary units from bottom to top are characterized by 1) backbarrier estuarine deposit composed of sandy mud, 2) a barrier shoreface and tidal deposit composed of muddy sand, and 3) the transgressive shoal deposit (reworked barrier island) consisting of sand and shell hash (Rodriguez et al. 1999 and 2004).

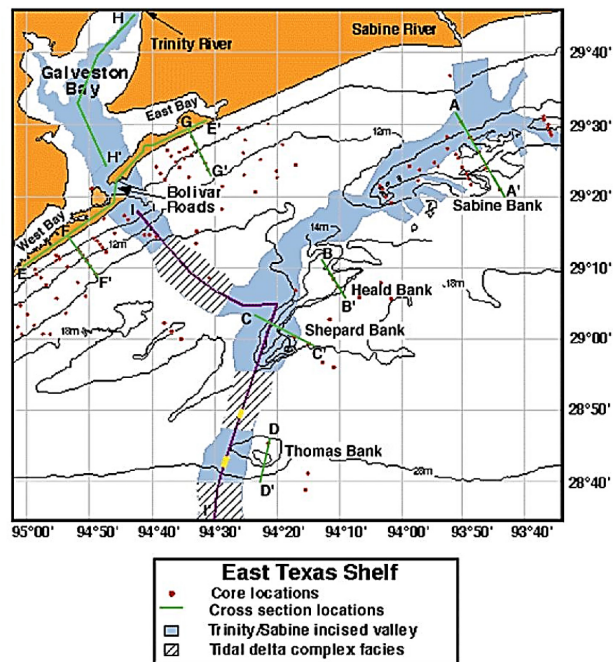


Figure 24. Map showing occurrence of sand banks relative to the Trinity/Sabine incised valley and tidal deposits.
From Rodriguez et al. (2004).

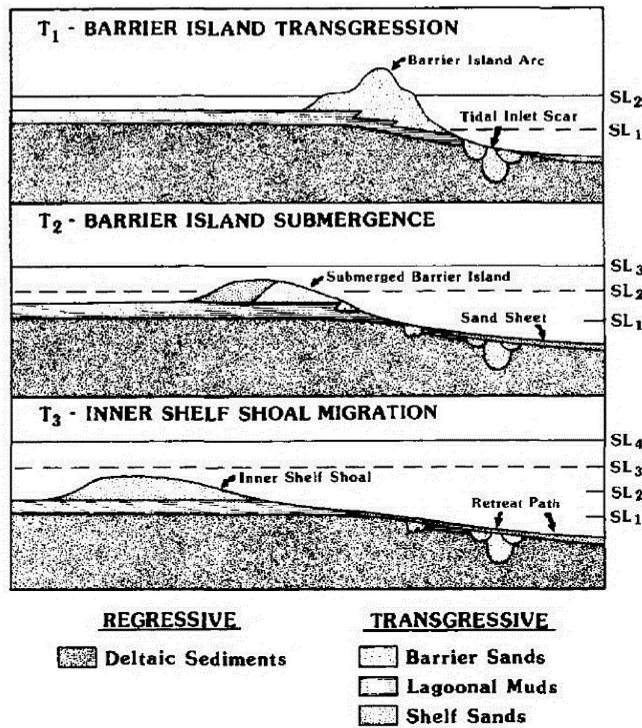


Figure 25. Three-stage conceptual model.

Illustrates the process of barrier island submergence and reworking of sands in the shelf setting, a process collectively referred to as transgressive submergence. Note that this differs from simple barrier island “drowning” models because the sands are continually reworked and migrate landward across the shelf after submergence. From Penland et al. (1988).

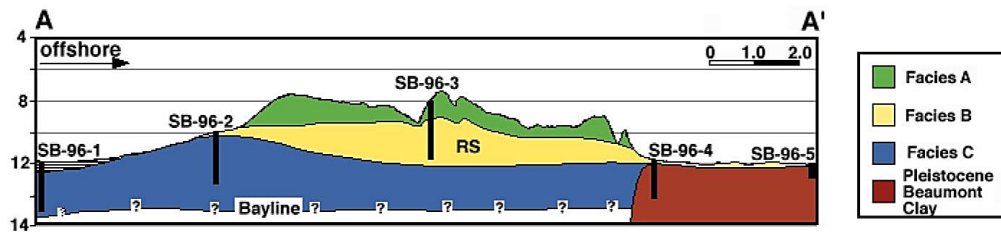


Figure 26. Dip-oriented cross-section across Sabine Bank.

Note the three (3) sedimentary units (facies) that comprise Sabine bank which coarsens upward from muddy estuarine deposits (A) into tidal deposits characterized as muddy sands (B) and capped with shoal sand and shell hash (C). (See map on **Figure 20** for location of section.) From Rodriguez et al. (2004).

An early estimate of Sabine Bank’s sand volume, based primarily on bathymetric relief and limited sediment cores, was estimated by Morton and Gibeaut (1995) to contain ~2.35 BCY of sandy deposits.

However, this overestimates beach-quality sand due to the vertical succession downward from shoal sands into relict tidal deposits as discussed above and in Rodriguez et al. (1999 and 2004).

3.1.7 Transgressive Ravinement

While the depositional response to sea level rise is manifested as incised valley fills and shelf sand bodies, response to wave and tidal current erosion (ravinement) dominated the study area and has resulted in removal of much of the upper sections of fluvial and coastal deposits associated with falling sea level (falling stage deltas and channel systems), lowstand (landforms that developed on interfluves), and early transgression (upper sections of incised valley fills and barrier island deposits). Preservation and even evidence of coastal deposits is extremely rare with the exception of the sand banks discussed above that actually represent reworked remnants of coastal deposits (Rodriguez et al. 2004; Anderson et al. 2015). Smaller stream channels that did not incise valleys or that were perched on interfluves are also rarely preserved (Anderson et al. 2015). The effective depth of transgressive ravinement in the study area was 25–35 ft (7.6-10.7 m) (and still is today along the modern shoreface; Wallace et al. 2010); therefore, the upper 25–35 ft (7.6-10.7 m) of all antecedent deposits were removed as the coastline migrated landward during the transgression (Wilkinson 1975; Siringan and Anderson 1994; Rodriguez et al. 2001). Recent work within the East Texas continental shelf found that this amount of ravinement acted to leave numerous older Pleistocene channel fills and channel belts close to the modern seafloor, with only coarse channel fill and point bar deposits preserved and minimal overburden associated with modern sediment deposition (APTIM 2021).

3.1.8 Highstand (~4,000 years ago to present)

Approximately 4,000 years ago the rate of sea level rise drastically slowed to an almost stable ~0.5 mm/yr allowing for the modern coastal system to mature as barrier islands prograded seaward and significant lateral spit accretion from headlands developed peninsulas such as Bolivar (Bernard et al. 1959; Wilkinson 1975). Much of the sand that exists in the modern coastal system was provided during transgressive ravinement of antecedent deposits on the shelf (e.g., falling stage deltas, transgressive barrier islands, shallow stream channels; Weight et al. 2011; Hollis et al. 2019). This concept of the modern coastal system being genetically related to preserved fluvial deposits on the shelf is an important consideration for assessing sand source suitability for beach nourishment.

Sand supply to the coast from the Trinity/Sabine system was non-existent by this time because the valleys had filled with estuarine deposits with their modern depocenters comprising bayhead deltas. The Brazos River continued to supply sand to the coast during highstand, but only intermittently during major flood events (Rodriguez et al. 2000).

3.1.9 Influence of Salt on Quaternary Geomorphology and Sediment Accumulation

As previously discussed, vertical migration of Jurassic salt diapirs up section can locally influence surface geomorphology due to uplift and contemporaneous/subsequent physical weathering of resulting topographic highs. Within the region, there are numerous examples of “salt domes” that produce

topographic highs along the coast including High Island and the “Five Islands” salt dome chain of Louisiana, all of which show significant displacement of Pleistocene strata (Autin et al. 1991). Erosion of the topographic highs results in development of radial or concentric gully drainage networks and an apron of coarse-grained colluvium flanking the slope toe of the highs (Autin et al. 1986; Autin and McCulloh 1995). A geologic map in **Figure 27** clearly shows the uplifted Pleistocene and the rim of colluvium surrounded by Holocene marsh deposits. This process of gully development and downslope accumulation of colluvium results in concentration of coarser material eroded out of the uplifted Pleistocene strata. It should be noted that the actual salt does not pierce the surface. In the shallow subsurface these features are characterized by radial fault sets and anticline structures, and geomorphic evidence suggests that uplift has continued through Quaternary times (e.g., Pleistocene fluvial deposits are uplifted; Autin and McCulloh 1995). The process of sand winnowing related to salt tectonics is important to consider given there are two salt domes on the shelf within the study area. Unlike those found on the coast, those that occur on the shelf within the study do not have any surface expression. Based on data from earlier sand prospecting activities in support of McFaddin Beach restoration, overlying the location of the McFaddin Dome, faulted and tilted Pleistocene strata (Beaumont Formation) outcrop on the seafloor and transgressive ravinement have truncated the upper section of the anticline (Gahagan and Bryant Associates, Inc. 2013; **Figure 28**). The concept that uplift, erosion, and downslope accumulation of coarse material associated with salt movement has been applied in hydrocarbon exploration on a much larger scale where “halokinetic sequences” of coarse-grained deposits that flank salt diapirs have been developed as hydrocarbon reservoir targets (Giles and Rowan 2012). The small scale halokinetic sequences of interest here can be preserved in the subsurface in two primary ways: 1) the slope-toe colluvium and gully fills accumulate contemporaneously with regional deposition and are buried, and 2) subsidence and brittle deformation associated with salt dissolution in the subsurface produces accommodation space for colluvium accumulation (Giles and Rowan 2012; **Figure 29**). As demonstrated by the chirp sonar profile in **Figure 28** that crosses the location McFaddin Dome, the structural and sedimentary response to salt diapirism produces complex stratigraphy that does not conform with conventional models that have informed shelf sand prospecting in the past (e.g., shelf sand shoals, paleochannel fills, etc.). The McFaddin Beach Restoration Project successfully developed this resource for construction, proving the utility as a sand resource, but also demonstrating the value of dense subsurface data coverage to accurately characterize the complex geology. Two more known near-surface salt diapirs have been identified within or proximal to the study area on the shelf (San Luis Pass and Bolivar salt domes), as well as other salt structures throughout the outer continental shelf. It should be noted, based on detailed geomorphic analysis of Louisiana salt domes, the sedimentary character of the colluvium is variable from one dome to another and dependent on the overlying, disrupted lithology (Autin et al. 1986; Autin and McCulloh 1995).

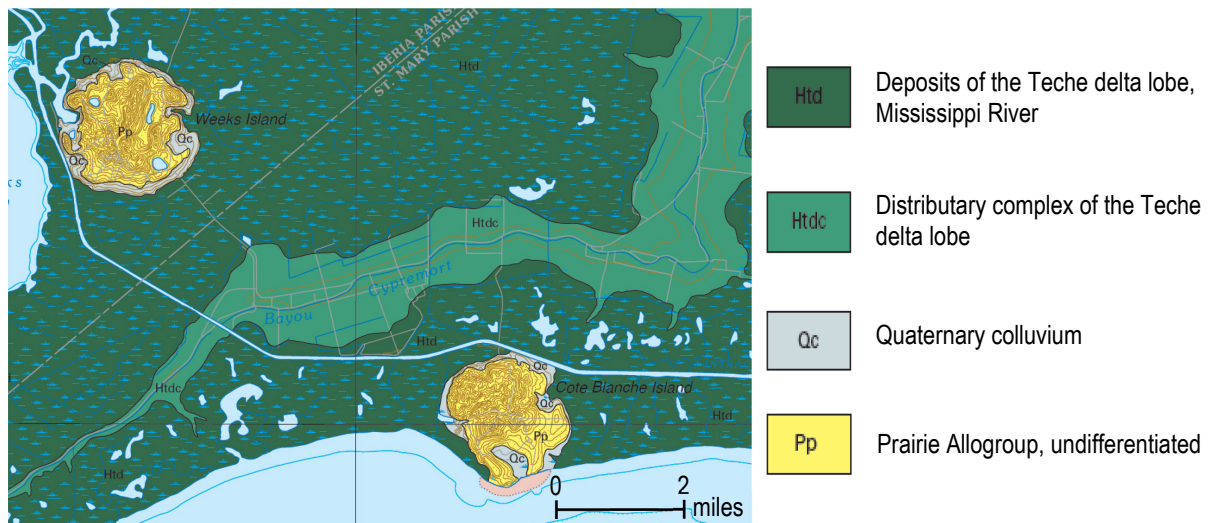


Figure 27. Geologic map showing Weeks Island and Cote Blanche Island salt domes in coastal Louisiana.

Note the older, uplifted Pleistocene (Prairie Allogroup is Beaumont Formation equivalent) deposits occur at higher elevations than the surrounding Holocene marsh and the colluvial apron (Qc) that flanks the uplifted Pleistocene. Modified from Morgan City 30 x 60 Minute Geologic Quadrangle, Louisiana Geological Survey (2012).

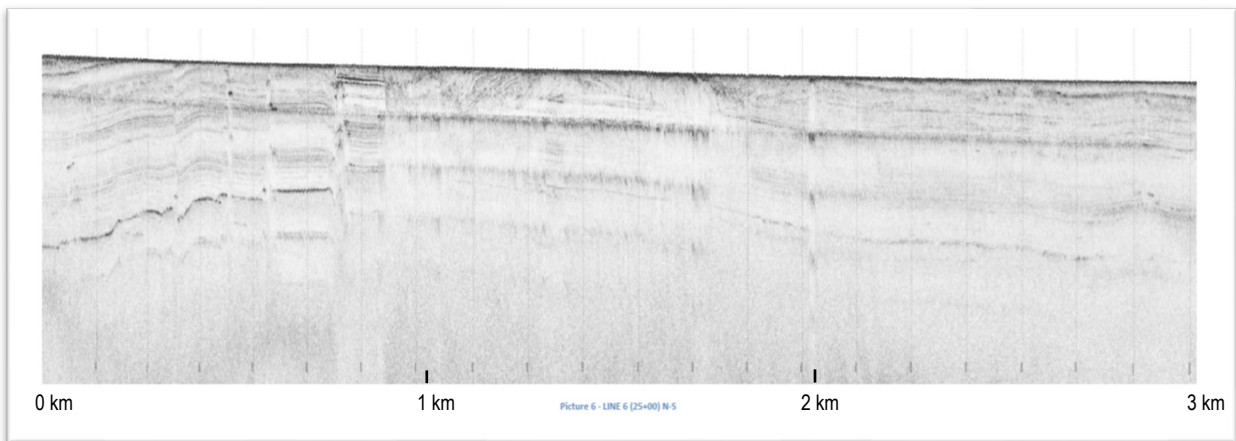


Figure 28. Chirp profile collected during the McFaddin Beach restoration sand search.

Profile crosses the location of the McFaddin Salt Dome (not visible in image). Note tilted strata on left side of image that outcrops at the seafloor. This is interpreted as uplifted and tilted Beaumont Formation that has been truncated by transgressive ravinement. This area is associated with a proven sand resource that has been partially excavated for construction of McFaddin beach. The original image did not include a vertical scale. From Gahagan and Bryant Associates, Inc (2013).

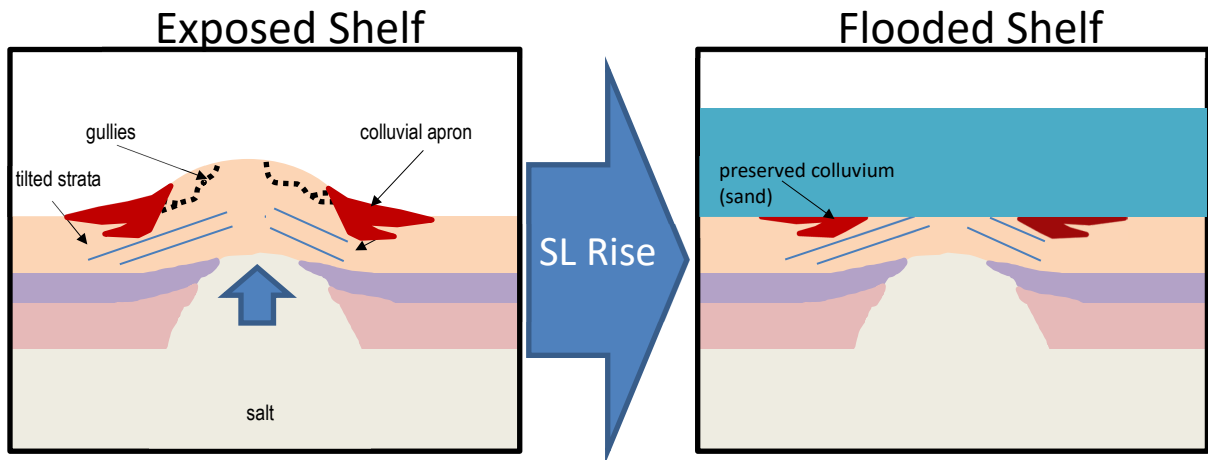


Figure 29. Conceptual model for development and preservation of salt dome colluvial aprons. Uplift and weathering produce colluvium and subsequent flooding as sea level rises and truncates former topographic highs, leaving the basal portion of gully fills and colluvial apron preserved in the subsurface.

3.2 Survey Planning

APTIM compiled and evaluated available reports, geophysical data, and geotechnical data to develop a geophysical data collection survey plan offshore Texas. The available sub-bottom data imported into SonarWiz together with historic reports indicate that the Sabine and Heald Banks along with smaller shoal features in their vicinities should be targeted as part of this effort. Potential sand deposits (surface sands, paleochannels, and sand shoals) and historic shapefiles of the delineated sand bodies were incorporated into the desktop study to assist with the planning of the survey area and line plan. The survey plan delineated from the data in the desktop study incorporate not only the already established Sabine and Heald Banks, but smaller potential shoals (**Appendix A**). Additionally, the banks sit above or in proximity to numerous paleo-channels and incisions that have yet to be explored for potential resources (Forde et al. 2009). The goal of targeting these smaller features is to potentially expand the boundaries of the available sand offshore Texas and increase the available volume of resources for future coastal restoration efforts. APTIM proposed to collect up to 1,050 nm of geophysical data (chirp sub-bottom, sidescan sonar, and magnetometer) and hydrographic (single-beam fathometer) survey data along Sabine and Heald Banks (and adjacent areas) on the OCS (**Figure 30**).

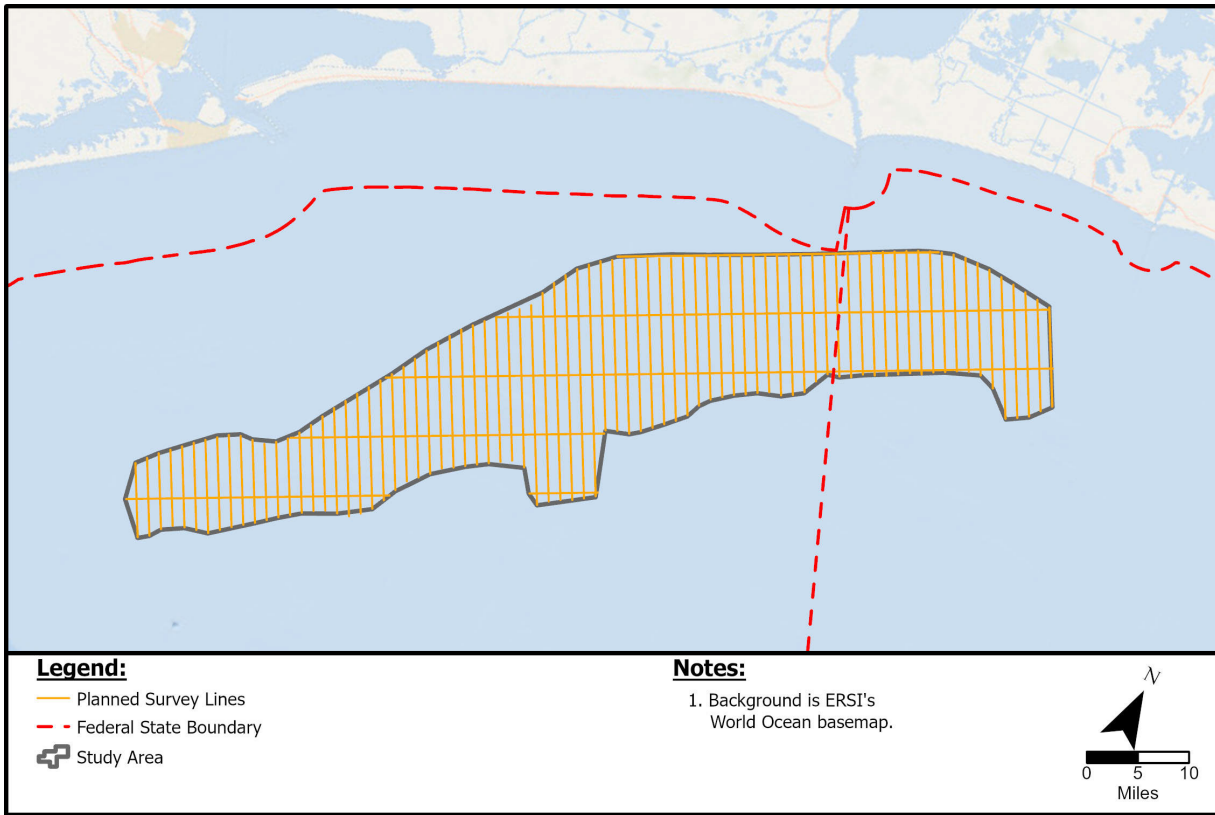


Figure 30: Planned survey lines from Desktop Study

Upon completion of discussions between APTIM, TWI, and the GLO, the final line plan map was submitted to the GLO for approval as part of the Desktop Study Report (**Appendix A**).

4 Task 2 Reconnaissance-Level Geophysical Survey

4.1 Geophysical Investigation

On October 23, 2020, the APTIM crew prepared the offshore vessel, M/V *Terry Bordelon*, for geophysical survey operations. From October 23, 2020 through November 14, 2020, APTIM conducted a comprehensive geophysical (chirp sub-bottom, sidescan sonar, and magnetometer) and hydrographic (single-beam fathometer) survey offshore western Louisiana and eastern Texas along Sabine and Heald Banks. APTIM conducted these investigations on the M/V *Terry Bordelon* 24-hours per day during favorable weather conditions. Over the course of 21 operational days, APTIM collected a total of 1,133 nm of geophysical data (**Figure 31** and **Table 1**) around the clock in 12-hour shifts, averaging a total of 56.65 nm per day. The total as-run data collection effort consisted of 1,067 nm of geophysical and single-beam data collection within the original study area with an additional 66 nm of data added in the field in order to connect the main federal study area to the Region 1 state-side work conducted by APTIM between August 19 through October 23, 2020. Due to inclement weather caused by named tropical system Zeta, and a merging cold front, survey operations were halted for two days.

Table 1. Geophysical investigations conducted in 2020.

	Date	Proposed (nm)	Collected (nm)
Geophysical data, primary lines (bathymetric, magnetometer, seismic and sidescan sonar)	October 23, 2020 through November 13, 2020	1,050	1,067
Geophysical data, add on secondary lines (bathymetric, magnetometer, seismic and sidescan sonar)	November 13, 2020 through November 14, 2020	55	66
Total	21	1,105	1,133

On October 23, 2020, the APTIM crew began mobilization for survey at Martin Midstream on Pelican Island in Galveston, Texas, aboard the *Terry Bordelon*. Once complete, the crew began transiting to the survey site in the afternoon of October 23, 2020. The crew arrived on site in the OCS in the late afternoon of October 23, 2020 and began data collection. The survey continued until October 27, 2020, when the vessel was forced to pull gear and retreat to Galveston due to inclement weather resulting from tropical storm Zeta and an encroaching cold front. The vessel arrived at dock in Galveston in the afternoon on October 27, 2020 and remained on weather standby for two days. New APTIM crewmembers boarded the vessel in the afternoon on October 30, 2020. The vessel transited to the survey site and resumed normal survey operations. On November 5, 2020, operations were shut down due to a Protected Species Observer (PSO) sighting (see **Appendix D**), and after roughly an hour, operations resumed. On November 13, 2020, APTIM began collecting the add-on geophysical tracklines within the study area to connect the recent state-side geophysical data to the OCS data and provide additional coverage of potential sub-surface formations/depositions. Survey continued smoothly until it was time for the next crew change on

the afternoon of November 13, 2020, and the vessel came to port in Sabine Pass to swap out crew. The new crew returned to the site offshore Sabine Pass to begin survey in the late afternoon. Survey resumed on November 13, 2020, and continued until the survey was completed in the morning of November 14, 2020, and the vessel and crew began transit back to dock in Houma, LA.

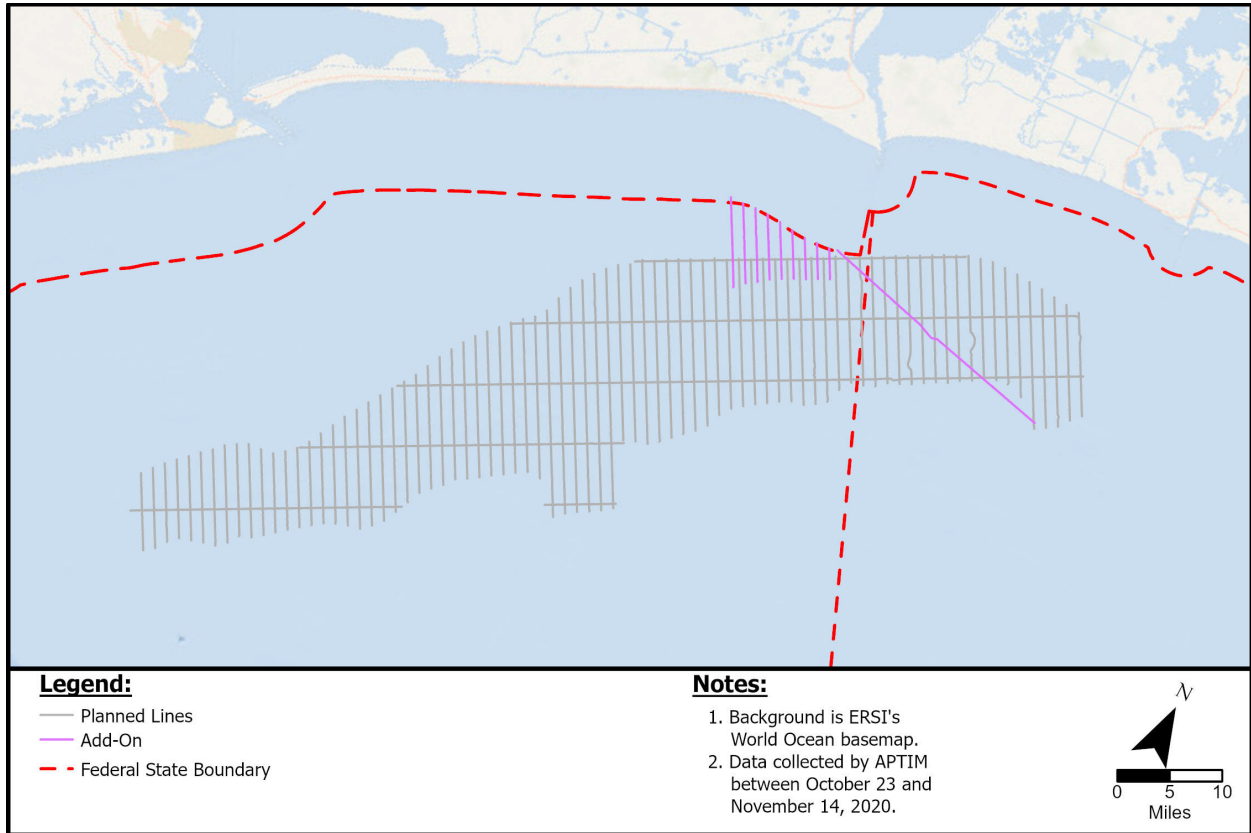


Figure 31. As run tracklines.

4.2 Equipment and Survey Methods

The Task 2 geophysical investigation included single-beam bathymetric, sidescan sonar, seismic reflection profiling, and magnetometer surveys. The survey systems are listed and discussed in detail below and presented in **Table 2**. The single-beam bathymetric, sidescan sonar, seismic reflection profiling, and magnetometer surveys were conducted concurrently using the setup illustrated on **Figure 32**. Geophysical data were collected under the responsible charge of Beau Suthard, a licensed Professional Geoscientist (Geology) registered in the State of Texas (License #12902).

Table 2. Equipment used during the geophysical investigation.

Equipment Type	Description	Acquisition Parameters
Navigation	Trimble Post Processing Kinematic, Differential Global Positioning System (Trimble SPS 461) interfaced with HYPACK®, TSS DMS-05	N/A
Odom Hydrographic Systems, Inc. "Teledyne E20" portable single beam Hydrographic Echosounder	Odom Hydrographic Systems, Inc. "Teledyne E20" portable Hydrographic Echosounder	200 kHz, 4-degree transducer
Sound Velocity Profiler	Valeport's SWIFT SVP.	N/A
Sub-Bottom Profiler (Seismic Reflection)	EdgeTech 3200 with SB-512i Sub-bottom Profiler	Pulse: 0.7-12 kHz, Power: 40% Ping Rate: 7.0 hz Acquisition Depth: 20m
Sidescan Sonar	EdgeTech 4200 300/600 kilohertz (kHz) sidescan sonar system	300 kHz, 230 m Range Scale 600 kHz, 120m Range Scale
Magnetometer	Geometrics G-882 Digital Cesium Marine Magnetometer interfaced with HYPACK Inc.'s HYPACK® software	0.02 nT P-P 0.1 second sample rate
Processing Software	HYPACK 2020®, Single Beam Max, ESRI ArcGIS 10.8.1, Golden Software's Surfer 12, HYPACK's MagEdit Software, EdgeTech's Discover-SB Software, Chesapeake Technology Inc.'s SonarWiz 7	N/A

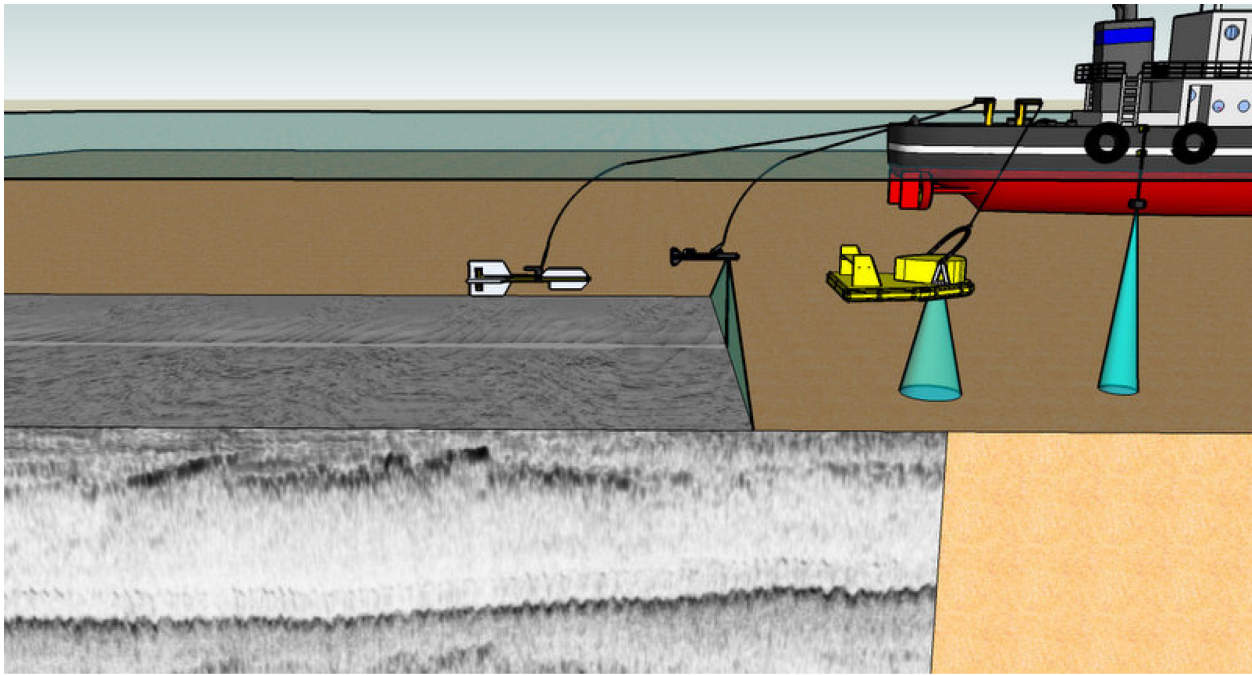


Figure 32. Schematic diagram showing the typical deployment of sensors.
Joint bathymetric, sub-bottom profiler, sidescan sonar, and magnetometer survey.

4.2.1 Navigation

The positioning system deployed for the survey was a Trimble SPS-461 Differential Global Positioning System (DGPS). The DGPS receiver was corrected by U. S. Coast Guard (USCG) navigational beacons. The receiver automatically acquired and simultaneously tracked the NAVSTAR satellites, while receiving precisely measured code phase and Doppler phase shifts that enabled the receiver to compute the position and velocity of the vessel. The receiver determined the time, latitude, longitude, height, and velocity once per second. Global Position System (GPS) accuracy with differential correction provided for a position accuracy of 1 to 4 ft (30 to 122 centimeters). A Trimble Global Navigation Satellite System (GNSS) receiver was used onboard the survey vessel to log GNSS positions for post processing GNSS data. GNSS data were logged at 5 hertz (Hz) during survey operations for accurate real time positions, and to aid in post-processing.

All coordinates presented in this report are in U.S. Survey Feet, relative to the North American Datum 1983 (NAD83), Texas State Plane Coordinate System, South Central. Elevations are presented in U.S. Survey Feet, relative to the North American Vertical Datum 1988 (NAVD88) relative to Geoid 18.

4.2.2 HYPACK Inc.'s HYPACK 2020® Data Collection and Processing Program

APTIM's navigation, magnetometer, and depth sounder systems were interfaced with an onboard computer and the data were integrated in real time using HYPACK Inc.'s HYPACK 2020® software. HYPACK is a state-of-the-art navigation and hydrographic surveying system. The location of the towfish tow-point and transducer mount were measured in relation to the center of mass of the vessel and the DGPS. Vertical and horizontal measurements were recorded and entered into the HYPACK survey program. The length of cable deployed between the tow-point and each towfish were also measured and entered into HYPACK to monitor the position of each system in real time. Online screen graphic displays included the pre-plotted survey lines, the updated boat track across the survey area, adjustable left/right indicator, as well as other positioning information such as boat speed, quality of fix measured by Position Dilution of Precision, and line bearing. The digital data were merged with the positioning data DGPS, video displayed, and recorded to the acquisition computer's hard disk for post processing and/or replay.

The positioning for the geophysical and bathymetric systems were calculated by establishing towpoint offsets for each system based on the vessels center of mass (see vessel diagram in **Appendix E**). Positioning for each geophysical system was provided by utilizing the towfish layback driver in HYPACK. This tool allows the user to set up towpoint offsets for each towfish and, during data acquisition, adjust cable out lengths, which will correct the final system position in real time by taking into account the towpoint offsets as well as the individual catenary factor established for each system. The catenary factor was calculated based on the weight of the system and its towing configuration. The final towfish position is then shared with each of the systems and raw geophysical data is collected with layback corrections. Positioning for the GPS, single beam and motion reference unit was calculated by measuring the offset of each system to the center of mass and utilizing the system offset set up within the HYPACK Hardware interface.

4.2.3 Bathymetric Survey

The Odom Hydrographic Systems, Inc.'s ECHOTRAC E20, a single frequency portable hydrographic echo sounder, was used to perform the bathymetric survey. The ECHOTRAC E20 operates at frequencies between 10 and 250 kHz and is a digital, survey-grade sounder. A 200 kHz, four (4) degree transducer was used for the bathymetric survey. Soundings were collected at maximum ping rates to provide an accurate depiction of the seafloor. Sounder calibration was performed periodically throughout the survey (typically at the beginning and end of each survey day). The sounder was calibrated via bar-checks and a sound velocity probe. Valeport's SwiFT Sound Velocity Profiler (SVP) measures the speed of sound through the water column with the average speed used to calibrate the ECHOTRAC E20. Bar checks were performed from a depth of 15 to 30 ft (4.6 to 9.1 m) (in 5 ft [1.5 m] increments) to verify the transducer draft and speed of sound. Echogram data showing the results of the bar check calibration were displayed on the sounder electronic charts during descent of the bar.

Real-time navigation software (HYPACK) was used to provide navigation to the helm to minimize deviation from the line azimuth. This software provided horizontal position to the sounding data, allowing real-time review of the data in plan view or cross section format. A TSS Motion Compensator was used

onboard the survey vessel to provide instantaneous heave, pitch, and roll corrections. Tie lines were collected to verify survey accuracies.

4.2.4 Magnetometer Survey

A Geometrics G-882 digital cesium marine magnetometer (**Figure 33**) was used to detect magnetic anomalies within the survey area. The magnetometer runs on 110 volts alternating current and is capable of detecting and aiding the identification of any ferrous, ferric, or other objects that may have a distinct magnetic signature. Factory set scale and sensitivity settings were used for data collection (0.004 nanotesla [nT]/ π Hz rms; typically, 0.02 nT peak-to-peak [P-P] at a 0.1 second sample rate or 0.002 nT at 1 second sample rate). The magnetometer was towed in an effort to maintain an altitude of no greater than 19.7 ft (6 m) above the seafloor and far enough away from the vessel to minimize boat interference. Navigation and horizontal positioning for the magnetometer were provided by the Trimble DGPS system via HYPACK and using a towfish layback correction. Magnetometer data were recorded in the native .raw HYPACK file format using HYPACK 2020's survey software. The purpose of the magnetometer survey was to detect the presence of potential underwater wrecks, submerged hazards, or other features that would affect borrow area delineation and dredging activities.

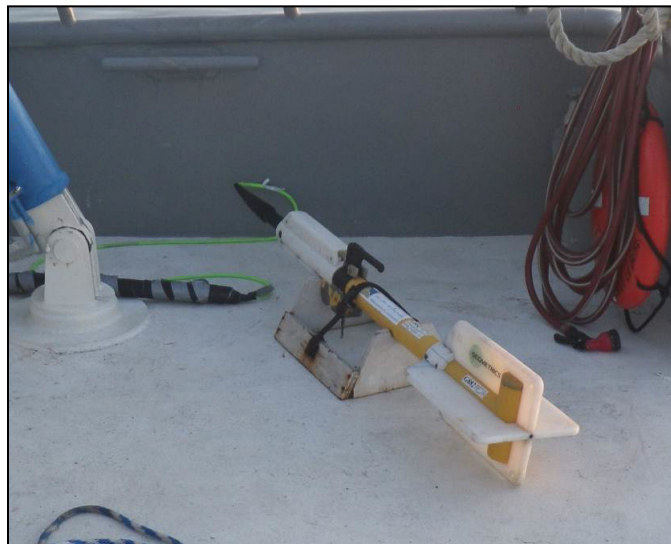


Figure 33. Geometrics G-882 Digital Cesium Marine Magnetometer.
Magnetometer is used investigate magnetic anomalies.

4.2.5 Sidescan Sonar Survey

APTIM utilized an EdgeTech 4200 sidescan sonar system (**Figure 34**) for this project. This system uses full-spectrum chirp technology to deliver wide-band, high-energy pulses coupled with high resolution and good signal to noise ratio echo data. The sonar packages included a portable configuration with a laptop

computer running EdgeTech's Discover® acquisition software and dual frequency towfish running in high-definition mode. The sidescan sonar data were merged with positioning data from DGPS via HYPACK, video displayed, and recorded to the acquisition computer's hard disk for post processing and/or replay. All sidescan sonar data were collected in the default EdgeTech jsf file format. This sonar system consists of dual frequency towfish operating at 300/600 kilohertz (kHz), with maximum range scales of 754 ft (230 m) to either side of the towfish (300 kHz), and 393 ft (120 m) to either side of the towfish (600 kHz). These range scales are the maximum manufacturer recommended ranges for the frequencies listed above. However, geophysicists in the field based the recorded ranges on the field conditions and may not have utilized the maximum range scales. For data acquisition during this survey, frequencies and range scales were at 300 kHz/230 m and 600 kHz/120 m with the operation range set to high-definition mode.



Figure 34. EdgeTech 4200 Sidescan Sonar Towfish.

4.2.6 Seismic Reflection Profile Surveys

Chirp sub-bottom/seismic-reflection data were used to show sedimentary stratigraphy and identify potential project-compatible sediment resources. The use of chirp sub-bottom data allowed common stratigraphic layers to be mapped throughout the study area while determining the thickness and extent of potential project compatible sediment.

An EdgeTech 3200 X-STAR with a SB-512i towfish was used to conduct the sub-bottom profile surveys (**Figure 35**). The X-STAR Full Spectrum Sonar is a versatile wideband FM sub-bottom profiler that collects digital normal incidence reflection data over many frequency ranges. Throughout the duration of the survey, operational parameters for the seismic system were a pulse frequency of 0.7-12 kHz, power of 40 percent (%) ping rate of 7.0 Hz and acquisition depth of 20 m This instrumentation generated cross-sectional images of the seabed (to a depth of up to 50 ft [15.2 m] in this survey). The X-STAR SB-512i transmits an FM pulse that was linearly swept over a full spectrum frequency range (also called a “chirp pulse”). The tapered waveform spectrum resulted in images that have virtually constant resolution with depth. The Chirp systems have an advantage over 3.5 kHz and “boomer” systems in sediment delineation because the reflectors are more discrete and less susceptible to ringing from both vessel and ambient noise. The full-wave rectified reflection horizons were cleaner and more distinct than the half-wave rectified reflections produced by older analog systems.

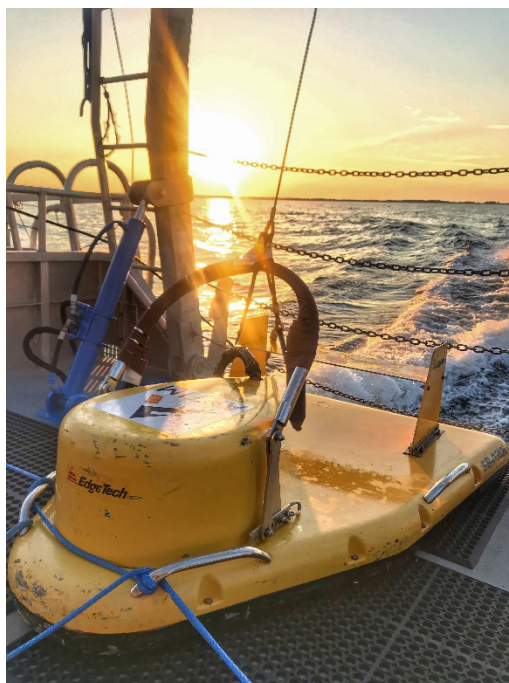


Figure 35. EdgeTech X-STAR SB-512i sub-bottom profiling system.

In order to minimize noise related to the survey vessel and sea conditions, the sub-bottom towfish (which operated as both the source and receiver for the sub-bottom system) was deployed and towed behind the research vessel. The sub-bottom system was interfaced with the DGPS system via HYPACK 2020® navigational software. The location of the fish tow point (as referenced to the DGPS antenna), together with the length of cable deployed from the tow point, were entered into HYPACK 2020® in order to account for the fish layback and provide accurate positioning of the sub-bottom fish during the survey. The sub-bottom system was operated by the Discover-SB® software program. At the start of the sub-bottom profiling survey, the sweep frequencies of the outgoing pulse together with the different gain settings available within Discover-SB® were adjusted to obtain the best possible resolution for the survey. The data were continuously bottom-tracked to allow for the application of real-time gain functions in order to have an optimal in-the-field view of the data. Automatic Gain Control (AGC) was used to normalize the data by strengthening quiet regions/soft returns while simultaneously reducing/eliminating overly strong returns by obtaining a local average at a given point. A Time-Varying Gain (TVG) was used to increase the returning signal over time in order to reduce the effects of signal attenuation. During the seismic data collection process, APTIM scientists were constantly monitoring the incoming data for areas where the sub-surface stratigraphy was indicative of sand. When these were observed, targets were made in HYPACK and/or notes were taken and reviewed.

All sub-bottom data were recorded on the acquisition computer's hard disk and transferred to a USB memory stick and/or portable hard drive at the end of each survey day to back-up raw survey data. After

every shift, the collected data were imported into Chesapeake Technologies, Inc.'s SonarWiz 7 program and general interpretations were made to verify and confirm field observations. Once a general feature was identified, an outline was made, and additional lines were generated to connect the study area to previous data collection areas. These add-on in lines allow for the better delineation and continuation of the boundaries of the deposit so that the GLO can have a better understanding of the volume and quality of material.

4.3 Mitigation Efforts to Minimize Potential High-Resolution Geophysical Impacts to Protected Species

4.3.1 Mitigation

While impacts to marine mammals were not expected, the following mitigation protocols were implemented to reduce the already small chance of High Resolution Geophysical (HRG) survey impacts to marine mammals. These protocols reflected the most recent federal regulatory coordination document to address HRG systems, the Final Environmental Assessment on Sand Survey Activities for BOEM's Marine Mineral Program produced by BOEM (May 2019), specifically Appendix B: Survey Requirements and Mitigation Measures.

The GLO and APTIM submitted a written Request for Mitigation Exemptions to BOEM on June 25, 2020 (see **Appendix C**). The GLO and APTIM requested exemptions from two mitigation measures, (1) Passive Acoustic Monitoring (PAM), and (2) Sea Turtle Frequency Modulation Requirements for Nighttime Operations. The written Request for Mitigation Exemptions provided information on the proposed geophysical survey equipment, the regulations for mitigation measures, proposed mitigation measures, as well as supporting documentation and reasoning for the mitigation exemption request. The Mitigation Exemption Request was granted (via email) by BOEM on July 30, 2020. On October 21, 2020, prior to commencing field operations, BOEM issued project specific "Survey Requirements and Mitigation Measures for all Marine Minerals Program (MMP) G&G" describing the necessary survey requirements. This document confirmed that nighttime PAM operation and the nighttime frequency modulation mitigation requirements were waived.

4.3.2 Seismic Survey Mitigation and Protected Species Observer Protocols

Geophysical surveys may have an impact on marine wildlife, although HRG surveys are the least impactful when compared with surveys utilizing airguns. Non-airgun HRG acoustic sources with frequencies greater than or equal to 180 kHz do not require mitigation because the frequency is outside the general hearing range of marine mammals (National Marine Fisheries Service [NMFS] 2020). The magnetometer produces no acoustic noise whatsoever, while the echosounder and the sidescan sonar utilize a higher frequency than 180 kHz; therefore, no mitigation plan was necessary for these three (3) systems. Since the EdgeTech 3200 512i chirp sub-bottom profiler operates at a frequency below 180 kHz, the survey implemented mitigation protocols consistent with Final Environmental Assessment on Sand Survey Activities for BOEM's MMP produced by BOEM (May 2019), specifically **Appendix B**: Survey Requirements and Mitigation Measures.

An Acoustic Exclusion Zone (AEZ) of 328-ft (100-m) was monitored during all sand survey activities. All survey operations were monitored by a NMFS approved, trained Protected Species Observer (PSO). One NMFS approved and trained PSO was always on duty during survey operations. Startup and shutdown requirements were followed every time the survey began. Nighttime operations did not require the use of PAM or any frequency modulation above 2 kHz (see Section 4.3.1). This exemption was supplemented with the nighttime PSO utilizing night vision goggles to monitor the AEZ, as well as the use of a thermal imaging camera system. These proposed nighttime mitigations provided the same visual monitoring standards proposed by the EA for daylight hours.

Throughout the survey operation, there was only one PSO shut-down due to a loggerhead turtle entering the exclusion zone on November 5, 2020. Operations were immediately suspended upon sight of the turtle. Once the turtle had vacated the AEZ, a PSO clearance was completed and a full seismic ramp up was done before survey was resumed. Additional sightings during operations consisted of bottlenose dolphins (both individuals and in pods), which did not require any shut-downs. All PSO sighting forms and operation reports are included in **Appendix D**.

4.3.3 Vessel Strike Avoidance and Injured/Dead Aquatic Protected Species Reporting Protocols

All efforts were made by the vessel operators and crew to avoid striking any aquatic protected species. A visual observer (e.g., captain and PSO) aboard the vessel monitored a vessel strike avoidance zone around the vessel to ensure the potential for strike was minimized. Vessel speeds were reduced to 10 knots or less when mother/calf pairs, pods, or large assemblages or any marine mammals were observed near the vessel. The vessel maintained a minimum separation distance of 100 m from sperm whales, and 500 m from any baleen whale to specifically protect the Gulf of Mexico Bryde's whale. The vessel maintained a minimum separation distance of 50 m from all other aquatic protected species, including sea turtles, with an exception made for those animals that approach the vessel. If aquatic protected species were sighted while the vessel was underway, the vessel acted as necessary to avoid violating the relevant separation distance. If aquatic protected species were sighted within relevant separation distance, the vessel reduced speed and shifted engine to neutral, and did not engage the engines until animals were clear of the area. This did not apply to any vessel towing gear (e.g., geophysical towfish). The above stated requirements did not apply in any case where compliance would create imminent and serious threat to a person or vessel or to the extent that the vessel was restricted in its ability to maneuver and, because of the restriction, was unable to comply

Any injured or dead aquatic protected species, regardless of whether the injury or death was caused by the survey vessel, would have been reported to the proper authorities specified in the Marine Mammals Protection Act (MMPA). No injured or dead aquatic protected species were observed.

4.3.4 Gulf of Mexico Marine Trash and Debris Awareness and Elimination Survey Protocols

Marine trash and debris pose a threat to fish, marine mammals, sea turtles, and potentially other marine animals, cause costly delays and repairs for commercial and recreational boating interests, detract from the aesthetic quality of recreational shore fronts, and increase the cost of beach and park maintenance. In order to mitigate this threat to the environment and marine animals, all personnel involved in conducting the HRG survey had Marine Trash and Debris Awareness Training. The program is conducted on an annual basis. All offshore employees and contractors actively engaged in offshore operations are required to view the Bureau of Safety and Environmental Enforcement (BSEE) You Tube video entitled “Keep the Sea Free of Debris. A look at preventing marine debris and some best practices” and review NTL 2015-G03. All policies and procedures outlined in this training were observed during vessel operations.

4.3.5 Navigation and Commercial Fisheries Operations Conflict Minimization Requirements

APTIM was required to file a Local Notice to Mariners with the appropriate USCG District. APTIM filed the Local Notice to Mariners prior to beginning the survey. Please see the USCG Published Local Notice to Mariners below.

LA/TX - GULF OF MEXICO - Geophysical Survey Operations

Continuing until approximately November 30, 2020, APTIM Environmental & Infrastructure, LLC., will be performing a High Resolution Geophysical Survey for the Texas General Land Office (TX GLO) covering TX GLO Region 1. The survey plan is to perform a reconnaissance high resolution geophysical survey along a 1-mile spaced survey grid within Outer Continental Shelf waters along the upper Texas and western Louisiana coast.

The Geophysical Survey will be bound by the following approximate positions:

NE Corner: 29-15-53.116N 093-15-53.116W,

NW Corner: 29-39-37.156N 093-25-07.291W,

SE Corner: 28-41-04.993N 094-37-53.345W and

SW Corner: 29-01-32.398N 094-51-29.447W.

Operations will be conducted 24-hours a day, 7-days a week. M/V TERRY BORDELON will monitor VHF-FM Channel 16. M/V TERRY BORDELON will be restricted in ability to maneuver. Mariners are urged to use caution when transiting the area.

Charts: 411 1116A 11330 11340

LMN: 43-20

5 Task 3 Data Processing and Data Interpretation

The results of the geophysical survey conducted by APTIM in the OCS are discussed below. Georeferenced features discussed in the sections below can be found in **Appendix P**, a digital deliverable in a gdb format, and a geoPDF map with most of the data discussed can be found in **Appendix O**. A copy of the SonarWiz 7 projects for both the sidescan sonar and seismic sub-bottom are included in the digital **Appendix V** and **Appendix W** respectfully. Raw .jsf files for the sidescan sonar and seismic sub-bottom data are included in the digital **Appendix X**.

5.1 Bathymetric Survey

Upon completion of the field work, data were edited and reduced with APTIM's internal software programs, Trimble Business Center (TBC), and HYPACK 2021®. The logged GNSS data were processed using TBC to aid with water level corrections. The GNSS derived water level corrections were compared with local National Oceanic and Atmospheric Administration (NOAA) water level gauges for verification purposes. The NOAA recording gauges compared well with the GNSS derived water levels in most areas. It was observed that the NOAA recorded water levels were more stable than the GNSS derived water levels in areas of long GNSS base lines from the Continually Operating Reference Stations station. The final water level solution was derived using the 8770822 Texas Point, Sabine Pass, TXNOAA recording water level gage (**Figure 38**). All digitized soundings were scanned for noise with errant and false soundings removed. Water depths within the study area ranged from -83 to -20 ft (-25.3 to -6.1 m) (NAVD88). Bathymetric maps are presented in **Appendix F**.

Data uncertainties were mitigated during both collection and processing phases using a range of instruments and procedures. Proper vessel mobilization, attentive and accurate data collection consistencies, as well as a stable processing method were used to ensure data quality and minimize uncertainties.

Prior to data collection, all instruments (including motion reference unit [MRU], GPS, and transducer) were mounted onto the vessel and offsets measured from the vessel center of mass. A vessel diagram depicting these offsets is presented in **Appendix E**. When installing the factory calibrated Teledyne TSS DMS-05 motion reference unit, field calibrations were also performed. During the calibration routine, the instrument measures average roll and pitch angles over an extended period while the vessel is not in motion. These averages are applied to the raw MRU data, which accounts for any mounting angle bias that may be present.

The transducer draft was measured using conventional instruments after mobilization, and periodically throughout operations to ensure accurate depth determination. Bar checks were performed to verify draft/sound velocity corrections and to ensure proper echosounder operation. Once draft/sound velocity measurements were taken, an acoustically reflective surface (bar) attached to a rope (or cable) is measured at a known distance from the waterline. Measurements are marked in five (5) ft increments, allowing the bar to be placed at a maximum depth of 30 ft from the waterline. Once lowered underneath the transducer at a specific depth the echosounder reading is compared to that the true depth of the bar verify digitized depth reading. A factory calibrated Valeport Swift Sound Velocity Profiler was used to measure sound velocity during the survey and is capable of collecting sound velocity casts while

underway. Sound velocity casts were collected at an interval of approximately one (1) ft throughout the entire depth range of the water column at least twice a day, once per 12-hour shift. Additional casts would be collected if deemed necessary (change in survey area, thermoclines observed, etc.). All casts were recorded for post processing of the soundings. The average velocity is applied to the echosounder after each cast. Sound velocity profiles are applied to the processed data within HYPACK to account for changes from the average velocity at depth.

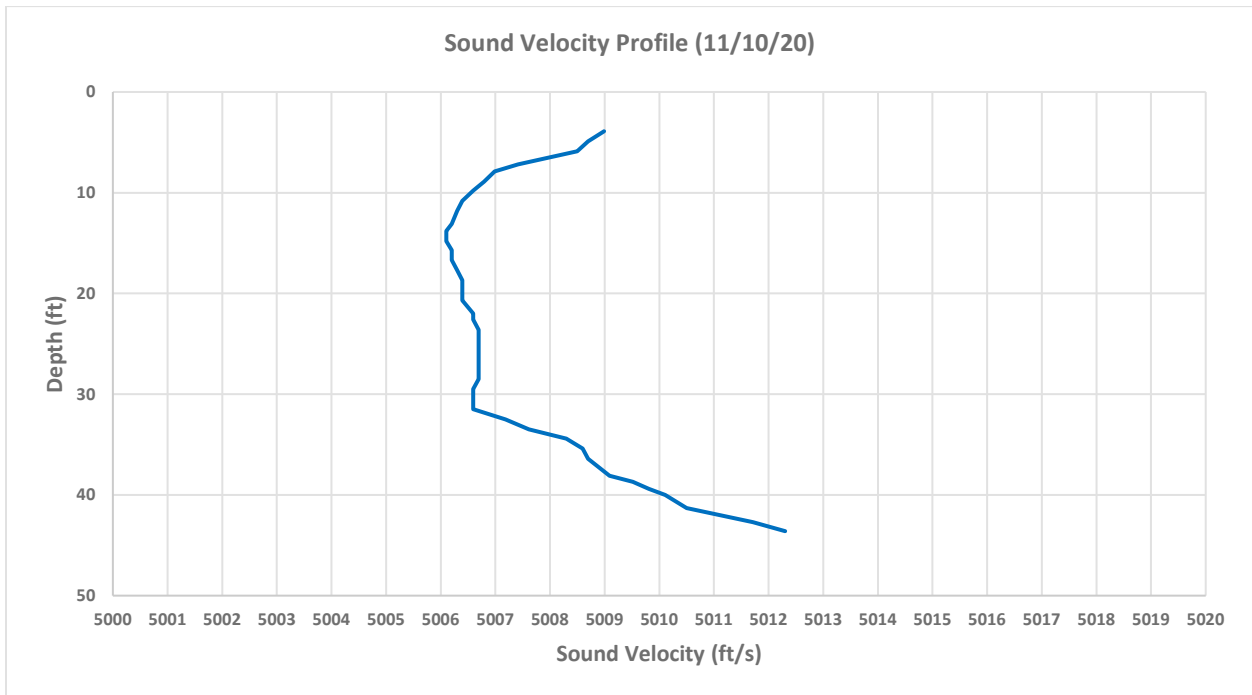


Figure 36. Sound Velocity cast profile example.

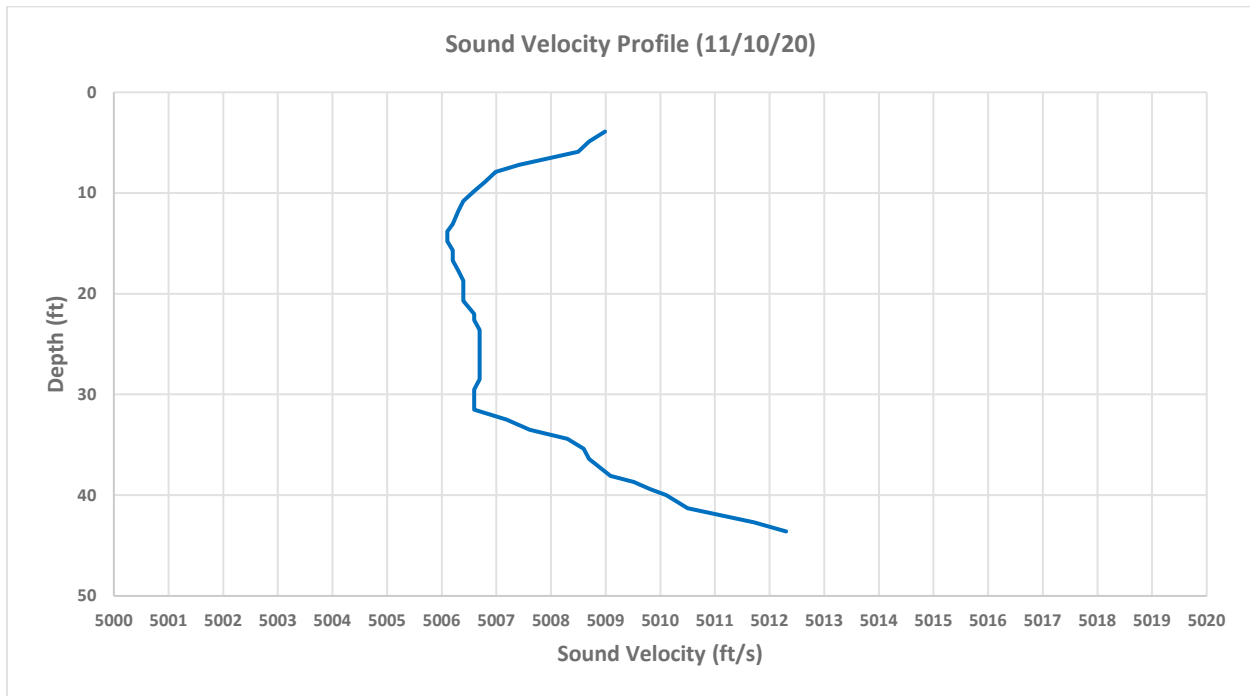


Figure 36. Sound Velocity cast profile example.

Following data collection, all data files were processed using HYPACK’s SBMAX64 program. A full sound velocity profile, tide adjustments and inertial measurement unit corrections were applied and analyzed for inconsistencies. Erroneous soundings were identified and removed within SBMAX64. HYPACK’s SORT Program was used to reduce sounding data and export to an XYZ file used to create bathymetric maps and is presented in **Appendix G**, which is a digital deliverable only and not a digital appendix in text. HYPACK’s Cross Check Statistics program was used to identify potential sounding inaccuracies. Cross Check Statistics provides detailed information regarding differences between data on intersecting lines at a user-defined search radius. The program displays the number of intersections within the given radius, standard deviation, difference mean, arithmetic mean, and minimum/maximum difference between intersections. **Table 3** below shows the Texas OCS Cross Check Statistical Report, generated using all main survey lines and tie lines. A graphical representation of sounding standard deviation is presented in **Figure 37**. Channels or large features within the survey area can have a major effect on minimum and maximum difference depending on the search radius used. These values are not always an accurate representation of uncertainties. Values such as standard deviation, absolute difference mean, and arithmetic mean are of greater importance when performing any quality assurance checks within a given dataset.

Table 3. Texas OCS Cross Check Statistical Report.

Cross-Statistics Analysis	
Number of Intersections	71
Theoretical Number of Intersections	23,051
Search Radius (ft)	25.0
Standard Deviation (ft)	0.381
Absolute Difference Mean (ft)	0.268
Arithmetic Mean (ft)	-0.174
Minimum Diff (ft)	-2.028
Maximum Diff (ft)	0.355

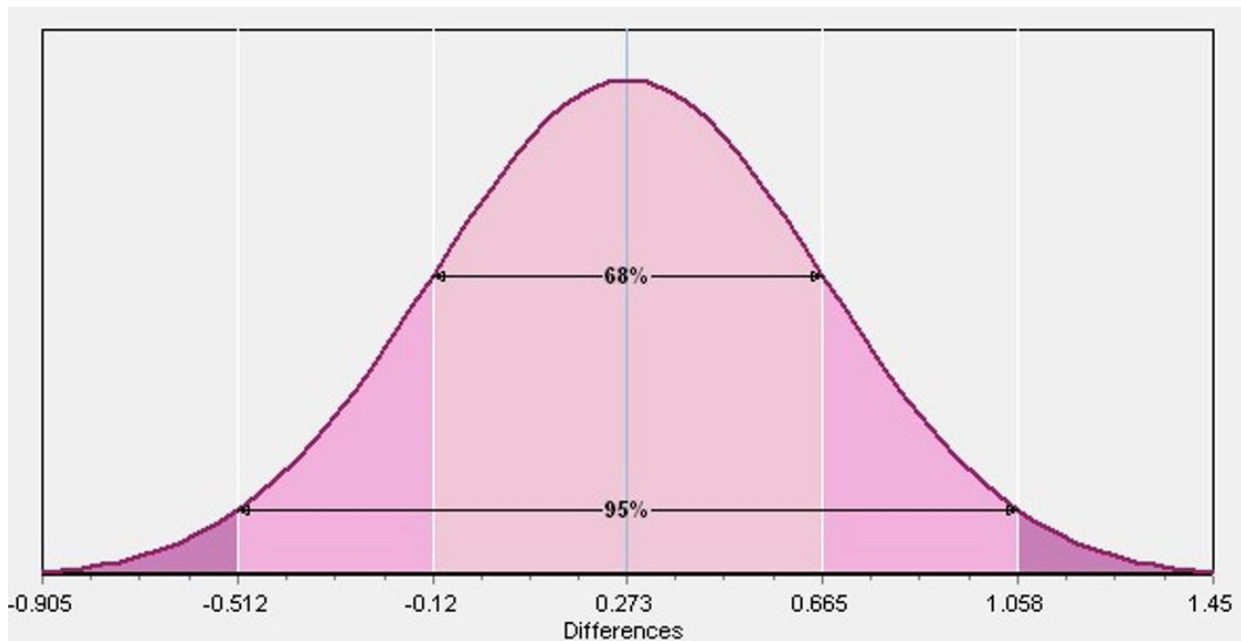


Figure 37. Texas OCS sounding standard deviation chart.

A Trimble SPS 461 Differential GPS system was used for heading and positioning data during operations. A Trimble R8-4 Receiver was also aboard, allowing for post-processing kinematic (PPK) tide corrections. PPK data were processed using TBC and multiple survey days were compared to two of the nearest NOAA water level gauges (8771341 Galveston Bay and 8770822 Sabine Pass) to ensure accurate water level corrections. An example comparison is shown in **Figure 38**.

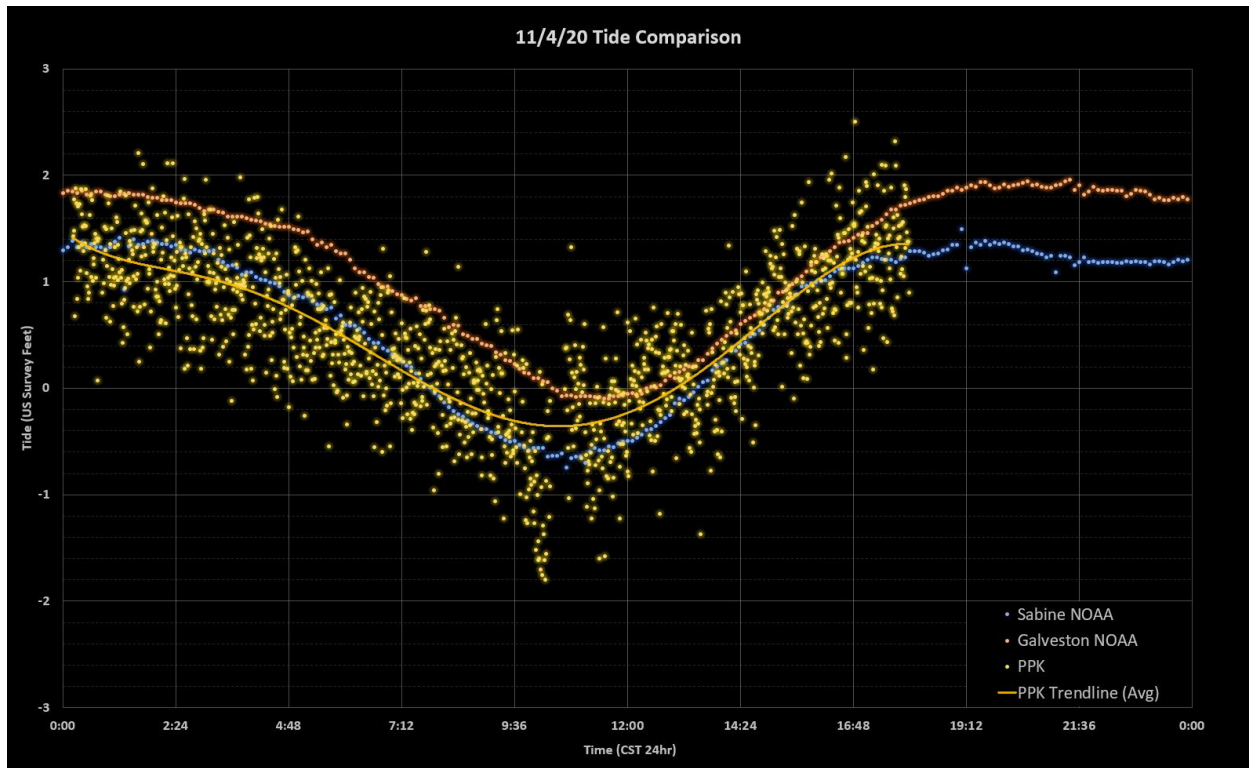


Figure 38. Tide Comparison Plot (11/4/20).

The final tide corrections were solely derived from the NOAA gauge (8770822 Texas Point, Sabine Pass). A base grid file was created with these xyz data using Surfer 21 (with the channel data removed) to interpolate between the data points. A spacing of 300 ft x 300 ft (91 m x 91 m) was used, which was a sufficient resolution for the line spacing that the xyz data were collected. The grid file was opened in ArcCatalog 10.8.2 and a coordinate system was assigned. The file was exported as a raster TIF file so it can be viewed in ArcGIS. The xyz data and the TIF file were opened in ArcGIS and a border shapefile was created, allowing interpolated raster data outside of the study area to be clipped out. To create the channel TIF file, the same procedure was followed, except only the deeper xyz channel data was used. Once the channel and base TIF files were clipped in ArcGIS to the correct extents, the two were merged using the Mosaic to New Raster tool. The deeper channel raster and the base raster were then merged into a single raster file. The raster file was then resampled to use a uniform pixel resolution, and then smoothed. A classified color ramp was applied to the raster file and contours were created based on the elevation of the merged raster TIF file using the Contours tool in ArcGIS.

5.2 Magnetometer Survey

The magnetometer data were processed with HYPACK 2020's Magnetometer Editing software to locate magnetic anomalies. The raw data files were imported into and normalized manually to clean and remove any abnormal spikes or irregularities in the magnetic profile and to account for unwanted interference in the record, such as the survey vessel's effects or environmental and diurnal variations. Objects that possess any ferromagnetic mass (e.g., iron) can be detected with the magnetometer and are indicated by changes in magnetic intensity and visualized as monopoles, dipoles, and multi-component signatures in the profile view of the data. These varying signals distinguish the anomalies from the natural environment.

Each survey line was reviewed and interpreted in detail for the presence of magnetic anomalies. Upon completion of this review, anomalies were plotted and examined together with shapefiles of sidescan sonar contacts, known oil/gas pipelines, wells, and platforms, charted shipwrecks and obstructions, miscellaneous easements, artificial reefs, and buried transmission cables to find associations between the datasets. The **Appendix I** map series shows the extent of the magnetometer data coverage of the investigation area and the spatial distribution of anomalies.

The magnetometer survey data revealed 971 magnetic anomalies within the OCS investigation area, as shown in **Appendix I** and the Magnetic Anomaly Table (**Appendix K**). Anomalies ranged from 5.01 to 18,852.96 nT in amplitude and from 1.69 to 1,961.63 ft (0.51 to 5,901.4 m) in duration. Anomaly signatures consisted of 577 monopolar, 244 dipolar, and 150 multicomponent anomalies. A total of 2 anomalies were potentially associated with, or representative of, side scan sonar contacts, and 412 anomalies were potentially associated with, or representative of, features mapped in the **Appendix P**.

5.3 Sidescan Sonar Survey

Sidescan sonar data were processed using Chesapeake Technologies, Inc. SonarWiz 7 software. The raw sidescan sonar data were imported into two (2) SonarWiz 7 projects, one (1) for low frequency and one (1) for high frequency data processing. Once the data were imported, they were bottom tracked to remove the water column (nadir) recorded in the data. Bottom tracking was achieved by applying an automated bottom tracking routine that determined the first return signal in the data and provided an accurate baseline representation of the seafloor that eliminated the water column from the data. In some cases, manual bottom tracking was necessary when the automated bottom tracking cannot accurately determine the first return in the sidescan sonar record. For these cases, the processor manually determined the first return in the data.

Once the data were bottom tracked, they were processed to reduce noise effects (commonly due to the vessel, sea state, or other anthropogenic phenomenon) and enhance the seafloor definition. All of the sidescan sonar data utilized Empirical Gain Normalization (EGN). An empirical gain normalization table was built including all of the sidescan sonar data files. Once the table was built it was applied to all of the sidescan sonar data. EGN is a relatively new gain function that works extremely well in most situations and can be considered a replacement for Beam Angle Correction. EGN is a function that sums and averages up all of the sonar amplitudes in all pings in a set of sonar files by altitude and range. The

amplitude values are summed and averaged by transducer (port and starboard) so there are actually two (2) tables. A given sonar amplitude sample is placed in a grid location based on the geometry of the ping. On the x-axis of the grid is range, and on the y-axis of the grid is altitude. The resulting table is used to work out the beam pattern of a sonar by empirically looking at millions of samples of data. Due to the sea state and some shallow water conditions observed in portions of the survey area, a small percentage of the sidescan sonar lines contain reduced data quality, resulting in noise and stripes. To try and aid in rectifying the noisy data, the Nadir Filter setting, and a De-Stripe Filter setting were utilized. The Nadir Filter is a special version of the AGC filter that runs only along the nadir stripe. It is designed to reduce the difference between the nadir pixel values and the values immediately outside the nadir. The De-Stripe Filter can be used to reduce the effects of a ‘pitching’ sonar that is characterized by a stripy pattern perpendicular to the direction of travel. This setting processes each ping by comparing the current ping brightness to a filtered version of the sonar file that has smoothed out the stripes.

After processing each line, the data were inspected and interpreted for areas of potential seafloor hazards, geologic formations, as well as other features of interest. Each potential area of interest on a line was digitized or highlighted and a shapefile was created for that particular bottom type. While APTIM geologists utilized the backscatter intensity, distribution, and texture to make best professional interpretations regarding the interpretation of features, it should be noted that these interpretations are based on the acoustic response (**Table 4**). Further ground-truthing is recommended for confirmation of acoustic interpretation.

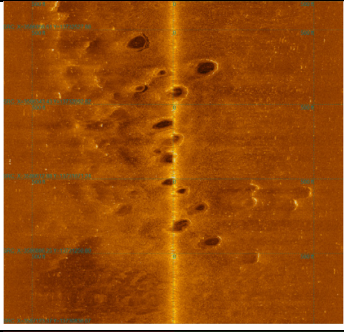
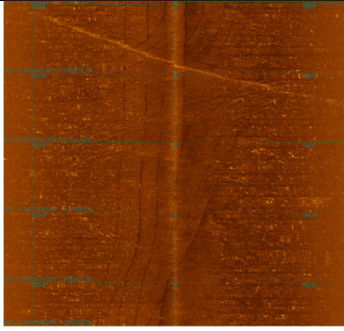
The widely spaced survey lines collected throughout the survey area covering the OCS region were collected with the EdgeTech 4200 towfish which provided a limited image of the seafloor. The maximum range of the system was 230 m (754 ft) on each side, or 460 m (1,508 ft) swath, which was insufficient to allow for full seafloor coverage or interpretation between lines given the 1 nm (6,076 ft) or 5 nm (30,380 ft) tie line spacing of the survey. Therefore, the digitized features were “isolated” to individual lines but provide a general location and description of areas/features of interest. Interpreted maps with digitized features delineated from the sidescan sonar data can be found in **Appendix H**. Identified sidescan sonar targets with magnetometer anomalies can be found in **Appendix I**. The sidescan sonar targets are also included within a contact report in order to highlight specific imagery, size characteristics, and location information of specific targets. The contact report is provided in **Appendix J**.

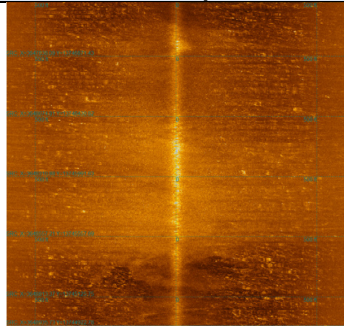
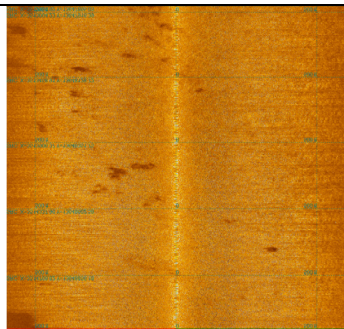
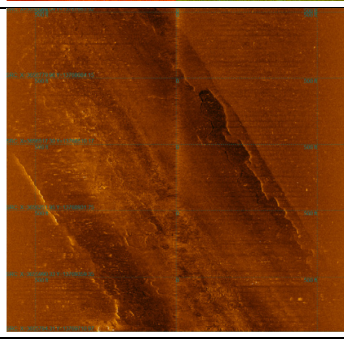
Based on the sidescan sonar interpretations, 179 contacts or targets were identified throughout the survey area. As displayed in **Appendix J**, contacts and targets include unknown debris and features, schools of fish and dolphins, fishing associated features (Shrimp Trawler Scour Marks), anchor scouring, exposed cables, and oil/gas infrastructure (Platforms, Wellheads, Associated Debris, and Exposed Pipelines).

As part of the processing of the sidescan data, APTIM correlated the targeted contacts to shapefiles of hazards, features, and known structures identified as part of the desktop study in order to assist with the classification of the contacts and provide some information on the general characterization of the seafloor. The Oil/Gas infrastructure has been correlated and labeled within **Appendix J** to the BSEE’s provided Platforms and Pipelines shapefiles. Several exposed pipelines and/or cables were identified across the survey area. The Sidescan Sonar Contact Report in **Appendix J** provides segment numbers on each exposed pipeline which were obtained from BSEE.

The vast majority of the survey area consists of sandy bottom (mid to high intensity backscatter) with large areas of high-intensity backscatter material, indicative of coarse sandy sediments, which are associated with both Sabine and Heald banks. Other prominent areas of high-intensity backscatter material, with no visual rippling also provide evidence to the presence of surface sands, which are indicative of smaller shoals within the study area. Areas of pockmarks are observed throughout the survey area. These pockmarks vary in size, but on average are roughly 40 to 60 ft (12.2 to 18.3 m) in diameter. Pockmarks are seabed depressions caused by the removal of seabed sediments by escaping fluids; in most instances, this fluid is gas. They vary in size according to the nature of the seabed sediments and are generally between a few meters and a few hundred meters across, and from less than 3 ft (1 m) to about 66 ft (20 m) deep (Hovland and Judd 1988). An unknown linear feature was identified east of the Sabine Navigational Channel extending for ~9 nm trending ENE to WSW. The sidescan sonar backscatter data displays a linear feature which may be interpreted as an exposed pipeline or a recently buried pipeline. APTIM is unsure of its relation but a dredge barge was identified operating in the area during the survey on November 10, 2020. APTIM has searched BSEE’s pipeline database, and no pipelines are observed in the area which can be associated with this unknown linear feature. APTIM has also searched the USCG District 8 Local Notice to Mariners notifications and could not find any operations in the area which may explain the unknown linear feature.

Table 4. Sidescan sonar bottom feature classification.

Bottom Feature/Description	Example
<p>Pockmarks</p> <p>Low-intensity backscatter formations surrounded by medium-intensity backscatter.</p>	 <p>Line 028.006</p>
<p>Exposed Pipeline/Cable</p> <p>High-intensity backscatter linear feature</p>	 <p>Line 014.002</p>

Bottom Feature/Description	Example	
<p>Sand</p> <p>High-intensity backscatter indicative of coarse sediments</p>		 <p>Line 018</p>
<p>Sand Ripples</p> <p>High-intensity backscatter indicative of coarse sediments with visible waves.</p>		 <p>Line 102.003</p>
<p>Sabine Pass Channel</p> <p>Low intensity</p>		 <p>Line 015.001</p>

5.4 Sub-bottom Profile Survey

Post collection processing of the sub-bottom data was completed using Chesapeake Technology, Inc.’s SonarWiz 7 software. This software allowed the user to apply specific gains and settings in order to produce enhanced sub-bottom imagery that were interpreted and digitized for specific stratigraphic facies relevant to the project goals.

The first data processing step was to calculate the approximate depth of the reflector below the sound source by converting the two-way travel time (the time in milliseconds that it takes for the “chirp pulse” to leave the source, hit the reflector and return to the source) to feet by utilizing an approximate value for the speed of sound through both the water and underlying geology. For this survey, a detailed

hydrographic and geologic sound velocity structure was not available, so APTIM geophysicists used an estimated sound velocity of 1.6 meters per millisecond (m/ms) to convert two-way travel time to feet. This estimate of the composite sound velocity is based on several assumptions including the speed of sound through water which is typically 1.5 m/ms as well as on the speed of sound through the sediment which can vary from 1.6 m/ms for unconsolidated sediment to >1.7 m/ms for limestone.

APTIM geophysicists then processed the imagery to reduce noise effects (commonly due to the vessel, sea state, or other natural and anthropogenic phenomenon) and enhance stratigraphy. This was done using the processing features available in SonarWiz; AGC, swell filter, and a User-Defined Gain Control (UGC). The SonarWiz AGC is similar to the Discover-SB® AGC feature, where the data are normalized in order to remove the extreme high and low returns, while enhancing the contrast of the middle returns. In order to appropriately apply the swell filter and UGC functions, the sub-bottom data was bottom-tracked to produce an accurate baseline representation of the seafloor. Once this was done, through a process of automatic bottom tracking (based on the high-amplitude signal associated with the seafloor) and manual digitization, the swell filter and UGC were applied to the data. The swell filter is based on a ping averaging function that removes vertical changes in the data due to towfish movement caused by the sea state. The swell filter was increased or decreased depending on the period and frequency of the sea surface wave conditions, however, special care was taken during this phase to not remove, or smooth over geologic features that are masked by the sea state noise. The final step was to apply the UGC. The SonarWiz UGC feature allows the user to define amplitude gains based on either the depth below the source, or the depth below the seafloor. For this survey, the UGC was adjusted so that the gain would increase with depth below the imaged seafloor (and not the source), mimicking a TVG. The user was able to remove the noise within the water column, increase the contrast within the stratigraphy, and increase the amplitude of the stratigraphy with depth, accounting for some of the signal attenuation normally associated with sound penetration over time. A blank water column function was also applied to eliminate any features such as schools of fish under the chirp system which produce reflected artifacts within the water column.

The primary objectives of initial sub-bottom data interpretation were three-fold: 1) delineate any surficial deposits that extend throughout the entire study area identified as Seismic Unit Q1, which includes the previously defined banks such as Sabine and Heald, 2) identify paleochannels and/or paleosols that could contain accessible sediments and, if necessary, revise the regional geologic model/framework and 3) inform vibracore locations that will be used to ground-truth geophysical data and provide sedimentological properties of units mapped based on geophysical data.

Processed sub-bottom profiler data were interpreted within SonarWiz. Interpretation involved the identification of seismic reflection horizons that serve as boundaries for different seismic facies packages (**Appendix L**). These horizons can represent erosional unconformities such as the basal scour surface of a lateral migrating fluvial channel, or contacts representing a change in environment and associated lithology such as transgressive flooding leading to estuarine fine-grained sediment draping over a previously exposed floodplain (Reijnenstein et al. 2011). The character of sub-bottom reflection horizons and geometries in continental shelf seismic stratigraphy can often be related to characteristics of silt, clay, sand, and the environment of deposition (**Figure 39**). These principles were used to interpret individual profiles that were combined to develop regional geologic conceptual models, such as defining the paths of

paleo-river channels. These conceptual models helped to identify zones with potential sand-bearing sediment. It must be cautioned that interpretation of lithology using sub-bottom profiler data must always be “ground-truthed” using geologic cores, and in the absence of core data for validation, these interpretations are regarded as preliminary.

Upon completion of interpretation and digitization, the sub-bottom data were exported as a “Web” based project of HTML/JPEG files viewable in standard web browser software packages (**Appendix M**).

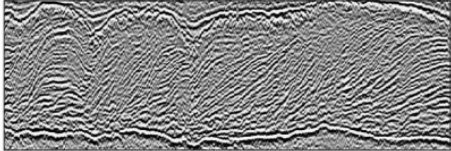
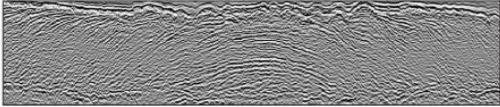

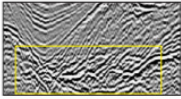
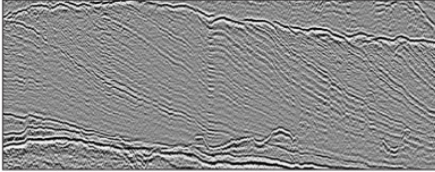
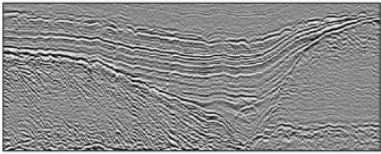
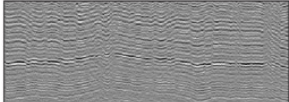
2-D Seismic Facies	Reflection Character / Sedimentologic Interpretation
	<p>Convex-up lateral accretion surfaces. High-amplitude inclined seismic facies</p> <p>Point-bar lateral accretion surfaces as seen in a dip-view cross section; Convex-up geometry with downdip increase in slope: 0.49° to 0.62° (point-bar tops) and 0.48° to 3.74° (basal point bar).</p>
	<p>Convex-up bidirectional downlap; High-amplitude inclined seismic facies</p> <p>Point-bar lateral accretion surfaces as seen in a strike-view cross section</p>
	<p>Low-amplitude chaotic seismic facies</p> <p>Reworked point-bar top deposits</p>
	<p>High-amplitude channel lag seismic facies</p> <p>Basal coarse-grained channel lag</p>
	<p>Concave-up clinoforms; Low-amplitude inclined seismic facies</p> <p>Cliniform deltaic mouth bar deposits; Concave-up geometry with downdip decrease in slope: 1.76° to 2.04° (clinoform tops) and 0.37° to 0.91° (basal section)</p>
	<p>High-amplitude, confined, laterally continuous reflections; Seismic terminations onlap against valley walls</p> <p>Early transgressive estuarine muddy facies</p>
	<p>Low-amplitude (transparent), laterally continuous seismic facies</p> <p>Open marine muddy facies</p>

Figure 39. Example classification of sub-bottom profiler data based on seismic horizon reflection character and geometry.

The first four are representative of sandy fluvial channel belt deposits, and the last three (3) represent deltaic, estuarine, and marine deposition. Modified from Reijnen et al. 2011.

5.4.1 Seismic Unit Quaternary 1 (Q1)

APTIM was able to identify and delineate a surficial unit that is continuous and extends across the majority of the investigation area and includes, but is not limited to, the previously defined bathymetric shoals. APTIM and TWI have named this unit Seismic Unit Quaternary 1 (Q1). Seismic Unit Q1 is defined as the uppermost unit resolved in the chirp data which overlies the transgressive ravinement and is upwardly bounded by the modern seafloor. Its full lateral/horizontal extent/limits are not constrained by the data collected as a part of this study as it extends to the north, west, and east beyond the dataset collected as part of this investigation. This unit forms the bathymetric highs, or shoals, and is laterally conformable across most of the study area and is commonly eroded/not present seaward of the shoals, where the transgressive ravinement appears to be coincident with the modern seafloor. The Seismic Unit Q1 assignment does not specify an environment of deposition or geologic interpretation and is used solely to refer to the uppermost regionally mappable seismic unit. Its seismic character includes acoustically chaotic massive units, laminar bedding, and acoustically transparent units. This unit is described as being Quaternary in age based on its relationship to underlying sediments that have been previously dated, but to avoid being overly specific in the absence of additional data.

Seismic Unit Q1, as defined in this report, includes the previously described Sabine, Heald and Shepard Banks identified within Rodriguez et al. 2005, and Dellapenna 2009 (Section 3.1.6) as well as the previously characterized facies and lithologic units (Facies A, B, C) which were units identified based on detailed geologic cores with paleo-environmental analysis designed to fit a model of coastal shoal evolution that interpreted them as overtopped, drowned, and subsequently reworked barrier islands (Rodriguez et al. 2005). Depending on the exact location, Seismic Unit Q1 may contain some or all of the previously identified units and facies of the various banks and/or surficial sediments. Our Seismic Unit Q1 is agnostic to specific environment of deposition or process as it is based on observed seismic facies which are variable within the bounding surfaces, indicating likely significant variability that requires further geological data to constrain. Additionally, contained within Seismic Unit Q1 are the Marine Minerals Information System (MMIS) Modeled Shoals, which represent bathymetric highs relative to the surrounding seafloor and include Sabine, Heald, Thomas, and Shepherd Banks. Much like Seismic Unit Q1, the Modeled Shoals appear to be a seismic unit constrained by the transgressive ravinement below and upward by the modern seafloor and so coincide with the Seismic Unit Q1.

Based on available historical geologic datasets the sediment composition of Seismic Unit Q1 is highly variable. Historic geotechnical data (**Figure 40**) were utilized to assist in the assessment of the properties of Seismic Unit Q1, however, existing vibrocore coverage is not sufficient for the delineation of sedimentologic and/or stratigraphic facies within the unit and serve more as a sparse baseline of sedimentological data to guide initial interpretation and inform future geological data collection needs. Additionally, historic datasets do not always provide a proper granulometric analysis, instead ranging from visual descriptions to modern grain size techniques. We identify five (5) general sediment classes from historic data that samples Seismic Unit Q1, which we detail in **Table 5**. These classes are solely a description of sediment types found in the region, and are not indicative of specific internal stratigraphic layers/units within Seismic Unit Q1. We provide a color code to represent these lithologic classes and serve as a visualization tool to be utilized when visualizing cores against the seismic data. As previously mentioned, the existing vibrocore coverage is not sufficient for the delineation of sedimentologic and/or

stratigraphic facies, therefore, we preliminarily find that Seismic Unit Q1 has variable sedimentological properties that range from 20-100% sand and additional geotechnical data collection is necessary in order to further constrain and quantify the areas of higher sand content within the Seismic Unit Q1, and identify sub-regions and units with the highest sand content.

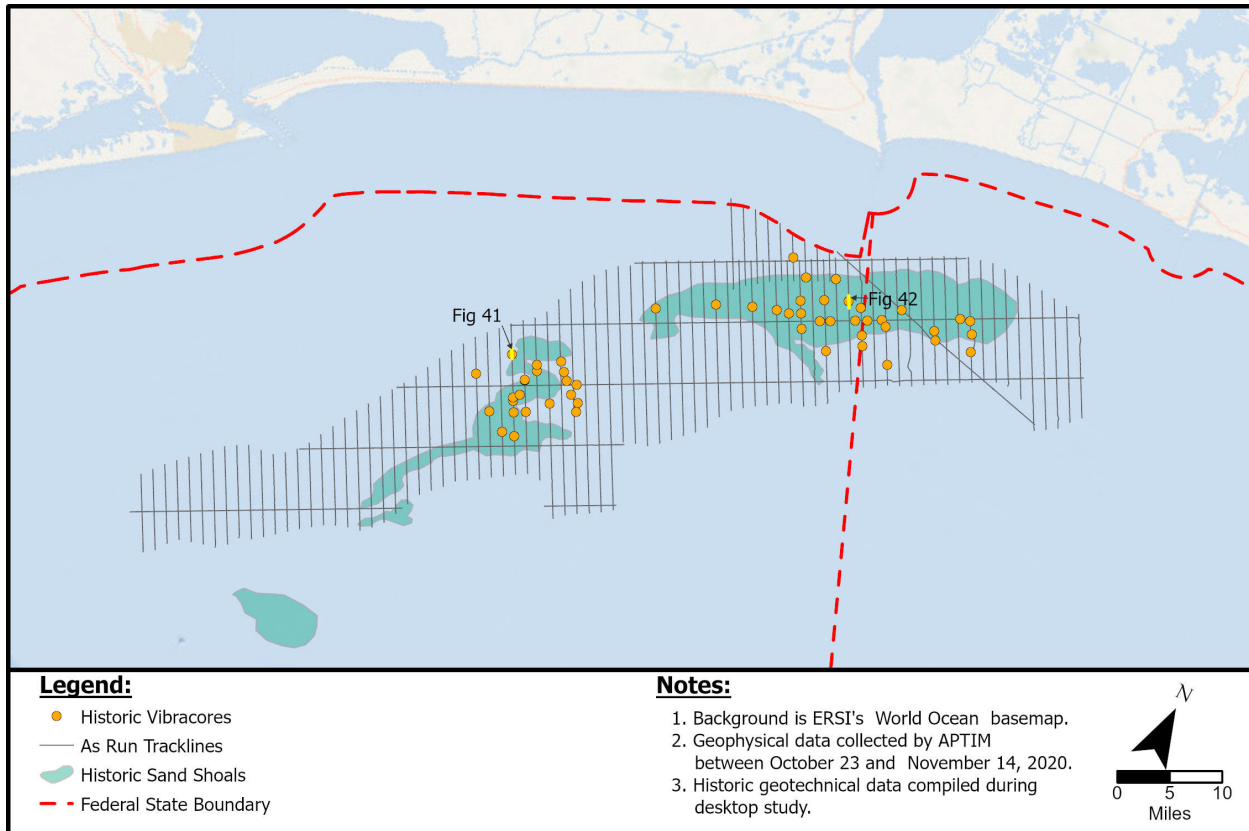


Figure 40. Historic vibracores utilized for geophysical data interpretation.
References to geotechnical data are part of the Desktop Study report submitted in **Appendix A**.

Table 5. Historic vibracore classification scheme.

Seismic Unit	Color Code	Sedimentological Properties
Seismic Unit Q1 (Purple)	Blue	Shelly, gravelly sands
	Green	>60% sand
	Yellow	40%-60% sand, fine grain sands
	Orange	20%-40% sand, muddy sand
N/A	Red	Clays, organic, mud

In order to correlate the historic vibracores and the seismic data, bottom tracked chirp sub-bottom profile lines were opened in SonarWiz to digitally display the recorded subsurface stratigraphy. Using the software's Sonar File Manager, color-coded vibracore descriptions were added directly to the chirp sub-bottom profiles. Using the color-coded vibracore descriptions as a guide, the chirp sub-bottom stratigraphy was interpreted and the stratigraphic reflector that best correlated to the transgressive ravinement was digitized within SonarWiz to create a color-coded boundary. These boundaries appear on the subsequent chirp sub-bottom imagery to allow for an easy, visual reference for the boundary representing the bottom of the Seismic Unit Q1. In areas with lacking geotechnical data (such as the southern portion of Heald Bank and Shepard Bank), the digitization was conducted utilizing the intersection feature within SonarWiz and cross-referencing lines to trace what is the bottom of Seismic Unit Q1. This boundary was used within SonarWiz to compute the thickness of the Seismic Unit Q1 (purple highlight) by calculating the distance between the digitized seafloor and the transgressive ravinement (Figure 41 and Figure 42).

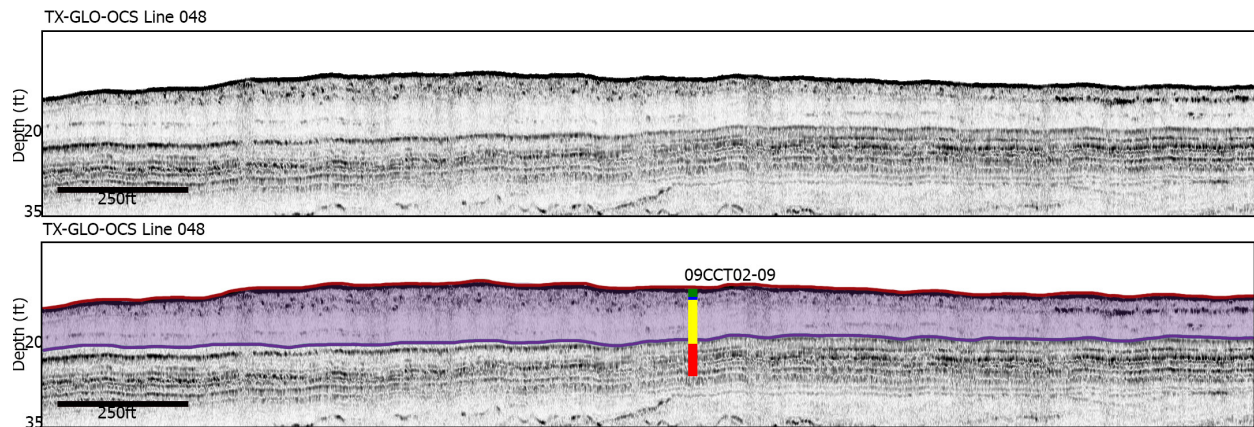


Figure 41. Seismic line 048.001.

The bottom of the Seismic Unit Q1 (transgressive ravinement) digitized in purple and highlighting the Seismic Unit Q1 thickness, with a historical vibracore collected as part of the 09CCT02 cruise (see Table 5 for vibracore color classification scheme).

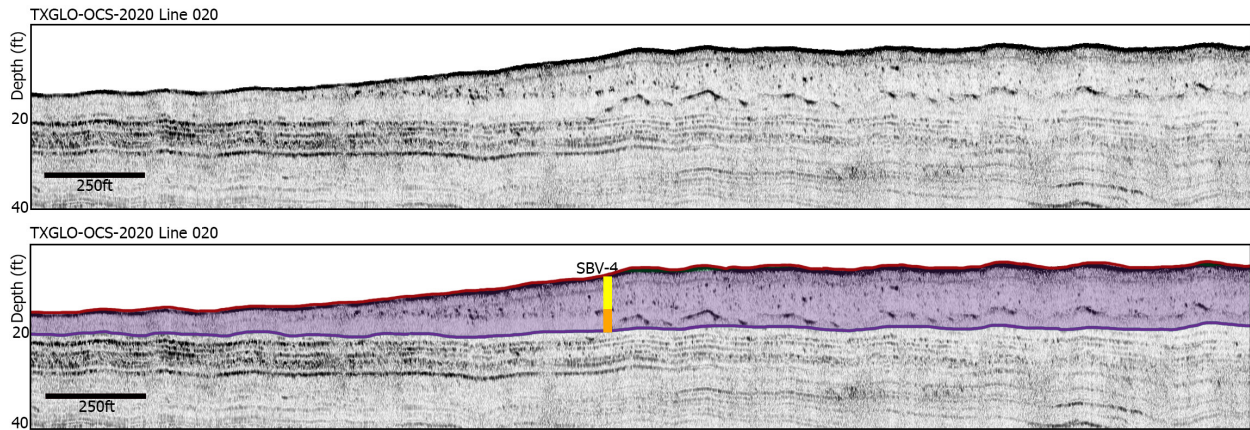


Figure 42. Seismic line 020.001.

The bottom of the Seismic Unit Q1 (transgressive ravinement) digitized in purple and highlighting the Seismic Unit Q1 thickness with a historical vibracore collected as part of the Morton and Gibeaut 1993 study report (see **Table 5** for vibracore color classification scheme).

An isopach (thickness as xyz) of the Seismic Unit Q1 was exported from SonarWiz, imported into Surfer 17, and gridded to create an interpolated surface depicting the general trend of the unit within the area (**Appendix N, Figure 1**). It is important to note that due to the wide line spacing, some smaller shoals within Seismic Unit Q1 could have been missed or the overall extents under-sampled due to gaps in the data coverage. As shown in **Figure 43**, Seismic Unit Q1 extends beyond the boundaries of the study area as well as the previously delineated Sabine, Heald and Shepard Banks, while containing these bathymetric features. Additionally, smaller shoals identified during the desktop study seaward of the northern portion of Heald Bank and on the southern and seaward end of Sabine Bank identified within MMIS Modeled Shoals are also contained within Seismic Unit Q1. Additional geotechnical data is necessary in order to determine the sedimentological properties of these areas within Seismic Unit Q1.

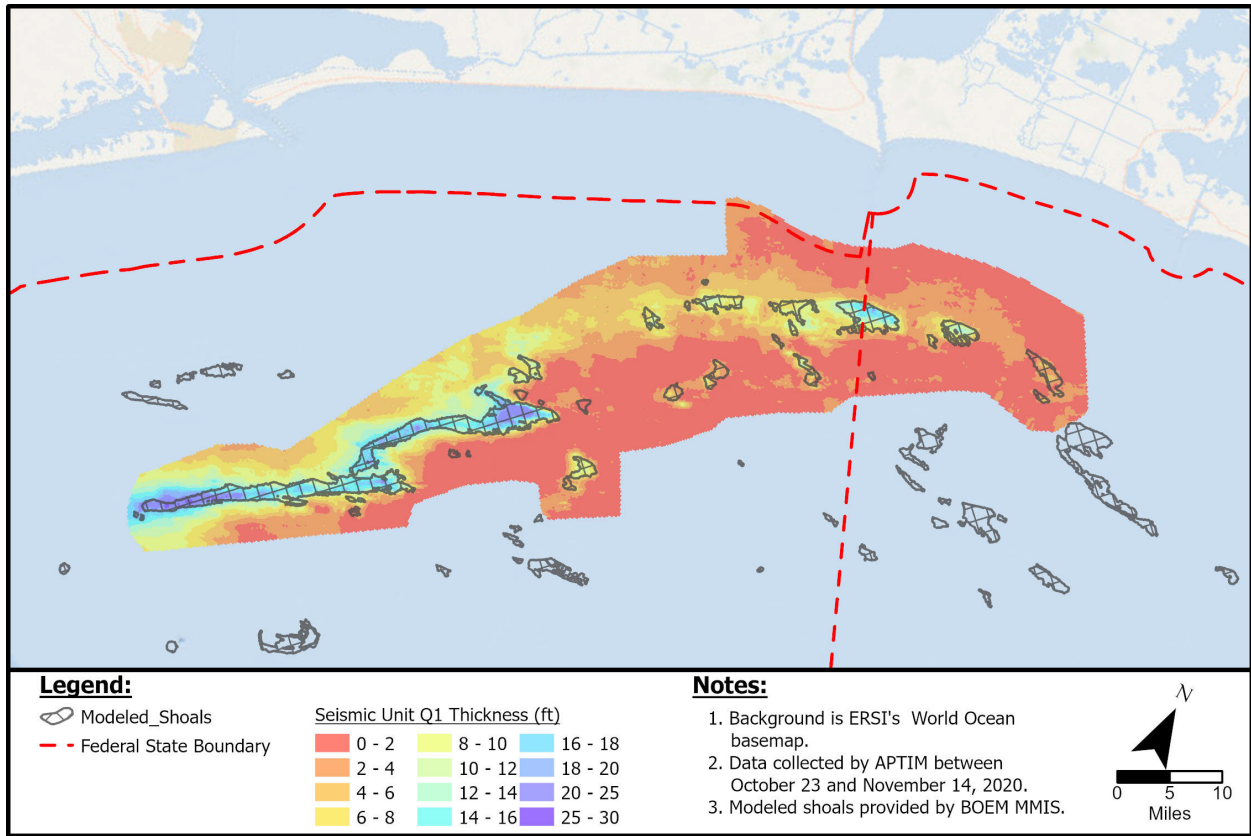


Figure 43. Seismic Unit Q1 isopach generated by APTIM compared to the Modeled Shoals provided by BOEM MMIS.

Confirms the findings of the seismic data interpretation and shoal delineation.

Once the thickness was gridded, APTIM conducted a preliminary volume calculation on Seismic Unit Q1 to determine the potential sediment contained within the unit. The volume presented in **Table 6** represents the potential gross volume above a zero-thickness plane. Additional geotechnical data are necessary in order to properly characterize the composition of this deposit and assess its variability throughout the entire area and further constrain its properties beyond likely containing 20-100% sand.

Table 6. Calculated potential gross volume.

Surface	Gross volume (cubic yards)
Seismic Unit Q1	5,920,850,000

5.4.2 Interpretation of Paleochannels, Potential Sand-Bearing Features, and Development of the Regional Geologic Model

In tandem with the mapping of features, interpreted surfaces were correlated where possible to generate the preliminary regional geologic model. This effort focused on identifying major regional fluvial systems responsible for delivering sediment to and constructing the shelf and interpreting the stratigraphy across the study area to provide for a conceptual model of regional framework geology linking sediment sources and sinks. The regional geologic model is built by systematically mapping the location, extents, and characteristics of these large-scale features and can be used to identify areas which are likely to contain sand-bearing stratigraphic elements. Potentially significant sand-bearing elements identified in the mapping and creation of the model have surfaces and isopachs generated from the mapped seismic horizons (**Figure 44**).

Overall, the east Texas OCS contains a significant number of potential sand-bearing units located within the study area in the form of fluvial deposits and sand bank/sheet features. The identified fluvial features are regionally correlative for 5-15 mi (8-24 km), outside of the major Sabine Incised Valley. Importantly, potential sand-resource bearing stratigraphy are interpreted with as little as 20 ft (6.1 m) of overburden across the study area on the seaward side of the Sabine incised valley, nearly all of which have never been previously identified. These potential resources have a gross volume of roughly 2.1 BCY (not including overburden) that could be available for future restoration efforts (**Table 7**). The following sections summarize the main findings for each stratigraphic unit.

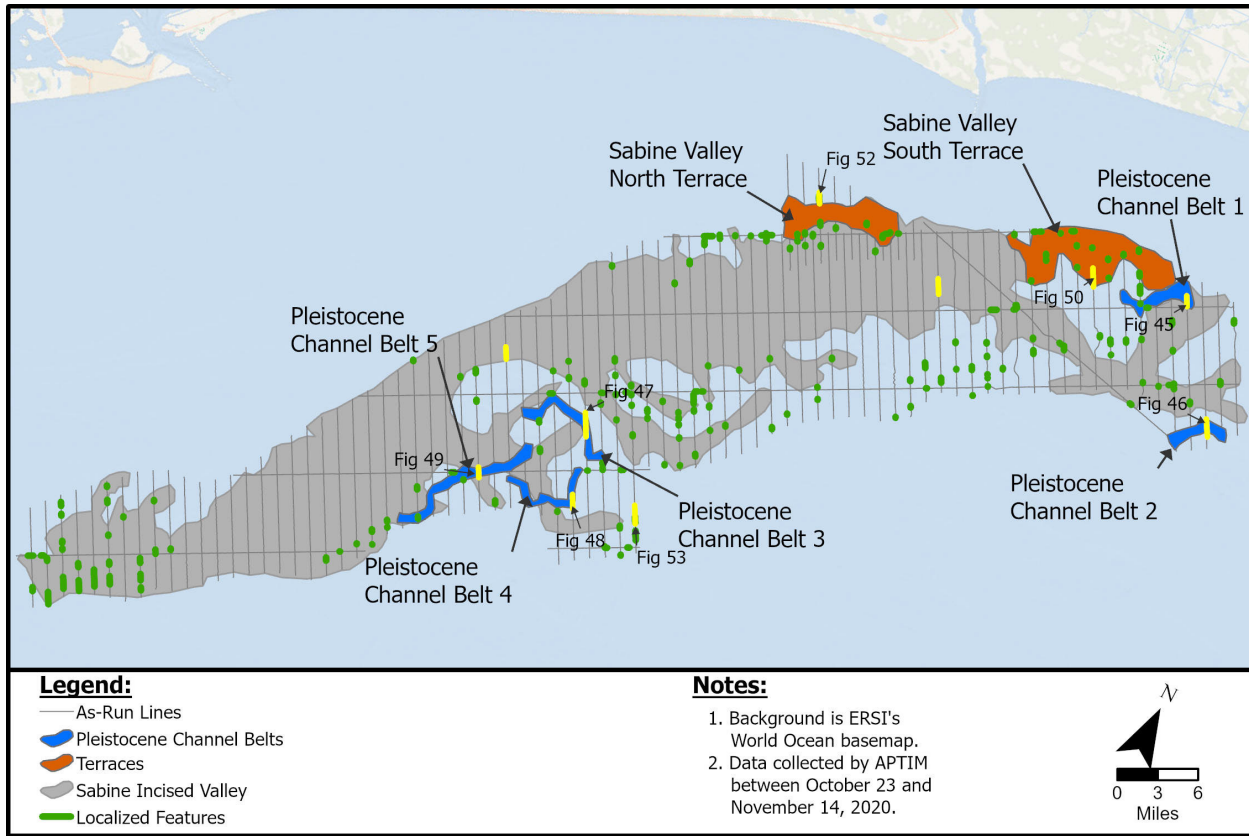


Figure 44. Mapped sub-surface geologic features.
Localized sub-surface features within the eastern OCS, offshore Texas.

5.4.2.1 Pleistocene Fluvial Channel Belts

Several potential sand-bearing stratigraphic units were identified within the study area, all located seaward of the main Sabine incised valley. Five discrete regionally conformable channel belts are interpreted and mapped in addition to numerous smaller channel forms and potential sand-bearing deposits located across the region that are not easily mappable from line to line. The easternmost channel belt features in the region are those located east of Sabine Pass (Channel Belts 1 and 2; **Figure 45** and **Figure 46**). These features are characterized by a basal erosional unconformity, when resolved on sub-bottom profiles, and overlaid by variable-amplitude, steeply-dipping clinoforms and occasional areas of semi-transparent to chaotic acoustic facies. The upper portion of these units is characterized by either a transition to a more-layered seismic facies or are truncated by transgressive ravinement. The potential sand-bearing portion of Channel Belt 1 is 25-50 ft (7.6-15.2 m) thick with 0-10 ft (0-3 m) of overburden. This channel belt is incisional within Beaumont Pleistocene stratigraphy. The overall orientation of Channel Belt 1 is northeast-southwest, similar to the trend of the Sabine Incised Valley (**Figure 44**). In

some portions to the east, the channel belt is cross-cut by a younger incisional drainage which appears to be a tributary flowing into the main Sabine Incised Valley.

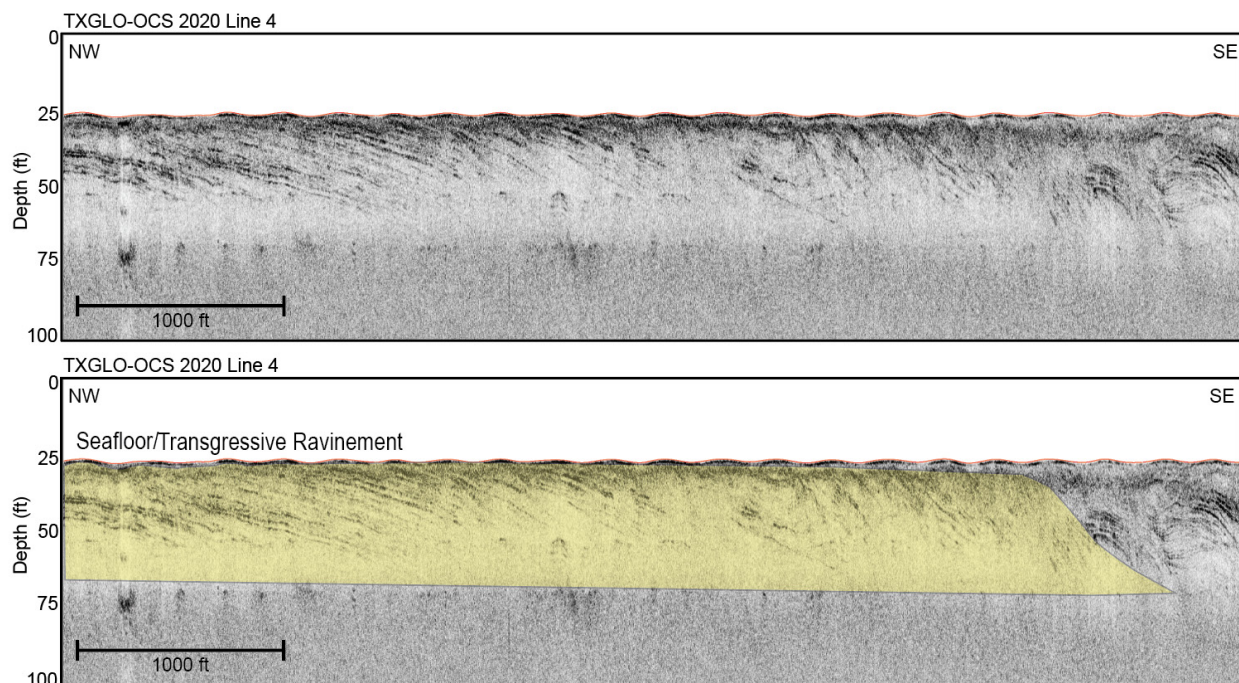


Figure 45. Example sub-bottom profiler data across Channel Belt 1.

Potential sand-rich clinoforms are highlighted in yellow. Note the relative absence of overburden.

Channel Belt 2 is also characterized by steeply-dipping clinoforms, occasionally semi-transparent to chaotic acoustic facies, and a basal erosional unconformity when resolved on the sub-bottom profiler record (**Figure 46**). Potential channel bar unit thickness is between 20-50 ft (6.1-15.2 m), with 0-5 ft (0-1.5 m) of overburden. Similar to Channel Belt 1, the channel belt is oriented northeast-southwest along the seaward flank of the Sabine incised valley. Also notable is the minimal overburden along the majority of the mapped feature extent. For much of the course of the channel belt, the seafloor appears erosional or non-depositional, with potential sand-rich clinoform packages outcropping at the seafloor (**Figure 46**).

Based on the stratigraphic architecture and seismic facies relationships present, where sand-rich paleochannel deposits (of Channel Belts 1 and 2) outcrop at the seafloor and underlie the shoals, a likely scenario is that the ravinement of these units provided a major source of sand that was subsequently reworked into the barrier systems that evolved into the modern shoals.

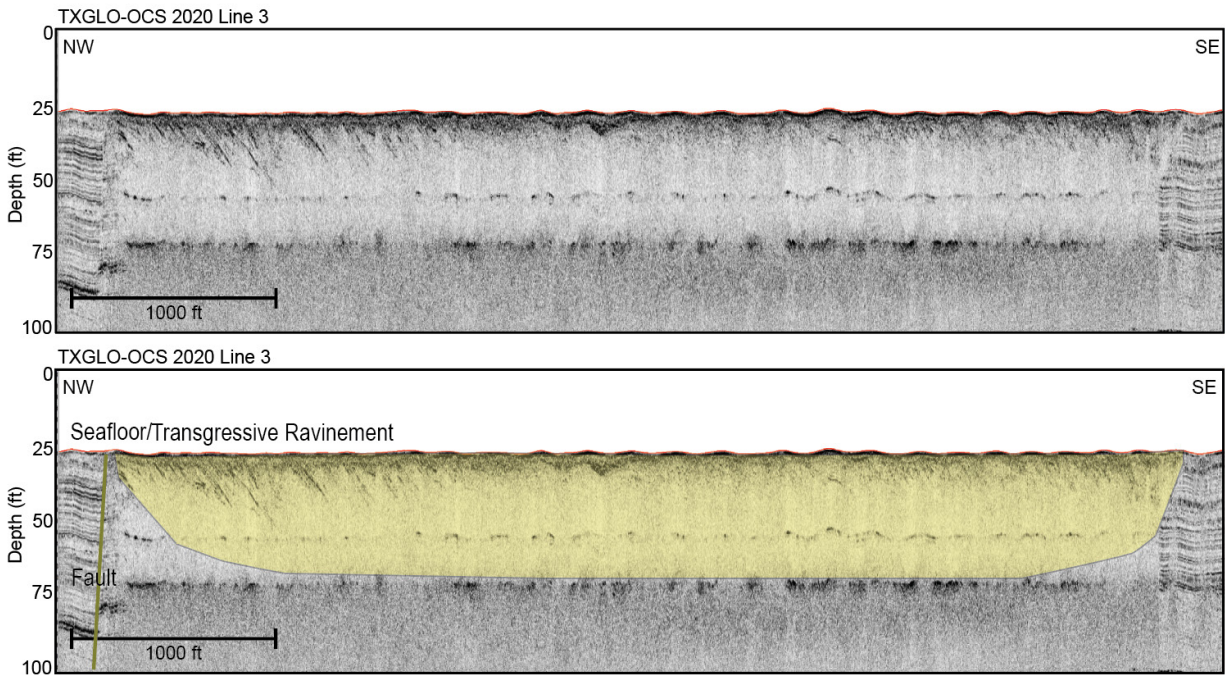


Figure 46. Example sub-bottom profiler data across Channel Belt 2.
Potential sand-rich clinofolds are highlighted in yellow.

The next set of large regional features (Channel Belt 3, 4 and 5; **Figure 47**, **Figure 48**, and **Figure 49**) are located in the central part of the study area, seaward, and under Heald Bank (**Figure 44**). These channel belt systems show variable geometry and occasional cross-cutting by incisional drainages feeding into Sabine Valley that poses challenges to interpretation, but overall can be mapped regionally for 5-15 mi (8-24 km) (**Figure 43**). All the potential channel belt features are composed of basal erosional unconformities overlain by steeply-dipping clinofolds that grade into U-shaped channel forms at the edge of the belt deposit (**Figure 47**). The potential sand-rich channel bar stratigraphy comprising the majority of the channel belt unit are 20-50 ft (6.1-15.2 m) thick with 0-20 ft (0-6.1 m) of overburden. Similar to those observed further to the northeast, many of the clinofolds appear to outcrop at the seafloor.

These systems are occasionally interrupted and eroded by the subsequent formation and incision of the Sabine valley and associated tributary drainages (**Figure 41** and **Figure 46**). The depth of this erosion and reworking is variable, but 5-15 mi (8-24 km) lengths of individual channel belts are still conformable. The most significantly eroded feature is Channel Belt 5 (**Figure 49**), which is the closest to the edge of the main trunk of the Sabine incised valley (**Figure 44**).

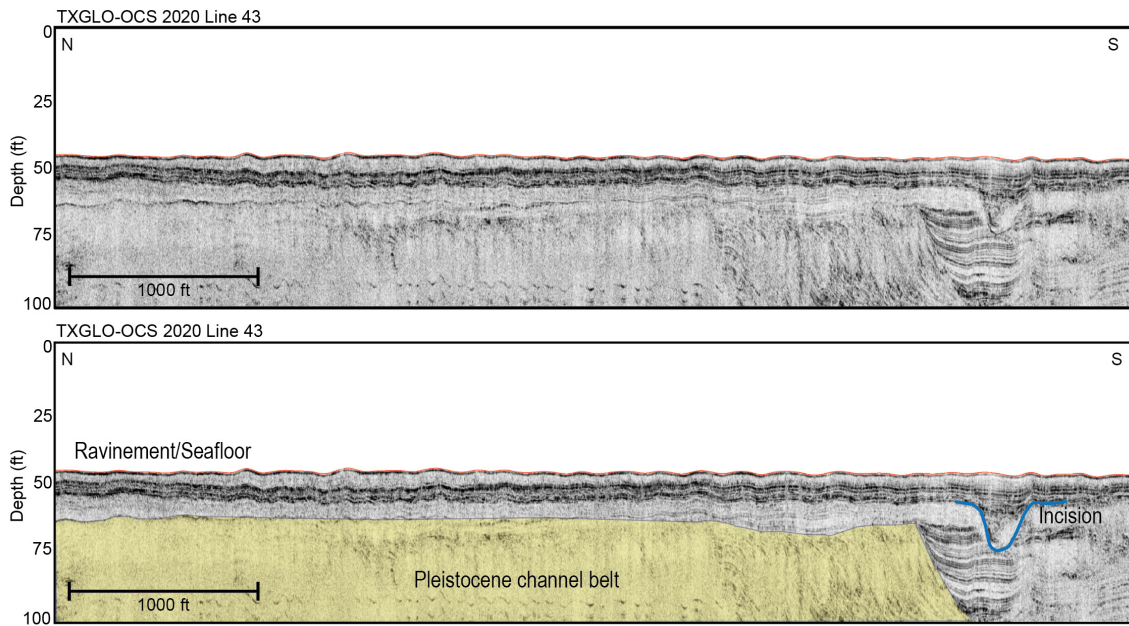


Figure 47. Example sub-bottom profiler data across Channel Belt 3.

Thick clinoform packages grading into a more layered channel form. The stratigraphic unit is incised again by a later generation of drainages.

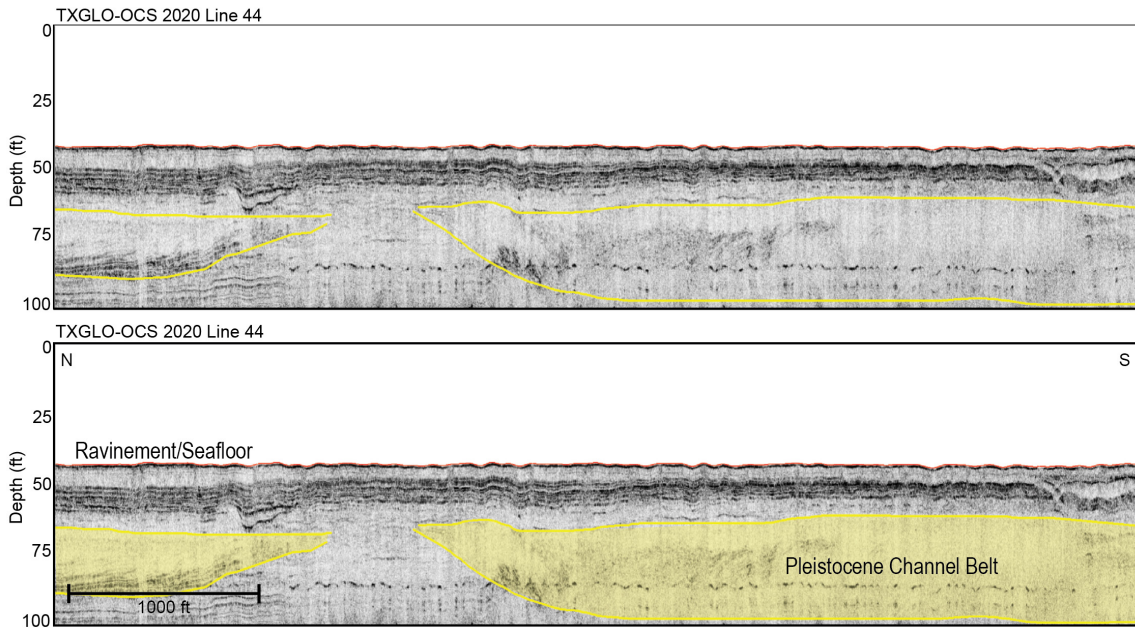


Figure 48. Example sub-bottom profiler data across Channel Belt 4.
Steeply dipping clinoforms composing the majority of the potential fluvial stratigraphic body.

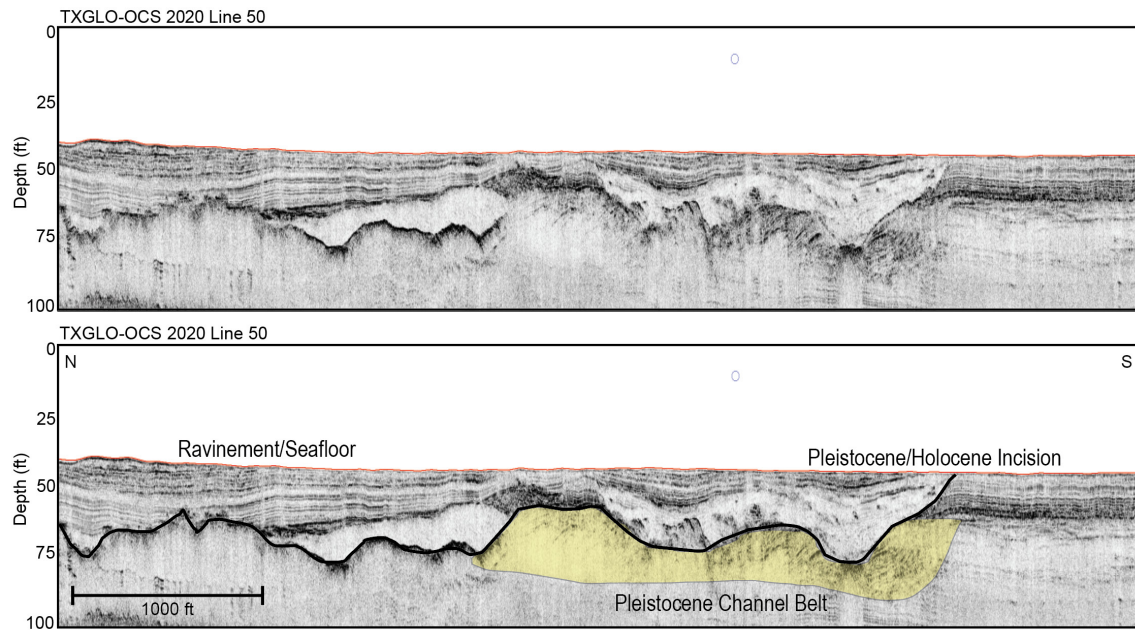


Figure 49. Example sub-bottom profiler data across Channel Belt 5.
Incision of potential channel belt point bar stratigraphy by a later generation of drainage formation.

5.4.2.2 Sabine Incised Valley and Terraces

The majority of the OCS survey area coincides with the location of the Sabine incised valley which trends northeast-southwest below the modern Sabine Pass before turning west (**Figure 44**; Anderson et al. 2015). At the northern edge of the northern portion of the survey area there are regions of relatively shallow, potentially sand-bearing deposits, the North and South Sabine Pleistocene Fluvial Terraces that may relate to fluvial terraces formed during the most recent falling stage and lowstand given their proximity to the Sabine incised valley. Both North and South terraces occupy areas immediately adjacent to the more deeply incised Sabine valley. The North and South Sabine Pleistocene Fluvial Terraces are characterized by steeply-dipping clinoforms that reach thicknesses of over 75 ft (22.9 m), and the base of which is not resolved on most chirp lines (**Figure 50**). These clinoforms often grade into channel fill seismic facies, with an associated transition to more layered seismic facies. The top of the clinoforms have a high-amplitude strong acoustic return and between zero and 15 ft (4.6 m) of overburden. The size of these clinoforms within the interpreted terraces are substantially larger than those observed within the modern and Holocene Sabine River, which is similar to the size differential observed within the coastal Sabine River valley where the Pleistocene Deweyville terraces preserve much larger fluvial channels than the modern system (Blum and Tornqvist 2000).

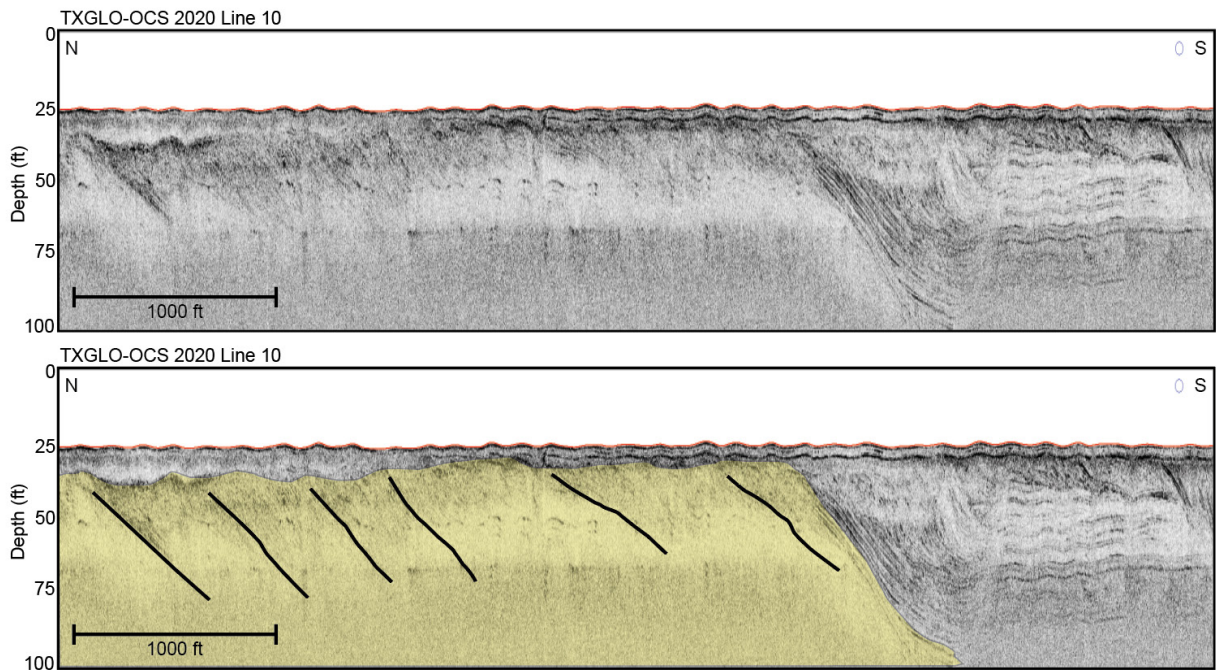


Figure 50. South Sabine Fluvial Terrace.

The Sabine Incised Valley itself has a similar internal stratigraphic architecture to that observed within the Trinity Valley and as observed by prior work (Thomas and Anderson 1994; Anderson et al. 2015).

The actual base of the valley is not resolved because it underlies a unit with a very high-amplitude acoustic return and little penetration beyond that (**Figure 51**). These facies are commonly observed within the Trinity and Sabine valleys and this basal unit correlates with an amalgamated sand-rich fluvial unit formed during the lowstand and early stage of the transgression (Swartz 2019). The basal unit is overlain by layered stratigraphy that is likely deltaic-estuarine in origin (Thomas and Anderson 1994). The thickness of the overlying estuarine unit is often 30-40 ft (9.1-12.2 m), but in some areas within the valley the fluvial section appears to shallow significantly to within 10 ft (3 m) of the seafloor (**Figure 51**). These shallow sections may represent terraces or late avulsions of the Holocene Sabine during the transgression and may be the most accessible fluvial sand-bearing stratigraphy within the Holocene valley itself. In general, however, the extent and thickness of the estuarine overburden limits the potential use of the basal valley sediments as a sand resource and so we do not quantify it within this report, but include it as a regionally important geologic feature.

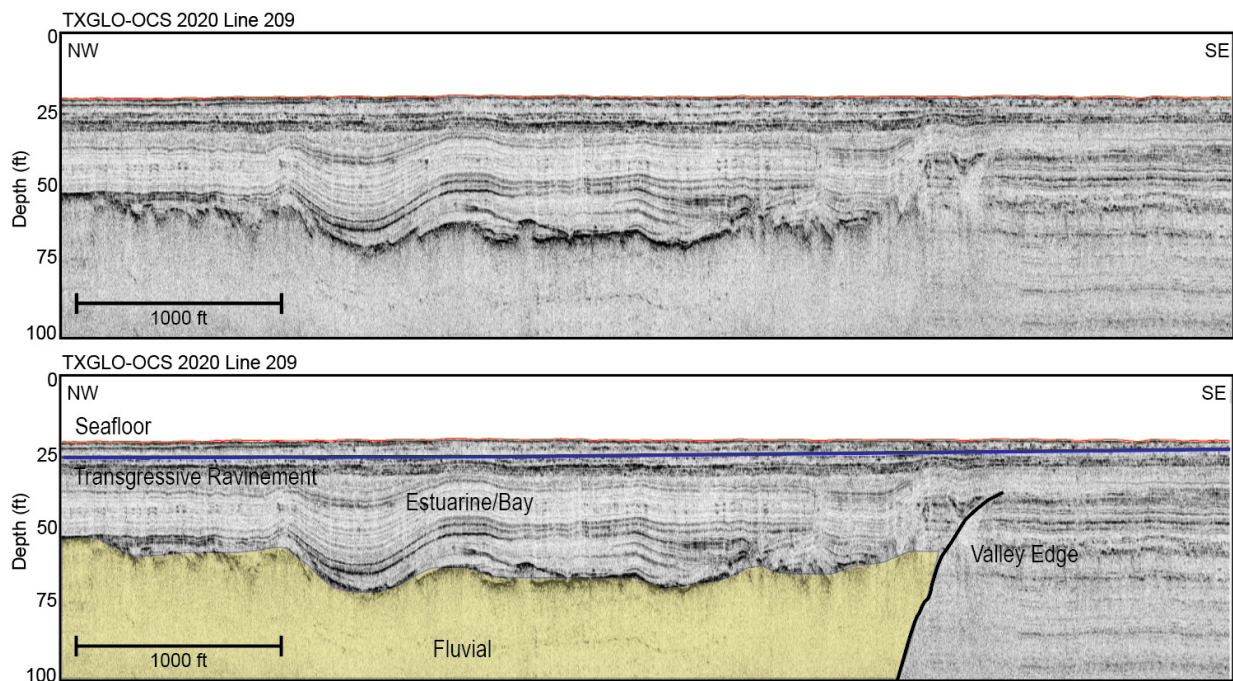


Figure 51. Sabine Incised Valley stratigraphy.

Table 7. Potential gross volume identified within study area.

Gross sediment volume does not include overburden.

Feature Name	Interpretation	Area (sq.ft)	Average Stratigraphic Unit Thickness (ft)	Average Overburden Thickness (ft)	Gross sediment volume (MCY)	Example Data Figure No.
Pleistocene Channel Belt 1	Pleistocene fluvial channel belt	125,430,000	31	0-10	121	Figure 45
Pleistocene Channel Belt 2	Pleistocene fluvial channel belt	85,460,000	18	0-5	49	Figure 46
Pleistocene Channel Belt 3	Pleistocene fluvial channel belt	149,300,000	14	0-20	78	Figure 47
Pleistocene Channel Belt 4	Pleistocene fluvial channel belt	116,020,000	7	0-20	67	Figure 48
Pleistocene Channel Belt 5	Pleistocene fluvial channel belt	219,030,000	20	0-20	107	Figure 49
Sabine South Terrace	Incised valley fluvial terrace	822,470,000	41	0-15	1240	Figure 50
Sabine North Terrace	Incised valley fluvial terrace	459,110,000	40	0-15	472	Figure 50
Sabine Incised Valley	Pleistocene/Holocene fluvial channel belt	n/a	n/a	n/a	n/a	Figure 51

5.4.3 Localized Features

In addition to the geologic features identified in Section 5.4.2, smaller, isolated features were also identified during data interpretation. These features are normally smaller pockets incised within the larger features (**Figure 52** and **Figure 53**) and have inconsistent stratigraphic properties between lines, which makes their correlation and delineation as a geologic feature potentially imprecise and/or incorrect, requiring additional geophysical and geotechnical data for further delineation. These areas (**Figure 54**) are characterized by their stratigraphic sequence and internal stratigraphy (or lack thereof) and the known properties of sediments that normally cause these types of attenuation and depositional patterns. Areas with specific sand-indicative depositional patterns (described in the sections above) were highlighted as part of the data interpretation phase of the project and some were targeted with vibracores since they have high sand-bearing potential. Lines with adjacent feature picks were analyzed for potentially correlative features that may indicate a larger depositional pattern/unit. If this assessment was inconclusive, the identified features were labeled as localized deposits which require additional geophysical data coverage to determine the boundaries of the deposit. As previously mentioned, additional ground-truthing would be necessary in order to verify and validate these potential deposits as a viable sediment resource.

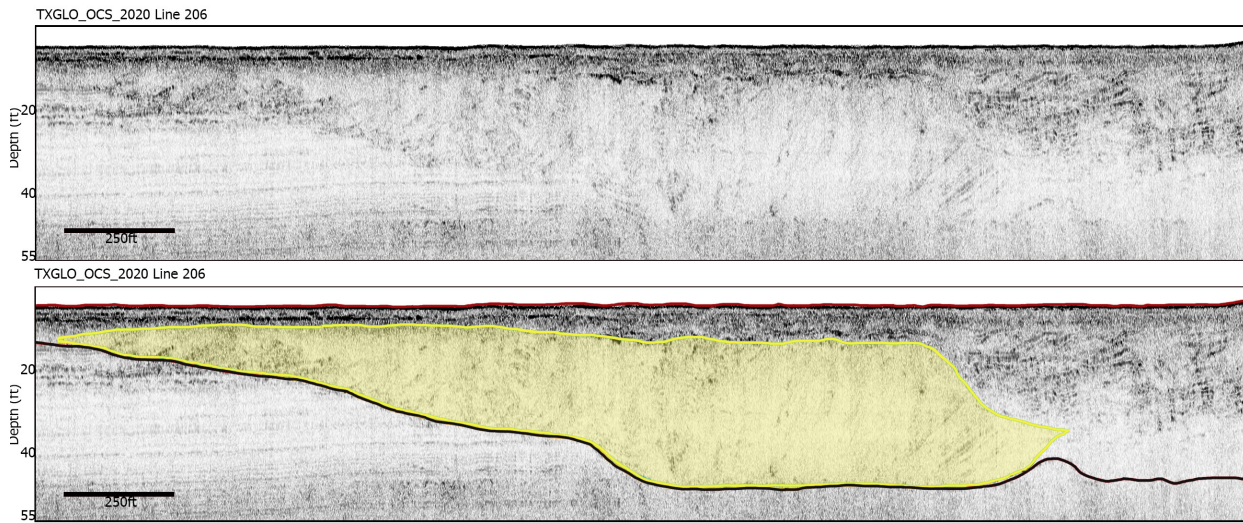


Figure 52. Localized potential sand deposit (yellow) in paleochannel (black) on seismic Line 206.

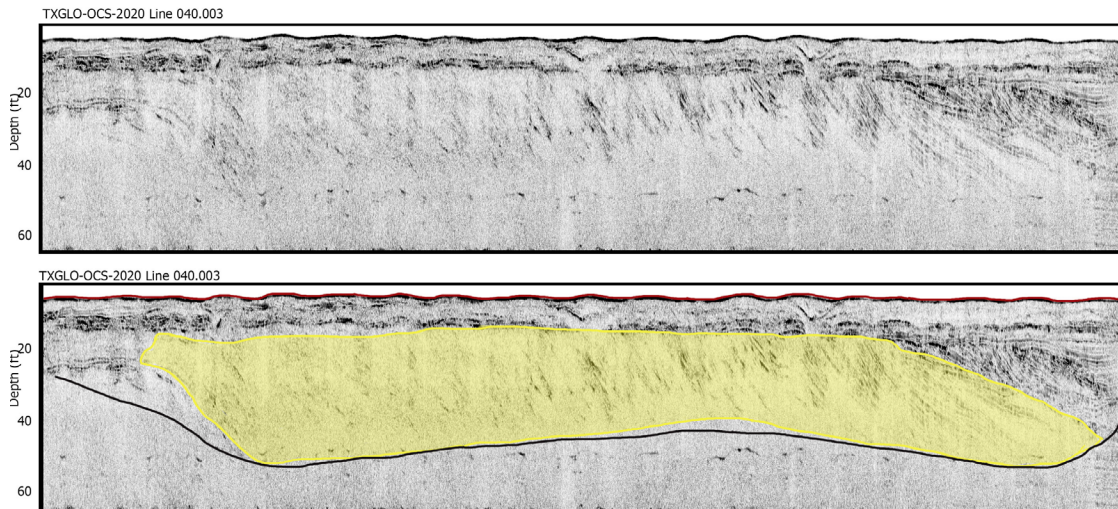


Figure 53. Seismic Line 040.003.
Localized potential sand deposit (yellow) in paleochannel (black).

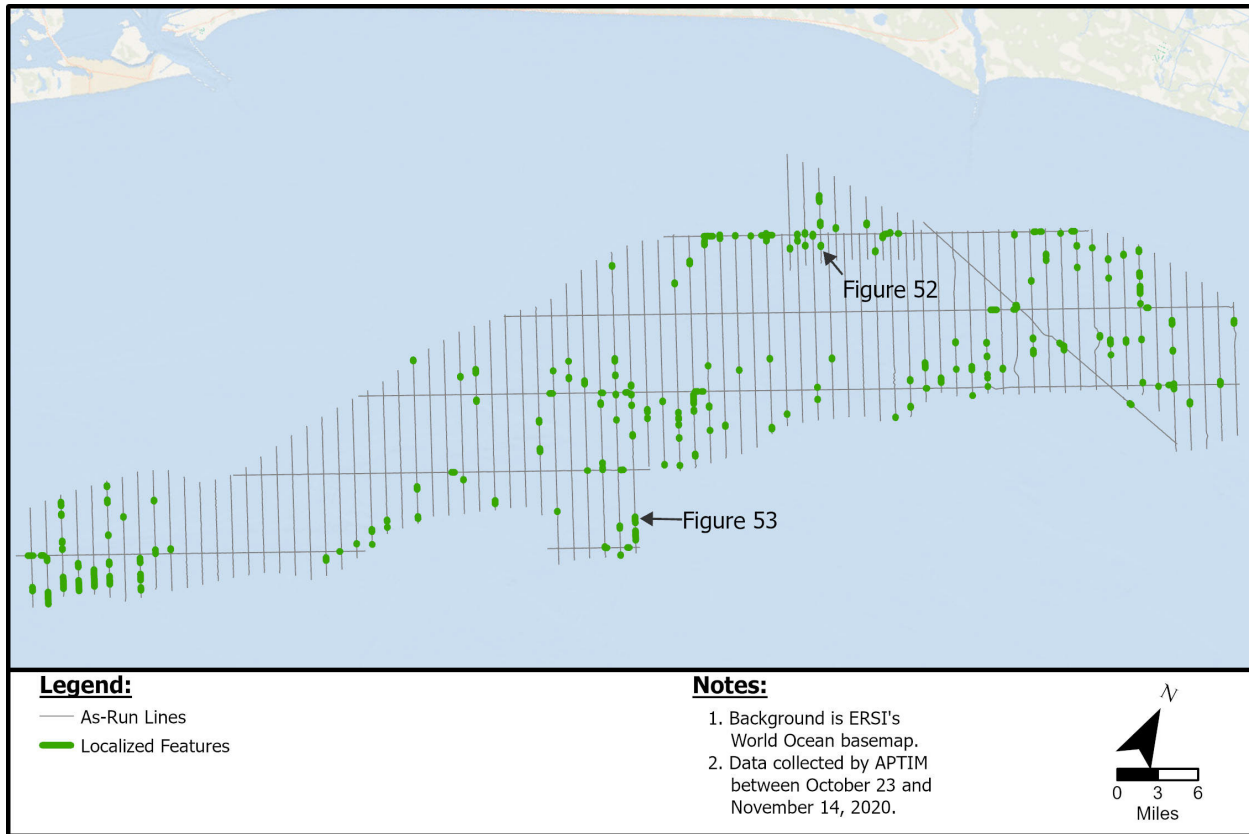


Figure 54. Localized features identified in the survey area.

5.4.4 Regional Geologic Summary

The Eastern Texas OCS contains numerous potential sand resources contained within regional-scale geologic systems such as the Pleistocene channel belt systems, Pleistocene terraces of the Trinity and Sabine Incised Valley, and the modern sand banks. Other significant potential sediment resources are found in localized features that are not regionally extensive due to survey spacing but are observed across the study area in the form of probable fluvial stratigraphy and near-surface sand sheets. While all geologic interpretations based on sub-bottom geophysical data must be held as preliminary until confirmed by geotechnical cores, these preliminary observations show the prominence of fluvial-related processes and stratigraphy across the OCS throughout the Pleistocene and Holocene. A generalized cross section was developed from the mapping of regional depositional systems and localized features (**Figure 55**). A key observation of this study is the amalgamation of Pleistocene and Holocene stratigraphy in the region which can lack clearly differentiated sequence boundaries separated by significant deposition as had been proposed in earlier work (Thomas 1991).

A generalized depositional sequence for the region can be summarized as:

1) Middle-Pleistocene falling stage and low-stand advances of deltaic and fluvial systems across the continental shelf, leading to the formation of inter-bedded prodelta and floodplain muds, sandy channel belt and distributary channel elements, and occasional preserved incised valley systems.

2) Middle-Pleistocene transgressions and high-stands leading to valley infilling, fluvial avulsion, and eventual reworking/erosion and the formation of internal sequence boundaries, commonly observed as regional erosional unconformities. Periods 1 and 2 together formed what is locally referred to as the Pleistocene Beaumont and Lissie formations, which can reach thousands of feet thickness across the inner continental shelf.

3) Late-Pleistocene falling stage and low-stand formation of incised valley systems, fluvial terraces, and associated erosional tributary drainages across the shelf, feeding shelf-edge delta systems.

4) Holocene transgression leading to backstepping of fluvial-deltaic systems within incised valleys, formation of Holocene estuarine and bay environments typically only preserved locally within incised valleys and tributary drainages, and localized avulsions of fluvial systems that “over-fill” valleys based on basin sediment supply.

5) Holocene to modern transgressive submergence and reworking of paleo-barrier island and formation of modern shelf sand bodies. Shelf sand shoals are likely not intact or in place barrier lithosomes but rather an actively evolving and moving shelf sedimentary system that may have initiated as a transgressed paleo-shoreline (**Figure 55**).

6) Modern sea-level high stand (current shoreline position) to develop extant barrier islands and coasts and the relatively mature (if still evolving) straightened shoreline observed today.

Key to this model is the recognition that within the upper section Holocene and Pleistocene fluvial systems may occur at equivalent depths below the seafloor, rather than be separated by large thicknesses of deltaic or marine deposition. Sequence boundaries, when observed, typically occur deep in the observed stratigraphy below the primary depth of investigation. This amalgamation and reworking leads to the “perching” of Pleistocene stratigraphic elements close to the modern seafloor.

East Texas Outer Continental Shelf Generalized Cross Section

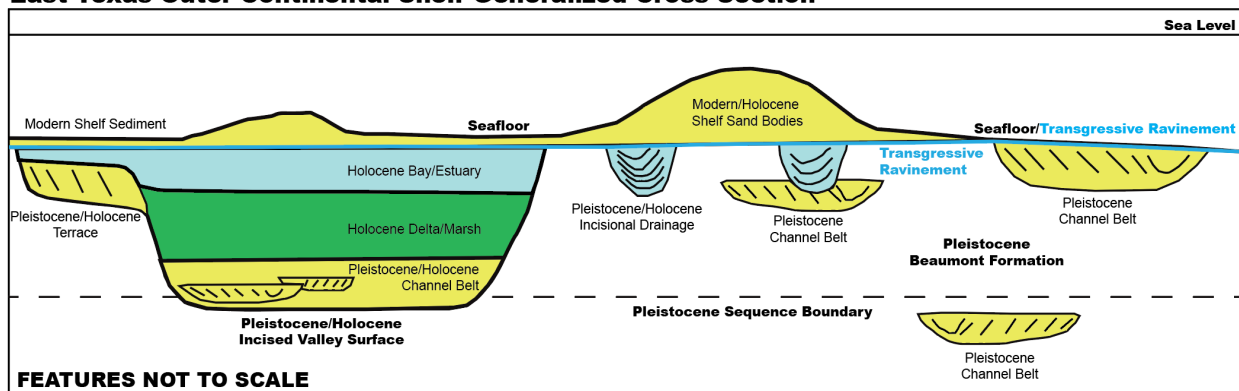


Figure 55. Generalized cross section of major features observed in the OCS.

Pleistocene stratigraphy often occurs at a level higher than Holocene fluvial stratigraphy.

While the location, character, and geologic history Trinity/Sabine Incised Valley systems has been well described by prior work, this new analysis shows the ubiquity of older fluvial channel belt systems relatively close to the modern seafloor. These older, likely Pleistocene, systems are not deeply buried within the Beaumont formation sediments as previously interpreted (Thomas 1991), but often occur at a depth equivalent to or even shallower than the more recent Holocene systems (**Figure 55**). In several areas the top of the potential fluvial stratigraphy is observed to outcrop at the seafloor, in contrast to the basal fluvial stratigraphy of the Sabine Incised Valleys which are often buried by 30-100 ft (9.1-30.5 m) of deltaic and estuarine sediments (Anderson et al. 2015). Also of importance is the observation of numerous channels that appear to have incised into the Beaumont formation during last sub-aerial exposure during sea level lowstand. These channels, drainages, and tributaries in some instances can be regionally mapped and their relationship to the larger incised valley systems observed, showing that they likely evolved together. These drainages and tributaries appear to be infilled in a manner similar to the larger incised valleys and the channel belt systems in that the base of the incisional drainages rarely appear to have a significant coarse-grained fluvial component, and so may not represent high-potential sand resources. Similar to the valleys they may contain localized sediment resources in the form of tidal deposits, but the scale of these features make correlation difficult at the regional level. The overall geologic history of the eastern Texas OCS appears to be comparable to that developed for the adjacent Southwest Louisiana shelf, where recent reviews found the ubiquity of fluvial stratigraphy and the potential for fluvial sand-bearing deposits to occur at almost every stage of sea level throughout the Pleistocene (**Figure 56**).

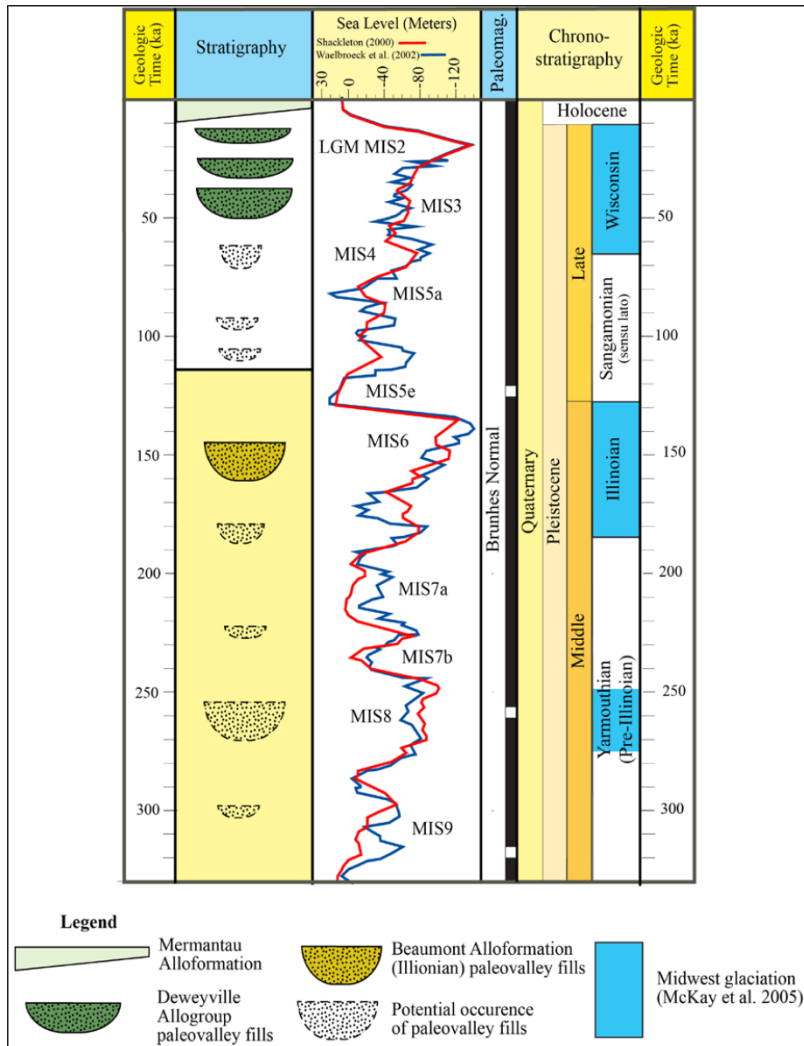


Figure 56. Late Pleistocene Stratigraphy of Southwest Louisiana.

Stratigraphy illustrates the ubiquity of fluvial stratigraphy at nearly all sea level stages. (Modified from Heinrich et al. 2020)

6 Vibracore Planning

The final goal of the OCS geophysical survey data collection, processing, and interpretation is the selection of vibracore sites for future collection. The purpose of collecting sediment samples is to ascertain the interpretations made from the seismic data, further characterize the sub-surface geology and stratigraphy, and establish a preliminary area of potential sediments that could be used in future coastal resiliency projects. Geologic samples are imperative for qualifying and quantifying a potential sand resource in terms of the available sediment volume as well as sedimentologic characteristics, such as grain size, color, carbonate content, shell content, etc. Therefore, the collection of vibracore samples would assist the GLO in determining the target compatibility of these potential deposits and if they would be a valuable resource for the Texas coastline.

Seismic interpretations are based on known sound attenuation signals caused in different sediment types and depositional environments. The difference in the available volume and behavior of coarse-versus fine-grained sediments throughout the various periods in geologic history causes different depositional patterns which are observed in the seismic record. Based on previous investigations along Sabine, Heald and adjacent areas, some seismic signatures have become indicative of sand deposits. These include paleochannels with some acoustic blanking/transparency, dipping depositional patterns such as clinoforms (suggestive of fluvial point bar deposits), or interbedded patterns indicative of small episodic depositional cycles within a continuous geologic period. Together with the information gathered from the geologic history in the desktop study, APTIM and TWI selected 74 geologic sampling sites assuming a 20 ft (6.1 m) maximum vibracore length (**Figure 57**). **Table 8** below includes all proposed sites as well as a description of the targeted geology and the feature/large sand body structures it is intended to characterize. Screen grabs of each proposed site can be found in **Appendix Q**, and a table with site name and coordinates are located in **Appendix R** along with a shapefile with the proposed locations in the digital **Appendix S**.

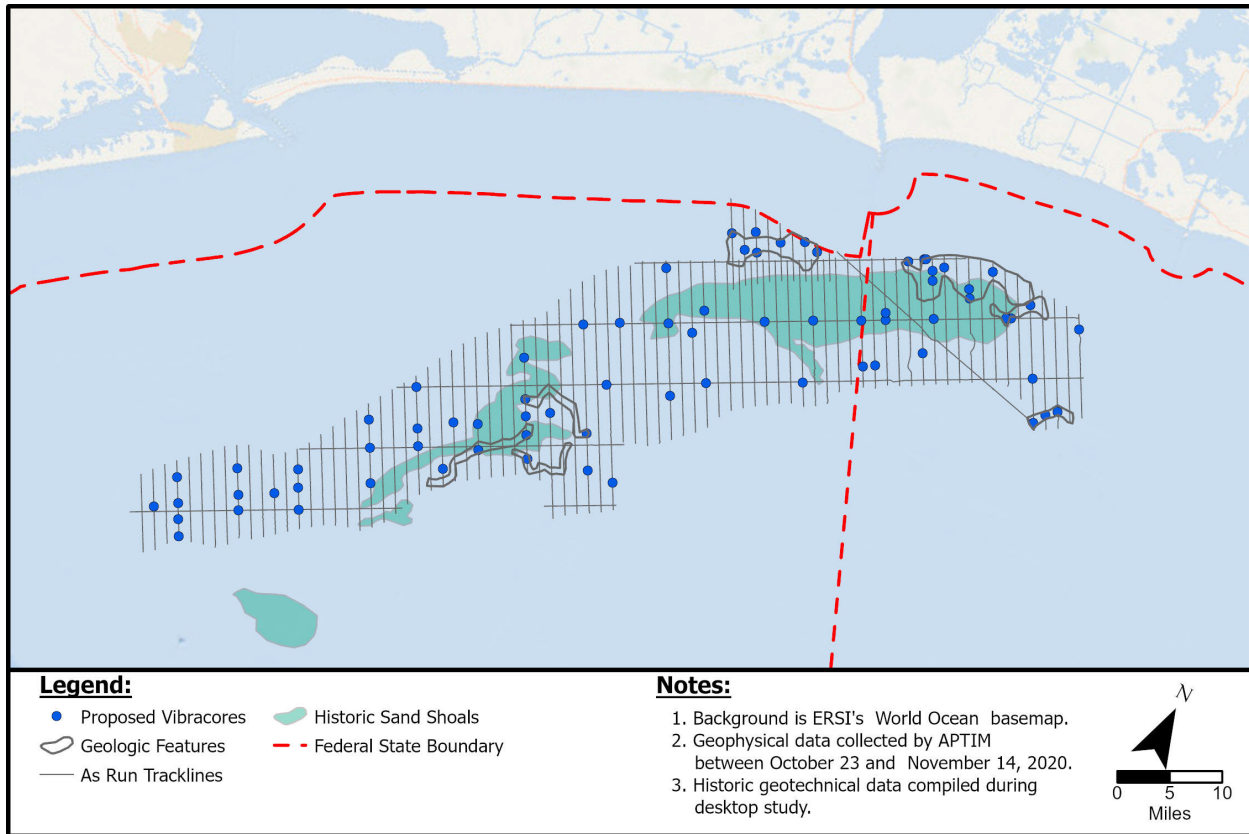


Figure 57. Proposed vibracore sites in the outer continental shelf study area.

Out of the 74 proposed sites, ten (10) are intended to provide geotechnical information on the Pleistocene Channel Belt systems. Two (2) are on the Pleistocene Channel Belt 1, three (3) are Pleistocene Channel Belt 2, two (2) Pleistocene Channel Belt 3, one (1) is in Pleistocene Channel Belt 4 and two (2) are in the Pleistocene Channel Belt 5. Five (5) samples were placed on the Sabine North Terrace. These samples are placed on acoustically transparent units with some prograding stratigraphy and/or chaotic deposition, which are all indicative of sandy deposits and have minimal overburden. Similarly, six (6) samples are placed on the Sabine South Terrace which has a similar stratigraphic pattern as the North Terrace, however with more isolated units with angular and prograding stratigraphic patterns. Other features that are not placed on large, delineated features were placed on smaller regional channel/drainage systems that are normally shallow (minimal overburden) with seismic facies highly indicative of a sand infill that are observed on a single or a few consecutive lines.

Most of the proposed sites (38) are placed on Seismic Unit Q1. The proposed vibracores placed on the topographic high, are intended to provide geotechnical properties on the likely sandier portion of the deposit and sample the surface “specked” chaotic deposit, which could be a coarser unit with some shells etc. Samples on the inshore portion of the study area aim at sampling the remaining portions of Seismic Unit Q1 which are not associated with bathymetric highs and would also sample the laterally continuous Beaumont/clay unit that is present throughout. The proposed vibracore coverage of the Seismic Unit Q1 would provide the GLO and BOEM with a more detailed understanding of the sedimentologic variability of the easily accessible surface deposit.

Table 8. Proposed Vibracore locations and general description of targeted stratigraphy.

Site Number	Seismic Line	Targeted Feature	Comments/Targeted Features/Site Description
1	Line_001	Localized Feature	Channel with prograding stratigraphy and acoustic blanking
2	Line_005	Localized Feature	Incised deposit with some prograding stratigraphy and acoustic blanking at bottom
3	Line_101	Localized Feature	Incised deposit with prograding stratigraphy, some acoustic blanking and chaotic deposition at the bottom
4	Line_003	Pleistocene Channel Belt 2	Incised channel with acoustic blanking and some prograding stratigraphy at edge
5	Line_004	Pleistocene Channel Belt 2	Incised channel with prograding stratigraphy overlaying an acoustically transparent layer
6	Line_209.002	Pleistocene Channel Belt 2	Incised channel with acoustic transparency and some angular deposit patterns
7	Line_005	Pleistocene Channel Belt 1	Channel with some mixed stratigraphy overlaying an acoustically transparent unit
8	Line_101	Pleistocene Channel Belt 1	Incised channel system with some acoustic blanking and prograding stratigraphy
9	Line_013	Localized Feature	incised unit with acoustic transparency and somewhat chaotic deposit
10	Line_100.002	Localized Feature	Incised deposit with prograding angular deposits overlaid by 10ft of overburden
11	Line_015	Localized Feature	Incised deposit with some acoustic transparency, prograding stratigraphy and some chaotic deposition at bottom
12	Line_008	Sabine South Terrace	Portion of incised deposit with angular stratigraphy
13	Line_010	Sabine South Terrace	Deposit with some acoustic blanking and angular deposits
14	Line_010	Sabine South Terrace	Terrace unit with prograding angular stratigraphy and some acoustic blanking
15	Line_012	Sabine South Terrace	Unit with acoustic blanking and some angular deposits
16	Line_013	Sabine South Terrace	Acoustically transparent unit with some chaotic portions
17	Line_100.002	Sabine South Terrace	Unit with acoustic blanking
18	Line_201	Sabine North Terrace	Unit with acoustic blanking and some angular deposits, with 10-15ft of overburden
19	Line_202	Sabine North Terrace	Acoustically transparent unit with some angular surface deposits

Site Number	Seismic Line	Targeted Feature	Comments/Targeted Features/Site Description
20	Line_204	Sabine North Terrace	Acoustically transparent unit with some angular bottom deposits
21	Line_207	Sabine North Terrace	Acoustically transparent unit with 10-15ft of overburden
22	Line_208	Sabine North Terrace	Acoustically transparent surface unit with some angular point-bar like deposits at the bottom
23	Line_013	Seismic Unit Q1	Surface unit with some laminated stratigraphy and acoustic transparency
24	Line_014	Localized Feature	Incised deposit with prograding stratigraphy and some chaotic deposition
25	Line_017	Seismic Unit Q1	Seismic Unit Q1 overlaying laminated strata
26	Line_101	Seismic Unit Q1	Seismic Unit Q1/acoustic transparency and laminated surface deposit overlaying laminated strata
27	Line_018	Localized Feature	Portion of incised channel that is acoustically transparent
28	Line_101	Seismic Unit Q1	Seismic Unit Q1/acoustic transparency and laminated surface deposit overlaying laminated strata
29	Line_019	Localized Feature	Channel edge with prograding stratigraphy/fluviial point bar and acoustic blanking
30	Line_023	Seismic Unit Q1	Seismic Unit Q1/chaotic deposition overlaying laminated strata
31	Line_024	Seismic Unit Q1	Seismic Unit Q1/chaotic deposition overlaying laminated strata
32	Line_027	Seismic Unit Q1	Seismic Unit Q1/chaotic deposition overlaying laminated strata
33	Line_206	Localized Feature	Localized deposit with some acoustic transparency and prograding deposits
34	Line_206	Localized Feature	Localized deposit with some acoustic transparency at the surface and angular point-bar like deposits at the bottom, with 10ft of overburden
35	Line_032	Seismic Unit Q1	Seismic Unit Q1/chaotic deposition overlaying laminated strata
36	Line_102	Seismic Unit Q1	Seismic Unit Q1/acoustic transparency and laminated surface deposit overlaying laminated strata
37	Line_033	Seismic Unit Q1	Seismic Unit Q1/chaotic deposition overlaying laminated strata
38	Line_035	Localized Feature	Incised deposit with prograding angular deposits overlaid by 10-15ft of overburden
39	Line_035	Seismic Unit Q1	Seismic Unit Q1/chaotic deposition overlaying laminated strata
40	Line_035	Seismic Unit Q1	Seismic Unit Q1/chaotic deposition overlaying laminated strata
41	Line_039	Seismic Unit Q1	Seismic Unit Q1/chaotic deposition overlaying laminated strata
42	Line_102	Localized Feature	Incised deposit with prograding stratigraphy and acoustic blanking, with 10-15ft of overburden
43	Line_040.003	Localized Feature	Incised channel deposit with point-bar like prograding stratigraphy and acoustic transparency
44	Line_042	Seismic Unit Q1	Seismic Unit Q1/chaotic deposition overlaying laminated strata
45	Line_042	Seismic Unit Q1	Seismic Unit Q1/chaotic deposition overlaying laminated strata
46	Line_042	Pleistocene Channel Belt 3	Incised deposit with prograding angular deposits overlaid by 10-15ft of overburden

Site Number	Seismic Line	Targeted Feature	Comments/Targeted Features/Site Description
47	Line_047.002	Pleistocene Channel Belt 3	Incised deposit with prograding angular deposits overlaid by 10-15ft of overburden
48	Line_047.002	Pleistocene Channel Belt 5	Incised deposit with prograding angular deposits overlaid by 10-15ft of overburden
49	Line_047.002	Pleistocene Channel Belt 4	Incised deposit with prograding angular deposits overlaid by 10-15ft of overburden
50	Line_051	Pleistocene Channel Belt 5	incised acoustically transparent unit with some stratigraphy at edges, overlaid with 10-12 ft of overburden
51	Line_045.001	Seismic Unit Q1	Seismic Unit Q1/chaotic deposition overlaying laminated strata
52	Line_047.002	Seismic Unit Q1	Seismic Unit Q1/chaotic deposition overlaying laminated strata
53	Line_047.002	Seismic Unit Q1	Seismic Unit Q1/chaotic deposition overlaying laminated strata
54	Line_051	Seismic Unit Q1	Seismic Unit Q1/chaotic deposition overlaying laminated strata
55	Line_053	Seismic Unit Q1	Seismic Unit Q1//chaotic deposition overlaying laminated strata
56	Line_054.002	Channel	Bottom of channel/channel edge with some prograding stratigraphy and acoustic transparency overlaid by 10ft of overburden
57	Line_056	Seismic Unit Q1	Seismic Unit Q1//acoustic transparency overlaying laminated strata
58	Line_056	Seismic Unit Q1	Seismic Unit Q1//chaotic deposition overlaying laminated strata
59	Line_056	Seismic Unit Q1	Seismic Unit Q1//acoustic transparency overlaying laminated strata
60	Line_060	Seismic Unit Q1	Seismic Unit Q1//acoustic transparency overlaying laminated strata
61	Line_060	Seismic Unit Q1	Seismic Unit Q1//acoustic transparency and chaotic surface deposit overlaying laminated strata
62	Line_060	Seismic Unit Q1	Seismic Unit Q1//acoustic transparency and chaotic surface deposit overlaying laminated strata
63	Line_066	Seismic Unit Q1	Seismic Unit Q1//acoustic transparency and chaotic surface deposit overlaying laminated strata
64	Line_066	Seismic Unit Q1	Seismic Unit Q1//acoustic transparency overlaying laminated strata
65	Line_066	Seismic Unit Q1	Seismic Unit Q1//acoustic transparency and chaotic surface deposit overlaying laminated strata
66	Line_068	Seismic Unit Q1	Seismic Unit Q1//acoustic transparency overlaying laminated strata
67	Line_071.002	Seismic Unit Q1	Seismic Unit Q1/acoustic transparency deposit overlaying laminated strata
68	Line_071.002	Seismic Unit Q1	Seismic Unit Q1/acoustic transparency overlaying laminated strata
69	Line_071.002	Seismic Unit Q1	Seismic Unit Q1/acoustic transparency and chaotic surface deposit overlaying laminated strata
70	Line_076	Seismic Unit Q1	Seismic Unit Q1acoustic transparency and laminated surface deposit overlaying laminated strata
71	Line_076	Seismic Unit Q1	Seismic Unit Q1/acoustic transparency and laminated surface deposit overlaying laminated strata
72	Line_076	Seismic Unit Q1	Seismic Unit Q1/acoustic transparency and laminated surface deposit overlaying laminated strata

Site Number	Seismic Line	Targeted Feature	Comments/Targeted Features/Site Description
73	Line_076	Seismic Unit Q1	Seismic Unit Q1/acoustic transparency deposit overlaying laminated strata
74	Line_078	Seismic Unit Q1	Seismic Unit Q1/acoustic transparency and laminated surface deposit overlaying laminated strata

7 Conclusion

This sand source reconnaissance geophysical investigation followed sequential survey procedures developed by APTIM. During Task I, a review of historical data found limited geologic data for marine sand resources offshore the Texas OCS along Sabine Bank, Heald Bank, and adjacent shoals. Based on this review, a Task 2 reconnaissance geophysical investigation collected 1,133 nautical line miles of geophysical data at a combined grid line spacing of approximately 1 x 5 mi (1.6 x 8 km) grid. The geophysical data were used to determine potential sand locations as well as determine where 74 future vibracores could be collected to further understand sediment distribution and quality and to ascertain the presence of material suitable for use for shore-protection projects.

The geophysical data were used to determine potential sand deposits, assess major regional stratigraphic features located in the study area, and develop a regional geologic framework of major depositional systems that have the potential to contain accessible sand resources. Within Seismic Unit Q1, APTIM determined that there is roughly ~5.9 BCY of potential surficial resources, which is a gross estimate based on the available data and would require additional geotechnical information in order to determine its grain size properties and composition.

In addition to the large regional units, smaller, isolated features were also identified during data processing. These localized features are observed throughout the study area, and many have a high-potential for sand-bearing deposits but are not observed on adjacent geophysical lines, making characterization and quantification of potential sand resources impossible at this resolution. These smaller features are normally isolated channels or sediment pockets, which are indicative of sand or mixed sediments.

The east Texas OCS contains a significant number of potential sand-bearing units located within the study area in the form of fluvial deposits and sand bank/sheet features. As part of this study, five (5) Pleistocene Channel belt systems were identified, along with two (2) terraces and the Sabine Incised Valley.

The Pleistocene Channel Belts 1 and 2 are located on the eastern side of the study area and are characterized by a basal erosional unconformity overlaid by variable-amplitude, steeply-dipping clinofolds and occasional areas of semi-transparent to chaotic acoustic facies, with the upper portion of these units being either a transition to more layered seismic facies or are truncated by transgressive ravinement. Channel Belts 1 and 2 are roughly 25-50 ft (7.6-15.2 m) thick with 0-10 ft (0-3 m) of overburden and 20-50 ft (6.1-15.2 m), with 0-5 ft (0-1.5 m) of overburden, respectively, and have a rough gross volume of 121 million cubic yards (MCY) and 49 MCY each (not including overburden).

Pleistocene Channel Belts 3-5 are located on the central portion of the study area, seaward and under Heald Bank. This channel belt system shows variable geometry and occasional cross-cutting by incisional drainages feeding into Sabine Valley and are characterized by basal erosional unconformities overlain by steeply-dipping clinofolds that grade into U-shaped channel forms at the edge of the belt deposit. The likely sandier portion of the system is roughly 20-50 ft (6.1-15.2 m) thick with between 0-20 ft (0-6.1 m) of overburden with a potential gross volume of 78 MCY, 67 MCY, and 107 MCY for Channel Belts 3, 4, and 5, respectively (not including overburden).

The two identified terraces are located to the north and south of the Holocene Sabine Incised Valley and are characterized as thick units with steeply-dipping clinoforms and 0 to 15 ft (0-4.6 m) of overburden. The Sabine North Terrace has a gross estimated volume of 472 MCY, and the Sabine South Terrace has an estimated gross volume of 1,240 MCY (without including overburden).

The Sabine Incised Valley system is a major stratigraphic unit across the entire study area. The edges of the system are well defined within this investigation; however, the actual base of the valley is not observed due to an amalgamated sand-rich fluvial unit formed during the lowstand and early stage of the transgression that has a very high-amplitude acoustic return and allows for little penetration past it. Therefore, this investigation was unable to estimate a gross volume of the Incised Valley system, though it is expected to be quite large, however, buried under a roughly 30-40 ft (9.1-12.2 m) thick estuarine unit, with some smaller areas being closer to the seafloor.

The features identified in this investigation are not exhaustive or inclusive of all potential sand-bearing stratigraphy within the region, but rather represent systems that are regionally extensive and contiguous to be confidently interpreted across the 1 x 5 mi (1.6 x 8 km) spaced survey grid. The major sub-surface geologic systems observed represent a cumulative that cumulative gross volume of 2.1 BCY (which does not include overburden) is contained within the major subsurface geologic systems (Paleochannel systems and terraces). The ~5.9 BCY represents the gross volume for the surficial unit Seismic Unit Q1. Existing vibracore coverage is not sufficient for the delineation of sedimentologic and/or stratigraphic facies, and therefore, our proposed Seismic Unit Q1 has variable sedimentological properties that range from 20-100% sand. The precise composition of these deposits is likely highly variable and requires more detailed geological investigation, detailed in the vibracore plan.

8 References

- Abdulah, K. C. 1995. The Evolution of the Brazos and Colorado Fluvial/Deltaic Systems During the Late Quaternary: An Integrated Study, Offshore Texas, Thesis submitted in partial fulfillment of the requirements for the degree Doctor of Philosophy, Rice University.
- Abdulah, K.C., J.B. Anderson, J.N. Snow, and L. Holdford-Jack. 2004. The late Quaternary Brazos and Colorado deltas, offshore Texas, USA—their evolution and the factors that controlled their deposition. In: Anderson, J.B., Fillon, R.H. (Eds.), Late Quaternary Stratigraphic Evolution of the Northern Gulf of Mexico Margin. *Society for Sedimentary Geology, Special Publication 79*, pp. 237-269.
- Anderson, J.B. 2007. The formation and future of the upper Texas coast: a geologist answers questions about sand, storms, and living by the sea (Vol. 11). Texas A&M University Press.
- Anderson, J.B., A. Rodriguez, K.C. Abdulah, R.H. Fillon, L.A. Banfield, H.A. McKeown, and J.S. Wellner. 2004. Late Quaternary stratigraphic evolution of the northern Gulf of Mexico: a synthesis. In: Anderson, J.B., Fillon, R.H. (Eds.), Late Quaternary Stratigraphic Evolution of the Northern Gulf of Mexico Margin. *Society for Sedimentary Geology, Special Publication 79*, pp. 1–23.
- Anderson, J.B., D.J. Wallace, A.R. Simms, A.B. Rodriguez, K.T. Milliken. 2014. Variable response of coastal environments of the northwestern Gulf of Mexico to sea-level rise and climate change: implications for future change. *Mar.Geol.*352,348–366.
- Anderson, J.B., D.J. Wallace, A.R. Simms, Robert W. Rodriguez, Z. Weighte, and Patrick Taha. 2015. Recycling sediments between source and sink during a eustatic cycle: Systems of late Quaternary Northwestern Gulf of Mexico Basin. *Earth-Science Reviews* 153 (2015) 111–138.
<http://dx.doi.org/10.1016/j.earscirev.2015.10.014>
- Anderson, J.B., D.J. Wallace, A.R. Simms, Robert W. Rodriguez, Z. Weighte, and Patrick Taha. 2016. Recycling sediments between source and sink during a eustatic cycle: Systems of late Quaternary Northwestern Gulf of Mexico Basin. *Earth-Science Reviews* 153 (2016) 111–138.
- Aptim Environmental & Infrastructure (APTIM). 2021. Texas General Land Office Region 1 Offshore Reconnaissance Geophysical Sand Search Survey: Geophysical Investigation. Final Report prepared for the Texas General Land Office. Contract No. 18-127-014: 86 p.
- Aptim Environmental & Infrastructure, LLC (APTIM) and The Water Institute of the Gulf 2022. Texas General Land Office Offshore Sediment Resource Inventory: Geological and Geophysical Data Collection and Processing for Identification of Outer Continental Shelf Mineral Resources Offshore of Texas. Final Report prepared for the Texas General Land Office. Contract No. 18-127-014: 94 p.

- APTIM-CPE. 2001. Holly Beach Breakwater Enhancement and Sand Management Plan, Appendix B. Boca Raton, FL: Coastal Planning & Engineering, Inc., 115 p (Prepared for the Louisiana Department of Natural Resources).
- Autin, W.J., S.F. Burns, B.J. Miller, R.T. Saucier, and J.I. Snead. 1991. Quaternary geology of the lower Mississippi Valley. *Quaternary nonglacial geology: Conterminous US*, 2, pp.547-582.
- Autin, W.J. and R.P. McCulloh. 1995. Quaternary Geology of Weeks and Cote Blanche Islands Salt Domes. *Gulf Coast Association of Geological Societies, Volume 45*, pp 39-46.
- Autin, W.J., R.P. McCulloh, and A.T. Davison. 1986. Quaternary geology of Avery Island, Louisiana. *Gulf Coast Association of Geological Societies, Volume 36*, pp. 379-390.
- Bernard, H.A., C.F. Major Jr., and B.S. Parrott. 1959. The Galveston barrier island and environments: a model for predicting reservoir occurrence and trend. *Trans. Gulf Coast Assoc. Geol. Soc.* 9, 221–224.
- Blum, M.D. and T.E. Törnqvist. 2000. Fluvial responses to climate and sea-level change: a review and look forward. *Sedimentology*, 47: 2-48. <https://doi.org/10.1046/j.1365-3091.2000.00008>.
- Blum, M.D. and D.M. Price. 1998. Quaternary alluvial plain construction in response to glacio-eustatic and climatic controls, Texas Gulf Coastal Plain. In Shanley, K., McCabe, P., eds., *Relative Role of Eustasy, Climate, and Tectonism in Continental Rocks*. Tulsa, OK, Society for Sedimentary Geology, *SEPM Special Publication 59*, 31-48.
- Buffler, R.T., W.A. Thomas, and R.C. Speed. 1994. Crustal structure and evolution of the southeastern margin of North America and the Gulf of Mexico basin. Phanerozoic evolution of North American continent-ocean transitions: *Boulder, Colorado, Geological Society of America, Decade of North American Geology, Continent-Ocean Transect Volume*, pp.219-264.
- Burke, K. 1975. Atlantic evaporites formed by evaporation of water spilled from Pacific, Tethyan, and Southern oceans: *Geology*, v. 3, p. 613–616.
- Dellapenna, T. M., Cardenas, A., Johnson K. and Flocks, J. 2009. Report of the Sand Source Investigation of the Paleo-Sabine-Trinity Marine Features (PSTMF). Texas General Land Office Cooperative Agreement Number MO7AC12518 Service Contract 09-109-000-3517
- Dellapenna, T. M., A. Cardenas, and J. Garrison. 2010. Report of the Re-Analysis of Sand Resources at Sabine and Heald Banks, East Texas Inner Continental Shelf. Texas General Land Office/U.S. Minerals Management Service/Bureau of Offshore Energy and Mineral Resource Extraction (BOEMRE). 47 p.
- Diegel, F. A., J. F. Karlo, D. C. Schuster, R. C. Shoup, and P. R. Tauvers. 1995. Cenozoic structural evolution and tectono-stratigraphic framework of the northern Gulf coast continental margin, in M. P.

- A. Jackson, D. G. Roberts, and S. Snelson, eds., Salt tectonics: a global perspective: *AAPG Memoir* 65, p. 109-151.
- Fisher, W.L., L.F. Brown, J.H. McGowen, and C.G. Groat. 1972. Environmental geologic atlas of the Texas coastal zone—Galveston-Houston area: The University of Texas at Austin, Bureau of Economic Geology, 91 p.
- Fisher, W.L., L.F. Brown, J.H. McGowen, and C.G. Groat. 1973. Environmental geologic atlas of the Texas coastal zone—Beaumont-Port Arthur area: The University of Texas at Austin, Bureau of Economic Geology, 93 p.
- Forde, A. S., S.V. Dadisman, J.G. Flocks, T.M. Dellapenna, J.M. Sanford, and D.S. Weise. 2009. Archive of Digital Chirp Sub-bottom Profile Data Collected During USGS Cruise 09CCT01 Offshore of Sabine Pass and Galveston, Texas, March 2009: U.S. Geological Survey Data Series 526. Online at <https://pubs.usgs.gov/ds/526/#Anchor-3591>
- Gahagan and Bryant Associates, Inc. 2013. Sand Resource Investigation for the McFaddin Wildlife Refuge Beach Nourishment TGLO CEPRA Project No. 1530.
- Galloway, W.E. 2008. Chapter 15 Depositional Evolution of the Gulf of Mexico Sedimentary Basin, in: *Sedimentary Basins of the World*. Elsevier, pp. 505–549. [https://doi.org/10.1016/S1874-5997\(08\)00015-4](https://doi.org/10.1016/S1874-5997(08)00015-4)
- Giles, K.A. and M.G. Rowan. 2012. Concepts in halokinetic-sequence deformation and stratigraphy. *Geological Society, London, Special Publications* 363, 7–31. <https://doi.org/10.1144/SP363.2>
- Heinrich, P.V., M. Miner, R. Paulsell, and R.P. McCulloh. 2020. Response of Later Quaternary Valley Systems to Holocene Sea Level Rise on the Continental Shelf Offshore Louisiana: Preservation Potential of Paleolandscapes 109.
- Hollis, R.J., D.J. Wallace, M.D. Miner, N.S. Gal, C. Dike, and J.G. Flocks. 2019. Late Quaternary evolution and stratigraphic framework influence on coastal systems along the north-central Gulf of Mexico, USA. *Quaternary Science Reviews*, 223, p.105910.
- Hovland, M., and A. Judd. 1988. Seabed pockmarks and seepages: Impact on geology, biology and the marine environment, Graham and Trotman, London.
- Louisiana Geological Survey. 2012. Morgan City 30 x 60 Minute Geologic Quadrangle.
- McGowen, J.H., C.V. Proctor, L.F. Brown Jr, T.J. Evans, W.L. Fisher, and C.G. Groat. 1976. Environmental geologic atlas of the Texas coastal zone—Port Lavaca area: The University of Texas at Austin. Bureau of Economic Geology.

- Mohrig, D.C., Heller, P.L., Paola, C., Lyons, W.J., 2000. Interpreting avulsion process from ancient alluvial sequences: Guadalupe-Matarranya system (northern Spain) and Wasatch Formation, (western Colorado). *Geological Society of America Bulletin* 112 (12), 1787–1803.
- Morton, R.A. and J. R. Suter. 1996. Sequence stratigraphy and composition of Late Quaternary shelf margin deltas, northern Gulf of Mexico. *AAPG Bulletin* 80, 505–530.
- Morton, R.A. and J.C. Gibeaut. 1993. Physical and Environmental Assessment of Sand Resources- Texas Continental Shelf, Prepared for the U.S. Department of the Interior Minerals Management Service Office of International Activities and Marine Minerals, Cooperative Agreement No. 14-35-0001-30635.
- Morton, R.A. and J.C. Gibeaut. 1995. Physical and Environmental Assessment of Sand Resources: Sabine and Heald Banks Second Phase 1994-1995: Report to the U. S. Department of the Interior 14-35-0001-30635, 62 p.
- Morton, R.A. and W.A. Price. 1987. Late Quaternary sea-level fluctuations and sedimentary phases of the Texas coastal plain and shelf, in Nummedal D., Pilkey, O.H., Jr., and Howard, J.D., eds., *Sea-Level Fluctuation and Coastal Evolution: SEPM, Special Publication 41*, p. 181–198.
- Morton, R.A., M.D. Blum, and W. A. White. 1996. Valley fills of incised coastal plain rivers, southeastern Texas. *Gulf Coast Association of Geological Societies. Volume 46*, pp 321-331.
- Nguyen, L.C. and P. Mann. 2016. Gravity and magnetic constraints on the Jurassic opening of the oceanic Gulf of Mexico and the location and tectonic history of the Western Main transform fault along the eastern continental margin of Mexico. *Interpretation*, 4(1), pp.SC23-SC33.
- Otvos, E.G. and W.E. Howat. 1996. South Texas Ingleside Barrier; coastal sediment cycles and vertebrate fauna. Late Pleistocene stratigraphy revised. *Trans. Gulf Coast Assoc. Geol. Soc.* 46, 333–344.
- Penland, S., R. Boyd, R., and J.R. Suter. 1988. Transgressive depositional systems of the Mississippi Delta plain; a model for barrier shoreline and shelf sand development. *Journal of Sedimentary Research*, 58(6), pp.932-949.
- Price, W.A. 1933. Role of diastrophism in topography of Corpus Christi area, south Texas. *AAPG Bulletin*, 17, 907–962.
- Reijnenstein, H., Posamentier, H. and Bhattacharya, J. 2011. Seismic geomorphology and high-resolution seismic stratigraphy of inner-shelf fluvial, estuarine, deltaic, and marine sequences, Gulf of Thailand. *AAPG Bulletin*, 95, 1959-1990. 10.1306/03151110134.
- Rodriguez, A.B., J.B. Anderson, F.P. Siringan, and M. Taviani. 1999. Sedimentary Facies and Genesis of Holocene Sand Banks on the East Texas Inner Continental Shelf, *SEPM (Society for Sedimentary Geology)* ISBN 1-56576-057-3, pp.165-178.

- Rodriguez, A.B., J.B. Anderson, F.P. Siringan, and M. Taviani. 2004. Holocene Evolution of the East Texas Coast and Inner Continental Shelf: Along-Strike Variability in Coastal Retreat Rates. *Journal of Sedimentary Research Vol 74* No. 3 pp 405-421.
- Rodriguez, Antonio B., John B. Anderson, Fernando P. Siringan, and Marco Taviani. 2004. Holocene Evolution of the East Texas Coast and Inner Continental Shelf: Along-Strike Variability in Coastal Retreat Rates. *Journal of Sedimentary Research* 74 (3): 405–421. doi: <https://doi.org/10.1306/092403740405>
- Rodriguez, A.B., M.L. Fassell, and J.B. Anderson. 2001. Variations in Shoreface Progradation and Ravinement Along the Texas Coast, Gulf of Mexico. *Sedimentology, Vol 48*, pp. 837-853.
- Rodriguez, A.B., M.D. Hamilton, and J.B. Anderson. 2000. Facies and evolution of the modern Brazos Delta, Texas: wave versus flood influence. *Journal of Sedimentary Research, 70(2)*, pp., 283-295.
- Salvador, A. (Ed.). 1991. Origin and development of the Gulf of Mexico basin, in: The Gulf of Mexico Basin. *Geological Society of America, U.S.A.*, pp. 389–444. <https://doi.org/10.1130/DNAG-GNA-J.389>
- Simms, A.R., J.B. Anderson, R. DeWitt, K. Lambeck, and A. Purcell. 2013. Quantifying rates of coastal subsidence since the last interglacial and the role of sediment loading. *Global and Planetary Change, 111*, pp.296-308.
- Simms, A.R., J.B. Anderson, Z.P. Taha, and A.B. Rodriguez. 2006. Overfilled versus underfilled incised valleys: lessons from the Quaternary Gulf of Mexico. In: Dalrymple, R., Leckie, D., Tillman, R. (Eds.), *Incised Valleys in Time and Space. SEPM Special Publication 85*, pp. 117–139.
- Siringan, F.P. and J.B. Anderson. 1994. Modern shoreface and inner-shelf storm deposits off the east Texas coast, Gulf of Mexico. *Journal of Sedimentary Research, 64(2b)*, pp.99-110.
- Swartz, J. 2019. Channel processes and products in subaerial and submarine environments across the Gulf of Mexico, Thesis submitted in partial fulfilment of the requirements for the degree Doctor of Philosophy. The University of Texas at Austin.
- Swartz, J.M., S.P.S. Gulick, and J.A. Goff. 2016, Formation of Heald Bank on the East Texas Inner Continental Shelf: Insights from Recent Geophysical Data: Geological Society of America, Abstracts and Programs, v 48, no. 1, South-Central Section Annual Meeting, Baton Rouge, Louisiana, March 21-22, 2016, doi: 10.1130/abs/2016SC-273680.
- Taha, Z.P. and J.B. Anderson. 2008. The influence of valley aggradation and listric normal faulting on styles of river avulsion: a case study of the Brazos River, Texas, USA. *Geomorphology* 95, 429–448.
- Thomas, M. A. 1991. The impact of long-term and short-term sea level changes on the evolution of the Wisconsinan-Holocene Trinity/Sabine incised valley system, Texas continental shelf. Diss., Rice University. <https://hdl.handle.net/1911/16488>.

- Thomas, M.A. and J.B. Anderson. 1994. Sea-Level Controls on the Facies Architecture of the Trinity/Sabine Incised-Valley System, Texas Continental Shelf. Incised-Valley Systems: Origin and Sedimentary Sequences, *SEPM Special Publication No 51*.
- Wallace, D.J., J.B. Anderson, and R.A. Fernández. 2010. Transgressive ravinement versus depth of closure: A geological perspective from the upper Texas coast. *Journal of Coastal Research*, 26(6), pp.1057-1067.
- Weight, R.W.R., J.B. Anderson, and R. Fernandez. 2011. Rapid Mud Accumulation On the Central Texas Shelf Linked To Climate Change and Sea-Level Rise. *Journal of Sedimentary Research* 81, 743–764. <https://doi.org/10.2110/jsr.2011.57>
- Wilkinson, B.H. 1975. Matagorda Island, Texas: the evolution of a Gulf Coast barrier complex. *Geological Society of America Bulletin*, 86(7), pp.959-967.
- Winker, C.D. 1979. Late Pleistocene Fluvial-Deltaic Deposition, Texas Coastal Plain and Shelf. *GCAGS Transactions* 29, 215.
- Young, S.C., T. Ewing, S. Hamlin, E. Baker, and D. Lupton. 2012. Updating the Hydrogeologic Framework for the Northern Portion of the Gulf Coast Aquifer 285.